

Differential Expression and MAL-dependent Targeting of the L-MAG and S-MAG Isoforms to Myelin Membranes

Inauguraldissertation

zur
Erlangung der Würde eines Doktors der Philosophie
vorgelegt der
Philosophisch-Naturwissenschaftlichen Fakultät
der Universität Basel

von

Michael Erb
aus Oberhof (AG)

Basel, 2003

Genehmigt von der Philosophisch-Naturwissenschaftlichen Fakultät
auf Antrag von

Dr. Nicole Schaeren-Wiemers
Prof. Markus Ruegg
Prof. Heinrich Reichert

Basel, den 10. Juni 2003

Prof. Marcel Tanner

Dedicated to Corinne

Table of contents

ACKNOWLEDGMENTS	7
ABBREVIATIONS	8
SUMMARY	10
INTRODUCTION	12
1. MYELIN	12
2. MYELINATING CELLS OF THE CENTRAL AND PERIPHERAL NERVOUS SYSTEM	13
2.1. SCHWANN CELLS.....	13
2.2. OLIGODENDROCYTES	13
2.2.1. <i>The Mouse Oligodendrocyte Cell Line Oli-neu</i>	15
3. ORGANIZATION OF THE MYELIN SHEATH	16
3.1. ARCHITECTURE OF THE PERIPHERAL NERVOUS SYSTEM MYELIN SHEATH	16
3.2. ARCHITECTURE OF THE CENTRAL NERVOUS SYSTEM MYELIN SHEATH	17
3.3. THE NODE OF RANVIER AND THE PARANODE	18
4. THE MYELIN PROTEINS	20
4.1. MYELIN-ASSOCIATED GLYCOPROTEIN - MAG	21
4.2. MYELIN AND LYMPHOCYTE PROTEIN - MAL	25
4.3. PROTEOLIPID PROTEIN - PLP	27
4.4. MYELIN BASIC PROTEIN - MBP	27
4.5. MYELIN/OLIGODENDROCYTE GLYCOPROTEIN - MOG	29
5. MYELIN LIPIDS	30
5.1. GENERAL.....	30
5.2. CHOLESTEROL.....	30
5.3. MYELIN GLYCOLIPIDS	31
6. LIPID-RAFTS	32
MOTIVATION AND AIM OF THE WORK	34
MATERIALS AND METHODS	35
1. MOLECULAR BIOLOGY	35
1.1. RNA ISOLATION AND cDNA SYNTHESIS	35
1.2. PRIMER LIST.....	35
1.3. SEMI-QUANTITATIVE RT-PCR	36
1.4. QUANTITATIVE RT-PCR	37
1.5. CLONING OF THE cDNA EXPRESSION CONSTRUCTS	37
1.5.1. <i>Cloning of the L-/S-MAG Expression Vectors</i>	37
1.5.2. <i>Cloning of the L-/S-MAG-GFP Expression Vectors</i>	38
1.5.3. <i>Cloning of the S-MAG-DsRed1 Expression Vector</i>	38
1.5.4. <i>Cloning of the S-MAG-VSVG Expression Vector</i>	38
1.5.5. <i>Cloning of the GFP-L-MAG/GFP-S-MAG Expression Vectors</i>	38
1.6. CLONING OF THE GENOMIC MOUSE MAG EXPRESSION CONSTRUCTS.....	39
1.6.1. <i>Cloning of the pmag-MAG-e13GFP Construct</i>	39
1.6.2. <i>Cloning of the pmag-MAG-e12GFP Construct</i>	41
1.6.3. <i>Cloning of the pmag-MAG-e12VSVG Construct</i>	41
1.6.4. <i>Cloning of the pmag-MAG-e12VSVG-e13GFP Construct</i>	41
1.6.5. <i>Cloning of the pmag-L-MAG-GFP Construct</i>	42
2. GENERATION OF TRANSGENIC MICE	44
3. CELL CULTURE	44

4. BIOCHEMICAL METHODS	44
4.1. GENERATION AND PURIFICATION OF AN ANTI-L-MAG POLYCLONAL ANTIBODY	44
4.2. IMMUNOCYTOCHEMISTRY	45
4.3. MYELIN PURIFICATION	46
4.4. MYELIN PROTEIN QUANTIFICATION	46
4.5. DIGS ISOLATION	46
4.6. SDS-PAGE AND WESTERN BLOT ANALYSIS	47
4.7. ANTIBODIES USED FOR BRAIN MYELIN WESTERN BLOT ANALYSIS	48
4.8. DENSITOMETRIC QUANTIFICATION OF WESTERN BLOT RESULTS	48
RESULTS	50
1. CHARACTERIZATION OF THE L- AND S-MAG MRNA LEVELS IN OLI-NEU CELLS UPON CYCLICAMP STIMULATION	50
2. MAG-GFP FUSION PROTEINS SHOW NORMAL BIOSYNTHESIS AND MEMBRANE INCORPORATION	51
2.1. L-MAG-GFP: C-TERMINAL GFP	52
2.2. GFP-L- AND GFP-S-MAG: N-TERMINAL GFP	52
2.3. COMPARABLE EXPRESSION PATTERNS OF L-MAG-GFP AND S-MAG-VSVG IN OLI-NEU CELLS	53
3. EXPRESSION OF INDIVIDUALLY TAGGED MAG ISOFORMS FROM GENOMIC EXPRESSION CONSTRUCTS	55
3.1. EXPRESSION OF L- AND S-MAG FROM A GENOMIC MOUSE MAG CLONE IN OLI-NEU CELLS	55
3.2. EXPRESSION OF L-MAG-GFP IN BIPOLAR OLI-NEU CELLS FROM PMAG-MAG-E13GFP	56
3.3. EXPRESSION OF S-MAG-GFP, OR S-MAG-VSVG IN RADIAL OLI-NEU CELLS FROM PMAG-MAG-E12GFP, OR -E12VSVG	58
3.4. SIMULTANEOUS EXPRESSION OF S-MAG-VSVG AND 'SOLUBLE GFP' FROM THE GENOMIC EXPRESSION CONSTRUCT PMAG-MAG-E12VSVG-E13GFP	59
3.4.1. <i>The Protein Expression Pattern of S-MAG-VSVG and L-MAG-GFP within Single Cells</i>	59
3.4.2. <i>L-MAG-GFP and S-MAG-VSVG mRNAs Show Normal Length and Regulation</i>	60
3.5. CONSTITUTIVE EXPRESSION OF L-MAG-GFP FROM THE GENOMIC EXPRESSION CONSTRUCT PMAG-L-MAG-GFP	61
4. GENERATION OF MAG-GFP TRANSGENIC MOUSE LINES	63
4.1. THE PMAG-MAG-E13GFP MOUSE LINE	63
4.2. THE PMAG-MAG-E12GFP MOUSE LINE	64
4.2.1. <i>The pmag-MAG-e12GFP Peripheral Myelin</i>	64
4.2.2. <i>The pmag-MAG-e12GFP Central Myelin</i>	66
4.3. THE PMAG-L-MAG-GFP MOUSE LINE	67
5. MAG BECOMES ASSOCIATED WITH RAFTS IN ADULT CNS MYELIN MEMBRANES	69
5.1. MAG IS NOT RAFT-ASSOCIATED DURING MOUSE CNS MYELIN FORMATION	69
5.2. MAG IS PARTIALLY RAFT-ASSOCIATED IN ADULT MOUSE CNS MYELIN	69
5.3. MAG IS ALMOST EXCLUSIVELY RAFT-ASSOCIATED IN THE ADULT HUMAN BRAIN	70
5.4. MAG-CONTAINING RAFTS IN THE HUMAN CNS ARE MORE RESISTANT TO DETERGENT EXTRACTION USING CHAPS THAN WHEN USING TRITONX-100	72
6. THE INCORPORATION OF MAG AND MBP INTO BRAIN MYELIN MEMBRANES IS DEPENDENT ON MAL	73
6.1. THE MYELIN PROTEIN LEVELS OF MAG AND MBP ARE DECREASED IN 4-MONTH-OLD MAL DEFICIENT MOUSE BRAINS	73
6.2. REDUCED MAG LEVELS IN THE DETERGENT-RESISTANT AND -SOLUBLE FRACTIONS ISOLATED FROM MAL-DEFICIENT MOUSE BRAIN MYELIN	73
6.3. QUANTIFICATION OF THE MYELIN PROTEIN LEVELS IN THE MAL-DEFICIENT MOUSE BRAIN MYELIN AND MYELIN-DIGS	75
6.4. MAG AND PLP PROTEIN LEVELS IN TWO-YEARS-OLD MAL-DEFICIENT MOUSE BRAINS	77
7. MAG AND PLP/DM20 TRANSCRIPTION ARE ALTERED IN THE MAL KNOCK-OUT BRAIN IN A COMPENSATORY MANNER	79
7.1. TOTAL-MAG AND L-MAG MRNA LEVELS ARE INCREASED IN THE ADULT MAL KNOCK-OUT BRAIN	79
7.2. DECREASED PLP/DM20 MRNA LEVELS IN ADULT MAL-DEFICIENT BRAINS	82
7.3. LACK OF EXON 1-CONTAINING MAL TRANSCRIPTS IN MAL KNOCK-OUT BRAINS	83

DISCUSSION84

DIFFERENTIAL EXPRESSION OF L- AND S-MAG IN OLI-NEU CELLS UPON CYCLICAMP TREATMENT84

THE EFFECT OF EXONIC INSERTIONS ON THE ALTERNATIVE SPLICING OF THE MAG PRE-MRNAs.....86

DIFFERENTIAL EXPRESSION OF L- AND S-MAG IN THE ADULT MOUSE BRAIN.....87

RAFT ASSOCIATION OF MAG DURING MYELINATION AND MYELIN MAINTENANCE89

DECREASED MAG AND MBP PROTEIN LEVELS IN THE BRAIN MYELIN FROM MAL DEFICIENT MICE91

OUTLOOK.....96

MAL KNOCK-OUT BRAIN MYELIN: ANALYSIS OF THE MYELIN PROTEIN COMPOSITION AT THE END OF THE MYELINATION PERIOD AND AFTER 2 YEARS OF MYELIN MAINTENANCE.....96

MAG-GFP EXPRESSING MOUSE LINES.....97

REFERENCES.....98

CURRICULUM VITAE108

Acknowledgments

The presented work was performed in the laboratory of Neurobiology at the Department of Research at the University Hospital Basel under the supervision of Dr. Nicole Schaeren-Wiemers and Prof. Andreas J. Steck.

First, I would like to thank Nicole and Prof. Steck for giving me the great opportunity to do my thesis project in their lab. I thank especially Nicole for giving me the opportunity to work independently and to find my own way. Furthermore, I want to thank her for her support in writing the publication, the grant applications and in particular the thesis.

I would like to thank in particular Beat Erne for his great help with stainings and microscopes and for being a really fine colleague during my past four years.

I would further like to thank all the people in the lab for the supporting environment during my thesis. It has been a pleasure to work together with Ursula Graumann, Frances Kern, Marc Sollberger, Thomas Zeis, Raffaella Lombardi, Andres Buser, Ralf Brunner, Nino Sansano, and Fabrizia Ferracin.

A special thanks goes to my collaborators, Prof. Ueli Suter from the ETH Cell Biology Institute in Zürich for the helpful discussions and for the support with mice and to Prof. Klaus Armin Nave from the Department of Neurogenetics, Max-Planck-Institute of Experimental Medicine in Göttingen for the critical reading of the paper and for the support with the MAG clone. Furthermore I would like to thank Dr. Anthony Heape from Oulu University in Finland for the critical reading of my thesis.

Finally, I would like to thank my parents and Corinne for their continuous help and support.

Abbreviations

3'-/5'-UTR	3'-/5'-untranslated mRNA region
aa	amino acids
Ab	antibody
bFGF	basic fibroblast growth factor
bp	base pair
cAMP	cyclic adenosine monophosphate
Caspr	contactin associated protein
cDNA	complementary deoxyribonucleic acid
CGT	ceramide galactosyl transferase
CMT1A	Charcot-Marie-Tooth disease type 1A
CNP	2'-3'-cyclic-nucleotide 3'-phosphodiesterase
CNS	central nervous system
Cx	connexin
DIGs	detergent-insoluble glycolipid-enriched complexes
DM20	small isoform of the proteolipid protein
DNA	deoxyribonucleic acid
ECM	extra cellular matrix
ESE	exon splicing enhancer
F3	F3/contactin
GalC	galactosylceramide
GAPDH	glyceraldehydes-3-phosphate dehydrogenase
GPI	glycosylphosphatidylinositol
HNPP	hereditary neuropathy with liability to pressure palsies
Ig	immunoglobulin G
IPL	intrapaper line
kb	kilo base pairs
kD	kiloDalton
ko	knock-out
L-MAG	large myelin-associated glycoprotein isoform
mAb	monoclonal antibody
MAG	myelin-associated glycoprotein
MAL	myelin and lymphocyte glycoprotein
MDL	major dense line
MBP	myelin basic protein
MOG	myelin oligodendrocyte glycoprotein
mRNA	messenger ribonucleic acid
Ngn	neurogenin
OD	optical density
OLP	oligodendrocyte precursor
P0	myelin protein zero
pAb	polyclonal antibody
PBS	phosphate buffered saline
PCR	polymerase chain reaction
PDGF α	platelet derived growth factor alpha

pH	negative logarithm of hydrogen ion concentrations
PLP	proteolipid protein
PNS	peripheral nervous system
QKI-5	quaking isoform 5 (nuclear factor)
RLR	RNA localization region
RT	room temperature
RTS	RNA transport sequence
RT-PCR	reverse transcriptase polymerase chain reaction
SC	Schwann cell
S-MAG	short myelin-associated glycoprotein isoform
Wt	wild-type

Summary

Many degenerative diseases of the nervous system, including Multiple Sclerosis and peripheral neuropathies, are triggered by an impaired interaction between the axons and their surrounding myelin sheaths. The cause for this disturbed axon-myelin interaction, and the secondary neuronal damage that produces the clinical symptoms, lies in a primary defect of the myelin sheath. The myelin sheath itself is formed and maintained by oligodendrocytes and Schwann cells, the myelinating glial cells of the central and peripheral nervous system, respectively.

The isoforms of the myelin-associated glycoprotein (MAG) are thought to be potential key elements of axon-myelin interaction, since these immunoglobulin-like cell signalling proteins are known to be localized in the periaxonal and paranodal myelin membranes. The MAG isoforms each display one of two possible intracellular C-termini as a result of alternative mRNA splicing. The C-terminus of the large isoform (L-MAG) has been shown to mediate downstream signals *via* the non-receptor tyrosine kinase Fyn, while the C-terminus of the short isoform (S-MAG) is thought to interact with the glial cytoskeleton.

We have investigated the regulation and differential expression of L- and S-MAG in oligodendroglial cells and in transgenic mice by the use of genomic constructs that encode individually green fluorescent protein-tagged MAG isoforms. In the oligodendroglial cells L-MAG was the dominant isoform prior to the stimulation of cells with cyclicAMP, whereas upon cyclicAMP stimulation, S-MAG was predominantly expressed in cells exhibiting advanced morphological differentiation. The investigation of our transgenic mice revealed that the two MAG isoforms are differentially expressed in distinct fibre tracts of the striatum and that S-MAG seems to be predominantly expressed in the long projecting fibres of the corpus callosum. Thus, the two MAG isoforms appear not only to be differentially expressed during development and in the adult, but they seem to mediate isoform-specific aspects of the axon-myelin interaction in distinct regions of the adult brain.

A major question in the formation and maintenance of the myelin-axon interaction concerns the coordinated targeting of myelin signalling molecules and lipids to the different myelin compartments. Recent results suggest that glycolipid-enriched microdomains, so-called 'lipid-rafts', are involved in special sorting and trafficking mechanisms of membrane proteins and lipids. Furthermore, they are thought to serve as platforms for signal transduction processes. This makes them to interesting candidates for axon-myelin interactions, as well as for interactions between the apposed myelin membranes. The integral membrane protein 'Myelin and Lymphocyte Protein' (MAL) is suggested to be involved in lipid-raft-mediated protein targeting and signalling in myelinating cells. Our investigation of adult brain tissue of MAL-deficient mice showed that the incorporation of particular myelin components, such as MAG, into myelin membranes was significantly reduced. Thus, the targeting of L- and S-MAG to the myelin membranes appears to be dependent on the lipid-raft protein MAL. Furthermore, the MAL-deficient mice showed several ultra structural alterations comparable to those of the MAG-deficient mice and that reflect an impaired axon-myelin interaction.

Our data supports the idea that-raft mediated trafficking of myelin constituents, such as MAG, to the different myelin compartments is a major task of adult oligodendrocytes in the context of maintaining the axonal contact of the myelin sheath.

With the use of the isoform specific tagged MAG expressing mice, it will be possible for the first time, to investigate their differential function in axon-glia interaction as well as their

dependence on MAL *in vivo*.

Introduction

1. Myelin

The myelin sheath is a unique and fundamental adaptation of both the central and peripheral nervous system (CNS and PNS) of vertebrates. The myelin sheath forms as a myelinating cell wraps layer upon layer of its own plasma membrane around an axon in a tight spiral, forming an electrically insulating sheath (Figure 1). This insulation is needed for rapid and efficient nerve impulse conduction along myelinated axons, known as saltatory conduction. The direct advantage of the saltatory conduction due to myelination is to increase the speed of conduction without requiring large increases in axon diameter and energy consumption. The myelin membrane sheaths are arranged as segments along the axon and are periodically separated by the non-myelinated nodes of Ranvier. It is within these restricted nodal sites that voltage-gated sodium-channels aggregate and the electrical activity of fibres are processed (for details, see Figures 3,4,5). However, the requirements for the myelin sheath are twofold, which is reflected by its architecture. On the one hand, almost all electrically conductive cytoplasm needs to be excluded from the myelin sheath for its insulating properties. On the other hand, access to all membranes within the sheath must be possible to maintain and nourish the whole structure. Therefore, non-compact myelin domains are found within the continuous myelin internodes.

The formation of myelin sheaths around large-calibre axons requires the coordinate interplay of distinct axonal and glial cell surface molecules. This complex and developmentally regulated process includes the coordinated expression of genes encoding myelin proteins and enzymes associated with the synthesis of myelin specific lipids (for review, see Garbay et al. 2000). The myelinating glial cells differ between the CNS and the PNS. The CNS myelin is produced by oligodendrocytes, whereas Schwann cells myelinate axons in the PNS. During development, both cells synthesize as much as 5000 μm^2 of myelin membrane per day, which they wrap tightly around the axon (Pfeiffer et al. 1993). Within the future compact myelin domains all cytoplasm gets excluded from the myelin spirals, resulting in the close apposition of both the intracellular and extracellular leaflets of the plasma membranes. These electron-dense structures are called major dense line (MDL) and intraperiod line (IPL), respectively (Figure 1).

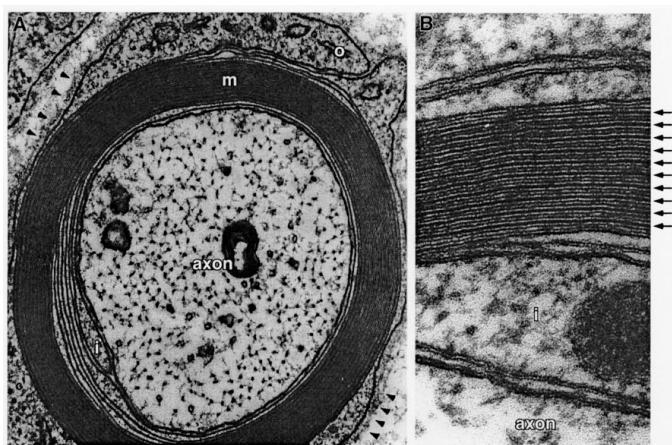


Figure 1 Ultrastructure of a PNS Myelinated Fibre

A This electron micrograph shows an axon, its myelin sheath (m), and basal lamina (arrowheads), as well as the inner (i) and outer (o) mesaxons.

B This image shows that the compact myelin sheath is composed of alternating major dense (arrows) and intraperiod lines. Note the “double nature” of the intraperiod line (Revel and Hamilton 1969).

One of the major biochemical characteristics that distinguish myelin from other biological membranes is its high lipid-to-protein ratio: isolated myelin contains 70-80% lipids and

20-30% proteins. This relatively high lipid content, and the particular characteristics of the lipids present in the sheath, provides the electrically insulating property required for the saltatory propagation of the nervous influx.

The inherited, or acquired failures of myelinating cells to form, or maintain the myelin sheath correctly results in severe neurological diseases, such as Multiple Sclerosis and demyelinating peripheral neuropathies (for review, see Garbay et al. 2000).

2. Myelinating Cells of the Central and Peripheral Nervous System

2.1. Schwann Cells

The Schwann cell precursor cells originate from the neural crest and, while they migrate into the periphery along the axonal tracts, they give rise to immature Schwann cells (Cameron-Curry et al. 1991). Their fate is tightly controlled by axonal signals, e.g. by \square neuregulin acting *via* the ErbB2/ErbB3 receptors and by fibroblast growth factor 2 (FGF2; Dong et al. 1999). On the one hand, immature Schwann cells can develop into pro-myelinating Schwann cells. The pro-myelinating Schwann cells form a 1:1 relationship with the large-calibre axons prior to myelination. This step is probably controlled by ATP, that acts as an activity-dependent axon-glia transmitter to inhibit Schwann cell proliferation, differentiation, and myelination (Fields and Stevens 2000). This inhibitory mechanism may help to coordinate Schwann cell development with the onset of functional activity in the nervous system and prevent premature Schwann cell differentiation (Fields and Stevens 2000). On the other hand, immature Schwann cells can develop into non-myelinating Schwann cells. Each non-myelinating Schwann cell ensheathes bundles of 5-30 axons (Friede and Samorajski 1968). Both types of Schwann cells, myelinating and non-myelinating, are surrounded by a basal lamina (Figure 1), which separates them from other components of the endoneurium in the peripheral nerve and anchors them to the extracellular matrix (Bunge 1993).

2.2. Oligodendrocytes

Oligodendrocyte precursor cells arise from neuroepithelial cells in the ventral spinal cord that generate both neurons and oligodendrocytes (Kessaris et al. 2001). These neuroepithelial cells of the subventricular zone are characterized by the expression of the transcription factor Olig2. They do first generate motor neurons, whereas later in development, they generate oligodendrocyte precursor cells (Zhou et al. 2001; Zhou and Anderson 2002). The combined expression of the transcription factors Olig2 and neurogenin-1 and -2 are thought to generate motor neurons (Figure 2, left). However, towards the end of spinal cord motor neuron induction, the expression of neurogenins is down-regulated (Zhou et al. 2001). This allows the overlapping expression of Olig1 and Olig2 and of the previously more ventrally expressed transcription factor Nkx2.2 (Figure 2, right), resulting in the generation of oligodendrocyte precursor cells (Zhou et al. 2001). In the absence of both Olig1 and Olig2, the cells that would normally give rise to motor

neurons and oligodendrocytes generate a specific class of interneurons and astrocytes (Zhou and Anderson 2002).

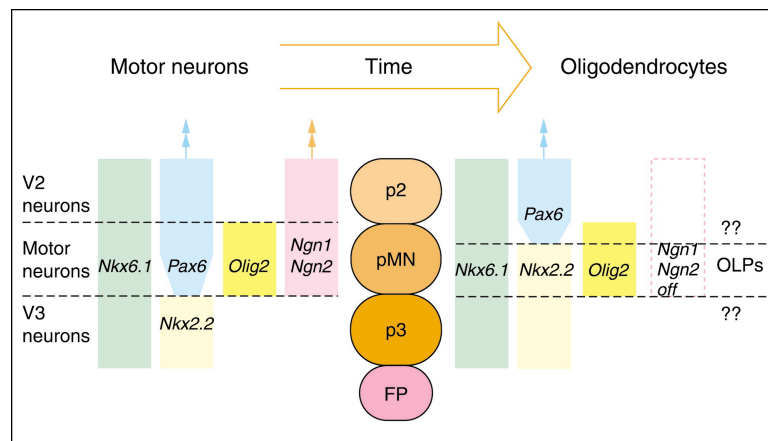


Figure 2 The Neuron-Oligodendrocyte Fate Switch in Chick Spinal Cord

At early times (E3–E5 chick), motor neurons are generated from the pMN domain under the influence of Olig2 in conjunction with Ngns. Later (E6–E7), Ngn1 and Ngn2 (neurogulin) are down-regulated in this part of the cord. Subsequently, the expression domains of Nkx2.2 and Olig2 shift relative to one another and generate a region of overlap. This triggers a switch in the activity of Olig2 in the overlap, which now generates oligodendrocyte progenitors (OLPs; according to Kessaris et al. 2001); FP: floor plate; pMN: motor neuron progenitor domain; p2,p3: V2 and V3 interneuron progenitor domain; Ngn,Olig: basic-helix-loop-helix transcription factors; Nkx,pax: homeodomain transcription factors.

Once committed to the oligodendrocyte lineage, precursors express cell surface antigens recognized by the monoclonal antibody A2B5 (Raff et al. 1984). *In vitro*, these cells have the capacity to give rise to both oligodendrocytes and astrocytes and have thus been termed oligodendrocyte-type-2 astrocyte (O-2A) progenitor cells (Raff et al. 1984). The combination of platelet-derived growth factor alpha (PDGF-A) and basic FGF (bFGF) promotes the extended proliferation of oligodendrocyte precursors (Bogler et al. 1990). These proliferating oligodendrocyte precursors can be identified through the expression of the PDGF receptor alpha (PDGF-RA; Pringle et al. 1992; Pringle and Richardson 1993), the expression of several myelin-associated components, including mRNA for the myelin genes 2',3'-cyclic-nucleotide 3'-phosphodiesterase (CNP), the DM20 isoform of the major myelin proteolipid protein (PLP) gene (Timsit et al. 1995), and the sulphated galactosylceramide (sulfatide) that is recognized by the monoclonal antibody O4 (Sommer and Schachner 1981). Further differentiation of oligodendrocyte precursors is characterized by a withdrawal from the cell cycle and expression of the major myelin glycolipid galactosylceramide (GalC; Raff et al. 1978). Promyelinating oligodendrocytes exhibit a multi-processed phenotype and their maturation results in the coordinated elevated expression of a number of major myelin components, such as myelin basic protein (MBP) and proteolipid protein (PLP; Roth et al. 1985; Lemke 1988).

A recent report identified adenosine as a novel antiproliferative and differentiating factor for oligodendrocyte precursor cells, which is derived from axons and promotes myelination in an activity-dependent manner. This axon-glial signalling mechanism provides a potent form of communication, coordinating oligodendrocyte proliferation, differentiation and myelination in response to action potentials in axons (Stevens et al. 2002).

Early silver impregnation studies identified four distinct morphologies of myelinating oligodendrocytes, and this was largely confirmed by ultra structural analyses in a variety of species (Stensaas and Stensaas 1968; Remahl and Hildebrand 1990). Oligodendrocyte

morphology is closely correlated to the diameter of the axons with which the cell associates (Butt et al. 1997, 1998a). Oligodendrocyte types I and II arise late in development and myelinate many internodes on predominantly small diameter axons, while oligodendrocyte types III and IV arise later and myelinate mainly large diameter axons. Oligodendrocytes that myelinate small diameter fibres (types I and II) express higher levels of carbonic anhydrase 11 (CA11; Butt et al. 1995; Butt et al. 1998a), while those myelinating larger axons (types III and IV) express the small isoform of the myelin-associated glycoprotein (S-MAG; Butt et al. 1998b). Whether such differences represent the response of homogeneous cell populations to different environments, or the existence of distinct cell lineages is unclear.

2.2.1. The Mouse Oligodendrocyte Cell Line Oli-neu

The cell line Oli-neu was generated by immortalisation of mitotic oligodendrocyte precursor cells with retroviral vectors containing the t-neu oncogene (Jung et al. 1995). *In vitro* and *in vivo* studies showed that the mouse oligodendrocyte cell line Oli-neu mimics the behaviour of primary oligodendrocytes in many aspects (Jung et al. 1995; Koch et al. 1997; Kramer et al. 1997; Kramer et al. 1999; Klein et al. 2002). Oli-neu cells express the typical myelin lipids, GalC and sulfatide (Jung et al. 1995), and have been shown to express the GPI-anchored proteins, F3/contactin and NCAM120 (Koch et al. 1997), and the microtubule associated proteins Tau-1 and Tau-5 (Klein et al. 2002), in a manner similar to that observed in primary oligodendrocytes. The interactions of Tau and the non-receptor kinase Fyn with tubulin have been shown to be responsible for process outgrowth in Oli-neu cells (Klein et al. 2002). Transplantation experiments into demyelinated CNS lesions showed that Oli-neu cells do express the components necessary for axonal interaction (Jung et al. 1995). Oli-neu cells grown in SATO medium proliferate and most of them have a bipolar shape. Under the influence of cAMP, Oli-neu cells stop their proliferation and develop a radial morphology with many processes. In parallel with their morphological maturation, they also up-regulate the expression of MAG (Jung et al. 1995).

3. Organization of the Myelin Sheath

3.1. Architecture of the Peripheral Nervous System Myelin Sheath

The PNS myelin sheath itself can be divided into two domains, compact and non-compact myelin (Figure 3). Compact myelin forms the bulk of the myelin sheath. Non-compact myelin is found at the lateral borders of the myelin sheath that flank the nodes of Ranvier (□ paranodal loops), in funnel-shaped interruptions in the compact myelin (□ Schmidt-Lanterman incisures), and in the inner and outer membranes of the myelin sheath (□ periaxonal and abaxonal membranes, respectively; see Figure 3 and for review Arroyo and Scherer 2000). One Schmidt-Lanterman incisure, that can be seen in a cross-section as a ring-like structure and in a longitudinal section as a V-shaped structure (Figure 3), is in fact a single spiral-shaped domain of Schwann cell cytoplasm that runs through the myelin sheath.

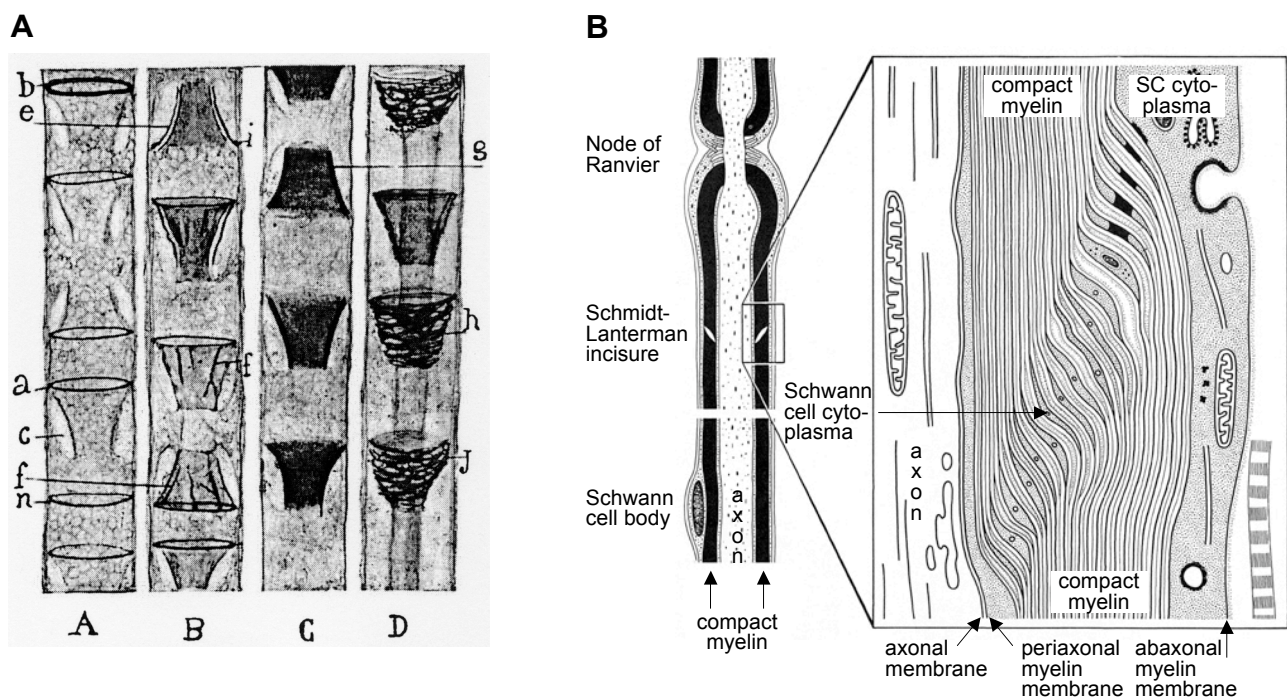


Figure 3 Schmidt-Lanterman incisures of the peripheral myelin sheath

A: Ramon y Cajal's depiction of incisures from 1928. B: Scheme of an incisure within a myelin sheath with an enlarged view of the incisure itself. The incisure represents a single, spiral-shaped domain of Schwann cell cytoplasm within the compact myelin sheath. The inner leaflets of the myelin membranes are separated by the cytoplasm, whereas the outer leaflets are still apposing each other, as in the compact myelin. SC: Schwann cell.

By analogy with epithelial cells, the basal/abaxonal surface of the PNS myelin sheath apposes the Schwann cell basal lamina (Figure 1, 4). This basal lamina contains laminin 2, type IV collagens, fibronectin, N-syndecan, and glypican (Bunge 1993; Scherer 1996). The underlying basal/abaxonal Schwann cell membrane contains integrin $\alpha 6 \beta 4$ and dystroglycan, both of which probably bind to laminin 2 (Einheber et al. 1993; Feltri et al. 1994; Rambukkana et al. 1998; Saito et al. 1999). The apical/adaxonal, or periaxonal, myelin membrane apposes the axon and is highly enriched in myelin-associated

glycoprotein (MAG), which may bind to molecules on the axonal surface (Yang et al. 1996; Sawada et al. 1999). The lateral borders of the Schwann cell membrane define the paranodes (Figure 5). The inner and outer edges of the Schwann cell membrane, which contact the adjacent layer of the myelin sheath, are called the inner and outer mesaxons, respectively. Adherens junctions (“desmosome-like” junctions) are found in both the inner and outer mesaxons as well as in paranodes and incisures (Fannon et al. 1995). The adherens junctions in the paranodes and incisures form a series of radially arranged junctions; these typically span many layers and are most prominent in the outer layers of the myelin sheath. Gap junctions were occasionally noted between the rows of adherens junctions (Yasargil et al. 1982). The gap junction protein connexin32 is localized to the same places (Bergoffen et al. 1993; Scherer et al. 1995; Chandross et al. 1996). Dye transfer studies demonstrated a radial pathway of dye diffusion across incisures, from the outer/abaxonal to the inner/adaxonal cytoplasm (Balice-Gordon et al. 1998). These findings provide functional evidence that gap junctions mediate a radial pathway of diffusion across incisures and, by extension, across the paranodes too. Such a radial pathway for diffusion could be about 3 million times faster than diffusion through the cytoplasm.

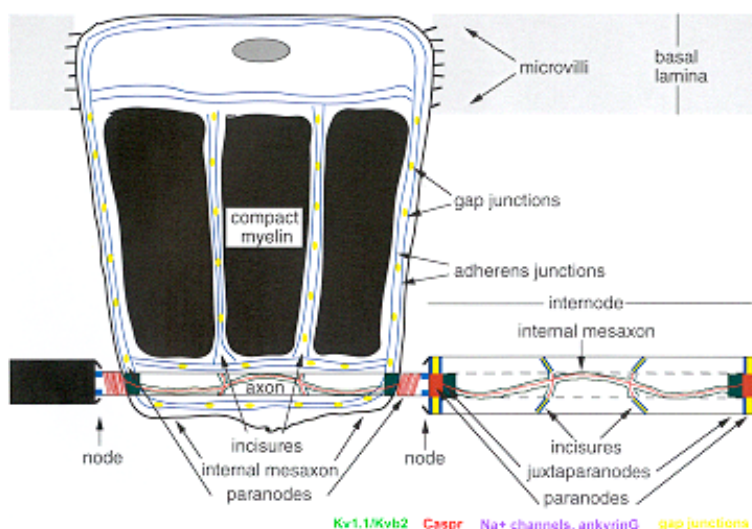


Figure 4 Schematic view of a myelinated axon in the PNS

One myelinating Schwann cell has been 'unrolled', revealing the regions that form the non-compact myelin, the incisures and paranodes. Adherens junctions are depicted as two continuous (purple) lines; these form a circumferential belt and are also found in incisures. Gap junctions are depicted as (orange) ovals; these are found between the rows of adherens junctions. The nodal, paranodal and juxtapanodal regions of the axonal membrane are colored blue, red and green, respectively (Arroyo et al., 2000).

The lateral borders of the Schwann cell processes are tipped with microvilli (Figure 4,5). These tips of the microvilli contact the nodal axolemma (Raine 1982; Ichimura and Ellisman 1991) and contain F-actin (Trapp et al. 1989), voltage-sensitive Na^+ channels (Howe and Ritchie 1990; Devor et al. 1993) and inwardly rectifying K^+ channels IRK1 and IRK3, which may allow them to accumulate K^+ during axonal activity (Mi et al. 1999).

3.2. Architecture of the Central Nervous System Myelin Sheath

Oligodendrocytes have neither a basal lamina nor microvilli like Schwann cells, and their “incisures” (Peters et al. 1991) have not distinguishing molecular markers, such as Cx32, MAG, or E-cadherin. “Perinodal astrocytes” contact CNS nodes (Black and Waxman 1988), and are thought to have a function analogous to Schwann cell microvilli (Figure 5). The molecular components of the CNS myelin sheaths partially overlap with those of the

PNS (Hudson 1990). Thus, in both the CNS and the PNS, compact myelin contains MBP and the adaxonal surface contains MAG (Trapp 1990). Like myelinating Schwann cells, oligodendrocytes also express Cx32, but mainly on their cell bodies and proximal processes; whether there is Cx32 in the paranodal myelin is not settled (Scherer et al. 1995; Kunzelmann et al. 1997). Unlike myelinating Schwann cells, oligodendrocytes express Cx45 and are coupled to other oligodendrocytes as well as astrocytes (Dermietzel et al. 1997; Kunzelmann et al. 1997). CNS myelin has a distinctive structural feature that is not seen in PNS myelin, the so-called “radial component” (Peters et al. 1991). The radial component is a series of radially arranged intralamellar strands that span the myelin sheath, usually in a single sector. These intralamellar strands look like tight junctions, and have recently been shown to contain claudin-11/oligodendrocyte-specific protein (OSP), a member of a large family of distantly related tight junction proteins (Morita et al. 1999; Bronstein et al. 2000). The functional significance of the radial component is so far unknown.

3.3. The Node of Ranvier and the Paranode

The first event in node formation is the clustering of axonal adhesion proteins, such as NrCAM and NF186. In the peripheral nervous system, this initial event is probably triggered by direct contact with the Schwann cell microvilli. In the central nervous system, this event might be controlled by a soluble factor released by the oligodendrocytes. In the peripheral and the central nervous systems, the next event is the recruitment of ankyrin G, with its multiple protein-binding sites that allow the clustering of Na⁺ channels with NrCAM and NF186 (Figure 5). The presence of α IV spectrin is a critical factor for the stability of these newly formed clusters. Heminodal clusters can form in contact with one myelinating cell and, as wrapping of the myelinating cell proceeds, be pushed towards the neighbouring heminode until they fuse to form a complete node (Vabnick et al. 1996; Rasband and Shrager 2000). While the periaxonal extension of the myelinating cell rolls around the axon and compact myelin is formed, the lateral loops of the myelinating cells become progressively compacted in a lateral direction, forming the paranodal region (Pedraza et al. 2001). In the paranodal region, the glial cell plasma membranes abruptly open out from compact myelin, creating cytoplasm-filled channels termed paranodal loops. The loops are held in register with one another at least in part through adherens junctions and MAG (Figure 5; Bartsch et al. 1989; Fannon et al. 1995; Rosenbluth et al. 1995). At this time, septate-like junctions that connect the glial paranodal loops with the apposing axonal membrane are formed in the paranodal region. The characterization of the molecular organization of the paranodal septate-like junctions started to emerge only in the past few years with the discovery of the axonal heterodimeric complex of F3/contactin and contactin-associated protein (Caspr; Einheber et al. 1997). Caspr is a neuronal transmembrane protein, highly concentrated in paranodal junctions. It has a large extracellular region, a single transmembrane segment, and a short intracellular region. On the extracellular side, Caspr was found to associate with F3/contactin. F3/contactin is a glycosylphosphatidylinositol (GPI)-anchored cell adhesion molecule of the Ig superfamily. An essential role in the targeting of Caspr to the plasma membrane has been recently demonstrated for F3/contactin. In the absence of F3/contactin, Caspr remains trapped in the endoplasmic reticulum (Faivre-Sarrailh et al. 2000).

F3/contactin associates with Caspr by its Ig domain and appears to guide it to the cell surface *via* the lipid-rafts (Boyle et al. 2001). In the absence of F3/contactin, Caspr remains associated with the endoplasmic reticulum and fails to accumulate at paranodes. These F3/contactin-Caspr complexes are connected to the axonal cytoskeleton through a meshwork that probably includes protein 4.1B.

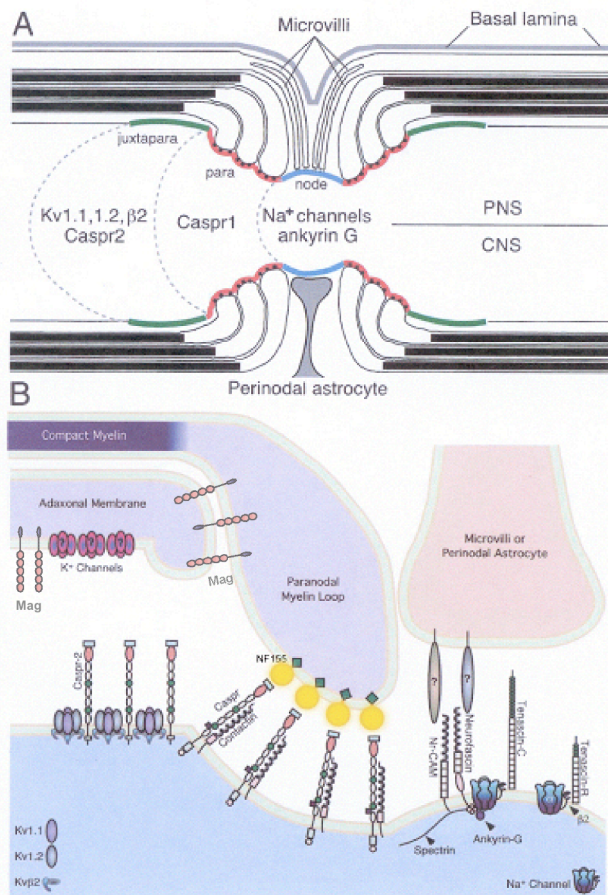


Figure 5 Scheme of the node of Ranvier

A: Schematic drawing showing the different compartments of the node, paranode, and juxtaparanode in CNS and PNS. Compact myelin is characterized by the absence of cytoplasm and extracellular fluid (black bars).

B: Schematic drawing of possible myelin-axon and myelin-myelin membrane interactions between the molecular components of nodes, paranodes and juxtaparanodes (copied and modified from Arroyo and Scherer, 2000)

The glial binding partner of the axonal F3/contactin-Caspr complex has been discovered only recently with the identification of the 155-kDa isoform of neurofascin (NF155; Tait et al. 2000; Charles et al. 2002). NF155 is a member of the L1 subgroup of the Ig superfamily and has been identified as a glial molecule enriched at the level of paranodal junctions, thus facing the F3/contactin-Caspr complex (Figure 5B; Tait et al. 2000). Recent *in vitro* studies have shown that NF155 binds specifically to the F3/contactin-Caspr complex (Charles et al. 2002). While the extracellular domain of Caspr might be simultaneously engaged in association with neuronal proteins (in cis) and partners expressed by the glial cell (in trans), its intracellular region connects it to the axonal cytoskeleton, perhaps stabilizing the complex and bringing it into close proximity with the signalling machinery. This role is underscored by the results in the Caspr knock-out mouse whose disorganized paranodes are characterized by the absence of the “transverse bands” (paranodal septate-like junctions) linking the axolemma to the glial membrane (Bhat et al. 2001). The enrichment of Caspr in paranodes is a relatively late event in myelination and the myelinating glial cells are required for the paranodal localization of Caspr, since in the ceramide-galactosyl-transferase (CGT) mutants, Caspr fails to accumulate at paranodes (Dupree et al. 1999).

Taken together, the paranodal axon-glial junction, which is a point of strong interaction of

myelinating glial cells with the underlying axon, has several important roles: it provides partial electrical insulation to the internodal region, allowing saltatory conduction of the nerve impulses; it restricts the lateral mobility of axonal membrane proteins, including ion channels; and it is likely to contribute to bi-directional signalling between axons and glial cells. The paranodal junctions appear to play important roles in the process of myelination and represent a site of early damage in several neuropathies and dysmyelinating disorders (Griffiths 1996).

4. The Myelin Proteins

Myelin formation involves complex interactions between at least two cell types, the neurons and the myelinating cells. Axonal contact and other environmental stimuli, such as matrix molecules and growth factors, induce oligodendrocyte precursor and Schwann cell proliferation (Salzer et al. 1980). In proliferating cells, certain myelin proteins may be expressed at low levels, but stable glial-axonal contact appears to be essential for the up-regulation of myelin-specific genes that accompanies myelin formation. Molecules that have been implicated in adhesion, or recognition, such as MAG, N-cadherin (Blank et al. 1974) and neural adhesion molecule L1 (Seilheimer et al. 1989; Letourneau et al. 1991), seem to participate in the earliest phases of myelination, where they assist in establishing glial-axonal contact and induce the expression of other myelin-specific genes. These genes encode proteins that play a role in the formation of the spiralling loops e.g. MAG, protein zero (P0), in the subsequent compaction of the myelin sheath e.g. P0, myelin basic protein (MBP) and proteolipid protein (PLP), in the determination of the correct myelin thickness e.g. P0, MBP, peripheral myelin protein 22 (PMP22), and in the maintenance of the myelin sheath e.g. MAG, P0, PMP22 and Connexin 32 (Cx32; see Figure 6 for a schematic representation of some compact and non-compact myelin proteins).

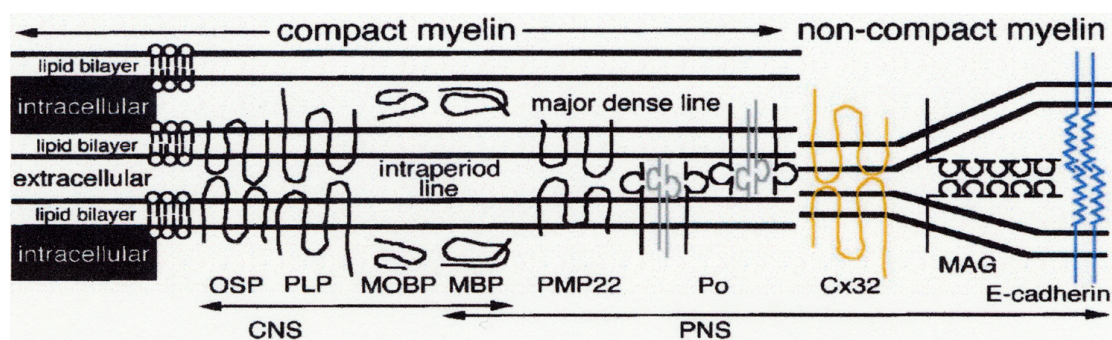


Figure 6 Schematic view of the proteins of CNS and PNS myelin sheaths

CNS and PNS myelin sheaths contain distinct sets of proteins. In the PNS, compact myelin contains protein zero (P0), peripheral myelin protein 22 kDa (PMP22), and myelin basic protein (MBP); in the CNS, it contains proteolipid protein (PLP), oligodendrocyte-specific protein (OSP), myelin-oligodendrocyte basic protein, and MBP. In the PNS, the non-compact myelin contains E-cadherin, myelin-associated glycoprotein (MAG), and connexin32 (Cx32). Note that P0 and MAG have extracellular immunoglobulin-like domains (semicircles), and OSP, PLP, PMP22 and Cx32 all have four transmembrane domains (reproduced from Arroyo and Scherer, 2000).

However, myelin-related cell surface molecules can play distinct, but also partially overlapping roles, during myelin formation and maintenance (for review, see Doyle and Colman 1993; Martini and Schachner 1997). The myelin and lymphocyte protein (MAL) does not belong to the cell surface or structural molecules of the myelin sheath, but is thought to be involved in lipid-raft-associated protein trafficking (Alonso and Weissman 1987; Schaeren-Wiemers et al. 1995b).

4.1. Myelin-Associated Glycoprotein - MAG

One cell adhesion protein that is expressed during myelin formation upon first contact with the axons is MAG (Quarles 1983). In the mature myelin sheath, MAG is restricted to the non-compacted regions, including the periaxonal location (Figure 7), suggesting a role for MAG in maintaining the interaction between the myelinating cell and the axon (Sternberger et al. 1979).

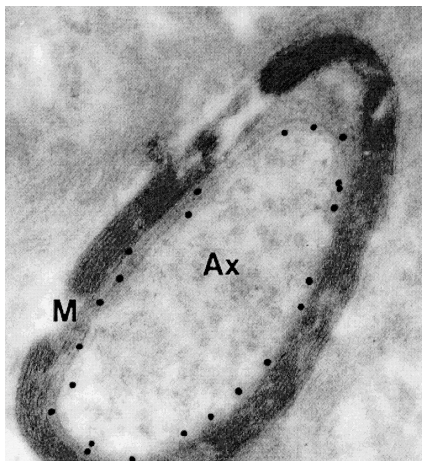


Figure 7 Ultrastructural location of MAG in the mouse optic nerve. When compact myelin (M) has formed, expression of MAG becomes restricted to the periaxonal space. Primary anti-MAG antibodies have been visualized with gold-conjugated secondary antibodies. Ax: axon; M: myelin sheath (reproduced from Bartsch et al., 1989).

The MAG protein is expressed as two isoforms: large MAG (L-MAG) and small MAG (S-MAG). They have identical extracellular and transmembrane domains and share a common sequence of 37 amino acids adjacent to the inner surface of the plasma membrane. But they differ at the C-terminal tails (Figure 8; Lai et al. 1987). The S-MAG specific C-terminal tail consists of 9 amino acids, resulting in a 46-amino-acid intracellular domain. The L-MAG specific C-terminal tail consists of 53 amino acids, resulting in a 90-amino-acid intracellular domain. The two isoforms are generated through the alternative splicing of exon 12. Exon 12 is the only alternatively spliced exon within the coding region. It encodes the S-MAG specific C-terminal tail, while the proceeding exon 13 encodes the L-MAG specific C-terminal tail (Miescher et al. 1997). Very recently, it could be shown that the nuclear localized quaking isoform 5 (QKI-5) directly represses alternative splicing of MAG pre-mRNA that is necessary for the formation of L-MAG (Wu et al. 2002). The natural occurring quaking mouse mutant lacks the QKI-5 nuclear factor and, therefore, does not express L-MAG.

The two isoforms are differentially expressed during myelin formation and maintenance. Early in the myelination process, the expression of L-MAG predominates, whereas S-MAG accumulates at later stages and in the adult. L-MAG is expressed in the adult CNS, but not in adult PNS myelin (Inuzuka et al. 1991). The cytoplasmic tail of L-MAG contains a

tyrosine phosphorylation site, suggesting a role in the regulation of L-MAG function (Jaramillo et al. 1994). Furthermore, the non-receptor tyrosine kinase Fyn, a member of the Src family, has been identified as a signalling molecule downstream of L-MAG. The analysis of the CNS of Fyn-deficient mice revealed a 50% reduction in the amount of myelin (Umemori et al. 1994). Beside Fyn, the calcium binding protein S100 β and the phospholipase C β have been shown to be isoform specific binding partners of L-MAG (Jaramillo et al. 1994; Kursula et al. 1999). Therefore, L-MAG seems to have, besides the properties of a cell adhesion molecule, characteristics of a transmembrane receptor that could transduce extracellular signals to the inside of oligodendrocytes and Schwann cells. The S-MAG specific domain has been reported to bind to tubulin and microtubules, supporting a role for S-MAG as a cell adhesion molecule linking the axonal surface and the myelinating glial cell cytoskeleton (Kursula et al. 2001).

The extracellular domain of MAG has eight sites for N-linked glycosylation and contains about 30% by weight carbohydrate (Spagnol et al. 1989; Burger et al. 1993). The oligosaccharides are very heterogeneous. Most are of the complex type and negatively charged, due to sialic acid and/or sulfate, and many are bisected by GalNAc. Like P0 and PMP22, MAG contains in many species the adhesion-related HNK-1 carbohydrate epitope (Bajt et al. 1990).

A very important, unanswered question about MAG concerns the identity of the putative axonal binding-partner(s). An important clue about its identity emerged from the determination that MAG is in a subgroup of the Ig superfamily, whose members exhibit high homology in the first two amino-terminal V and C2 type Ig-like domains and bind to sialic acid-containing oligosaccharides (Crocker et al. 1998). This is the 'siglec' family for 'sialic acid-binding immunoglobulin-like lectins', and members differ in their affinity for different sialyloligosaccharides, depending on the carbohydrate configurations. There are now at least 10 members of this family, including sialoadhesin, CD22 and CD33, most of which are expressed primarily on cells of the immune system (Crocker 2002). MAG (Siglec-4a) was reported to bind best to oligosaccharides with α 2,3-linked sialic acid (2,3-SA) on a core structure of Gal β 1-3GalNAc (Kelm et al. 1994). As such, MAG showed a preference for binding to O-linked oligosaccharides on glycoproteins and to some gangliosides, such as the major GD1a and GT1b brain gangliosides (Kelm et al. 1994; Yang et al. 1996). However, an investigation of glycoproteins in a neuroblastoma cell line that bound to MAG demonstrated that most binding was to N-linked oligosaccharides with terminal 2,3-SA, so the reported specificity for glycoproteins with O-linked oligosaccharides is not absolute (Strengel et al. 1999). However, the fact that MAG binds to oligosaccharides on both glycoproteins and gangliosides indicates that there are likely to be several binding partners on the axolemma. A particularly interesting aspect of this argument is that mice engineered to lack complex gangliosides exhibit some of the same abnormalities of myelinated axons as MAG-null mice (Sheikh et al. 1999). Recently, a novel glycosylated form of microtubule-associated protein 1B (MAP1B) expressed at the surface of axonal membranes, was identified as a binding partner of MAG (Franzen et al. 2001), which could be relevant to the effects of MAG on the microtubular cytoskeleton and stability of myelinated axons.

In 2002, several reports appeared implicating GD1a and GT1b gangliosides and/or a GT1b/neurotrophin receptor p75 complex as functional MAG-binding partners involved in the inhibition of neurite outgrowth (Figure 8; Vyas et al. 2002; Yamashita et al. 2002). However, another very recent paper reported that MAG inhibits neurite outgrowth by acting as an additional ligand for the Nogo receptor (Figure 8; Domeniconi et al. 2002).

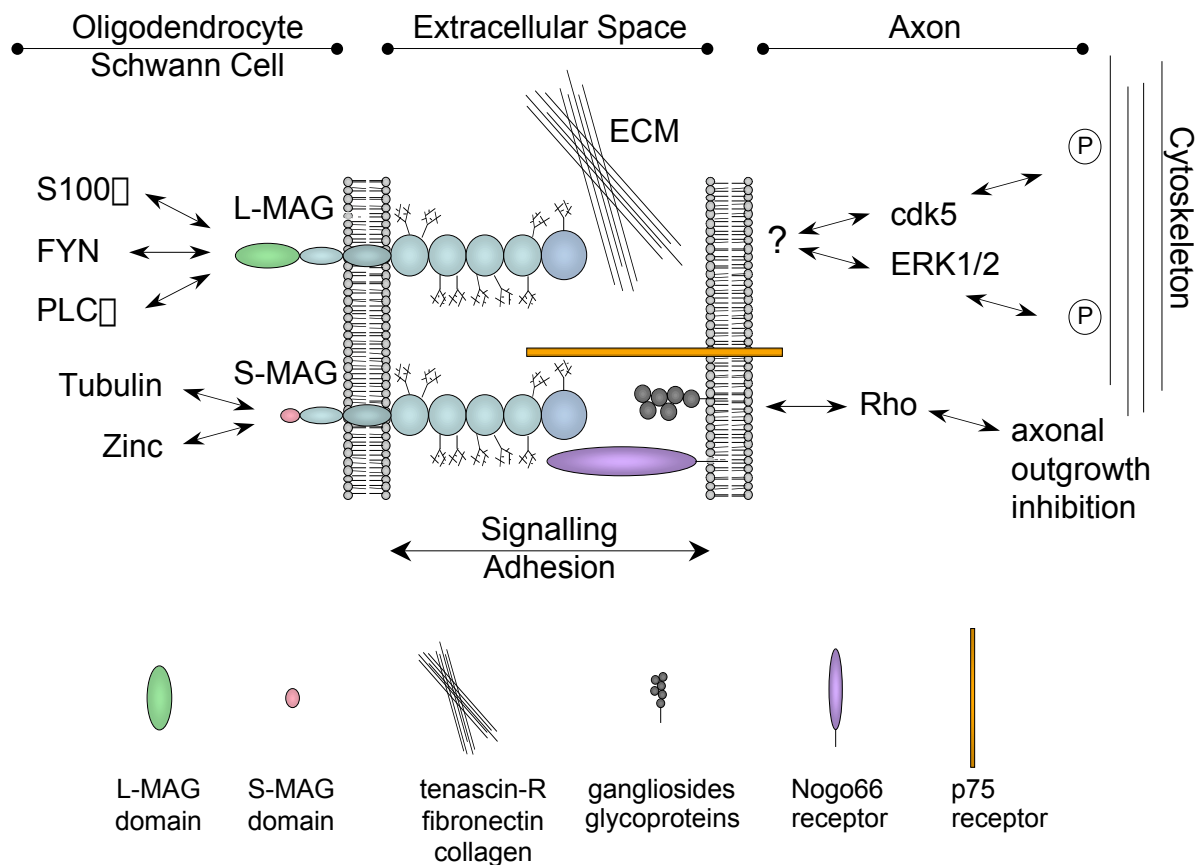


Figure 8 Schematic summary of the mechanisms by which MAG may mediate interactions and signaling between myelin-forming cells and axons.

The extracellular domain of MAG mediates axon-glia interactions by binding to an unknown component on the axonal surface membrane. Because MAG has lectin properties and binds to oligosaccharides with 2,3-SA, its axonal binding partner is likely to be a ganglioside or a glycoprotein. In the PNS, the primary role of MAG in the Schwann cell periaxonal membrane appears to be as a ligand that binds to an axonal receptor, which activates a signal transduction cascade that is necessary for the normal maintenance of myelinated axons. The signaling causes increased phosphorylation of neurofilaments by cdk5 and ERK 1/2, leading to greater axonal caliber. In the CNS, the most important signaling appears to be in the reverse direction with MAG acting as a receptor to enhance the vitality of oligodendrocytes and their capacity to form and maintain myelin. The different C-termini of the L and S isoforms of MAG are shown in green and red, respectively, and may interact selectively with the various glial components shown as part of MAG's function.

Binding of MAG to the ganglioside GT1b on neuronal cells results in p75 dependent activation of Rho, leading to inhibition of neurite outgrowth. MAG can also bind the Nogo receptor in a sialic-acid-independent manner and is functionally important in MAG-dependent neurite inhibition.

The binding partners discussed above are those on neuronal membranes that could interact with MAG in the periaxonal glial membranes, but MAG localized in mesaxons, loops and incisures of Schwann cells may interact with the same, or different molecules on adjacent Schwann cell membranes. These structures are very dynamic during the process of active myelination. Along this line, MAG has been shown to bind to extracellular matrix components such as collagen (Probstmeier et al. 1992; Bachmann et al. 1995), tenascin-R (Yang et al. 1999) and fibronectin (Strengel et al. 2001). However, the physiological relevance of its binding to components of the extracellular matrix is not clear, because most MAG is localized in sequestered periaxonal and other spiralled glial membranes. Binding to these molecules could be relevant to MAG's effect on neurite outgrowth, and tenascin-R was shown to neutralize the inhibition of neurite outgrowth by MAG (Yang et al. 1999).

In vitro experiments showed that MAG can influence neurite outgrowth in a bifunctional manner. Whereas it promotes neurite outgrowth of neurones at early stages of development, such as in embryonic dorsal root ganglia, it inhibits neurite outgrowth of neurons at later stages, such as in adult dorsal root ganglia or early postnatal cerebellum (Mukhopadhyay et al. 1994; DeBellard et al. 1996). A very recent study showed that L-MAG, but not S-MAG, promotes neurite outgrowth of cerebellar neurons (Shimizu-Okabe et al. 2001).

Mice with a null mutation in the MAG gene show a delay in CNS myelin formation (Li et al. 1994; Montag et al. 1994; Bartsch et al. 1997). Moreover, oligodendrocytic cytoplasmic collars of mature CNS myelin are frequently missing or reduced. Compact myelin containing an increased presence of oligodendroglial cytoplasmic loops and compact myelin coursing away from the axon were other abnormalities associated with MAG deficiency. The biochemical analysis of myelin from mice lacking MAG indicated pathological abnormalities in oligodendrocytes. Substantial reductions of CNPase, N-CAM120, tubulin and Fyn tyrosine kinase were found in 14-month-old mice, and reductions of CNPase and N-CAM120 were already found in 2-month-old mice, showing that abnormalities begin at a relatively early age (Weiss et al. 2000). In contrast, PNS myelin formation proceeds normally in MAG mutant mice, but older mutants display PNS axonal and myelin degeneration, indicating that MAG plays a critical role in maintaining PNS integrity (Fruttiger et al. 1995). Furthermore, axon calibres in peripheral nerves of MAG mutants surrounded by morphologically intact myelin were significantly smaller than in wild-type controls. Reduced axon calibre correlated with reduced neurofilament spacing and a decrease in neurofilament phosphorylation (Yin et al. 1998). These data demonstrate that the MAG null mutation might have deleterious secondary effects on neurons. Recently, an isoform-specific L-MAG mutant mouse line was generated, displaying most of the CNS, but not the PNS, pathological features of the MAG null mutant (Fujita et al. 1998). These observations demonstrate a differential role of the L-MAG isoform in CNS and PNS myelin and indicate that S-MAG may be sufficient for PNS myelin maintenance.

Although the neurological deficit in MAG-null mice is mild, double knockouts, in which the absence of MAG is combined with the genetic ablation of other proteins, results in more severe phenotypes than either knockout alone and have provided further insight into MAG function. One example is provided by mice in which both MAG and Fyn tyrosine kinase are absent (Biffiger et al. 2000). It is well established that Fyn has an important role in the formation of CNS myelin, and the CNS of Fyn-null mice is hypomyelinated. However, in the absence of both Fyn and MAG, there is a much more severe hypomyelination of the CNS. This may relate to the report of a direct Fyn-MAG interaction in signal transduction (Umemori et al. 1994). Another example, in which combining a MAG deficiency with the absence of another oligodendroglial component exacerbates CNS pathology, is the MAG/UDP-galactose:ceramide galactosyl transferase (CGT) double knockout (Marcus et al. 2002). CGT-null mice are unable to synthesize galactocerebroside (GalC) or sulfatide, which are characteristic lipids of myelin and lipid-rafts (for more aspects of the CGT mutant, see below in section 5.3.). Similarly to the MAG-null mice, myelination is not dramatically impaired in these mutants, but they exhibit a more severe pathology in the CNS with aging and die at about 90 days. Particularly noteworthy are defects in axo-glia interactions, such as splitting of the periaxonal space along the internodes and a severe disorganization and breakdown of the tight glia-axon junctions in the paranodal regions. The normal developmental increase in the amount of the small MAG isoform relative to the

large isoform in the CNS is impaired in the CGT knockouts (Coetzee et al. 1998). In MAG/CGT double knockouts, the defects of axon-glia interactions are much more severe, and the degeneration in the paranodal region progresses much more rapidly, leading to death by about 3 weeks of age. Interestingly, careful examination of the paranodal region in the CNS of single MAG knockouts revealed mild degeneration of these structures, but they did not progress to the extent that occurs in the CGT single knockout, or in the double knockout. It is of interest that the paranodal junctions in the PNS of CGT and MAG/CGT double knockouts are only mildly affected. Thus, there appears to be some overlap of function between MAG and galactolipids in glia-axon interactions of the CNS, despite the very different structure and properties of these molecules. Furthermore, because MAG is localized in the internodal periaxonal membrane, it is easy to understand how its absence contributes to splitting at this location. However, since it is not clear if MAG is expressed in the CNS paranodal loops, although there is at least one report claiming so (Bartsch et al. 1989), it is much less easy to understand how the absence of MAG contributes to the degeneration of the loops. If MAG is in fact expressed in the paranodal loops, the absence of the adhesion properties of MAG and/or the absence of the autotypic MAG-mediated signalling (glia-glia) between adjacent membranes could cause a loosening of this structure. Alternatively, if MAG is not expressed in this region, MAG-mediated signalling (axon-glia) could provide trophic support that increases the vigour of oligodendrocytes in general, and its absence may exacerbate the structural or functional defects caused by the absence of galactolipids.

The culturing of oligodendrocyte precursor cells on a substratum containing N-CAM, or MAG itself, increased both cell survival and the generation of myelin-like membranes (Gard et al. 1996). The effect of MAG suggests the possibility of autotypic MAG-mediated signalling between adjacent, loosely spiralled, oligodendroglial membranes that enhances the myelination process.

4.2. Myelin and Lymphocyte Protein - MAL

The myelin and lymphocyte protein, MAL, has been cloned independently by several groups from different tissues. In 1987, MAL was cloned from human T lymphocytes (Alonso and Weissman 1987). In 1995, MAL was cloned from rat primary oligodendrocytes (Schaeren-Wiemers et al. 1995a) and from the kidney cell line MDCK (Zacchetti et al. 1995). Furthermore, MAL was shown to be expressed in the myelinating glial cells of both the peripheral and the central nervous systems (Schaeren-Wiemers et al. 1995b). Colocalization of MAL with MBP and PLP, shown by immunoelectron microscopy, suggested a main localization in compact myelin (Frank et al. 1998). Recently, MAL was shown to colocalize with MAG in the Schmidt-Lanterman incisures of peripheral myelin (Erne et al. 2002). During development of the CNS, MAL became detectable at P10 in the rat spinal cord, and at P15 in the cerebellum, which was about 5-6 days later than MBP and PLP (Frank et al. 1999). In the rat PNS, MAL was detectable at E17 and at birth MAL was also widely expressed in Schwann cells that had not formed myelin (Frank et al. 1999).

In the kidneys, MAL is expressed at the apical lamina surface of the tubuli (Frank et al. 1998; Frank 2000). Besides the kidney, MAL is also expressed in the apical plasma membrane of the gastro-intestinal tract (Magyar et al. 1997), including the stomach (Frank

et al. 1998), and in the thyroid (Martin-Belmonte et al. 1998). MAL was originally identified as a marker of human T lymphocytes (Alonso and Weissman 1987) and is in fact expressed in various human T cell lines and in the human thymus. However, in rodents, MAL transcripts were only detectable in the spleen and not in the thymus (Schaeren-Wiemers et al. 1995b).

The proteolipid MAL is a tetraspan protein with 153 amino acids and a molecular mass of 17 kDa (Alonso and Weissman 1987). All cloned cDNAs show an amino acid identity of about 90% relative to the human homologue. Proteolipids are defined as proteins extractable into organic solvents under conditions used to isolate cell lipids (Schlesinger 1981). Along this line, extraction of kidney and spinal cord plasma membranes, as well as myelin membrane, with chloroform/methanol trapped MAL in the organic phase (Frank et al. 1998).

Lipid rafts can be isolated as DIGs (detergent-insoluble glycolipid-enriched complexes) after extraction with Triton X-100 or CHAPS at 4°C (see below: Introduction, Chapter 6: Lipid-rafts). MAL has been isolated from DIGs of MDCK cells, human mature T cells, human peripheral blood lymphocytes, rat thyroid cells, primary mature oligodendrocytes, as well as of rat kidney and spinal cord plasma membranes (Kim et al. 1995; Zacchetti et al. 1995; Millan et al. 1997a; Frank et al. 1998). The C-terminal LIRW sequence of MAL was postulated to be necessary for its incorporation into DIGs (Puertollano and Alonso 1998). However, this LIRW motif is not sufficient to direct other proteins into DIGs, indicating that other features of MAL, such as lipid-binding or global physical properties are also required (Puertollano et al. 1997; Frank et al. 1998; Puertollano and Alonso 1998).

Increasing the gene dosage of MAL controlled by its own regulatory elements in transgenic mice resulted in increased MAL levels in organs and tissues that also express MAL in the wild-type animal. These include the kidney, the stomach and the nervous system. Whereas peripheral myelin appeared normal, a striking segregation of non-myelinated axons became pronounced with increasing age. In the CNS, signs of mild hypomyelination with an increased number of unmyelinated axons and focal myelin alterations were observed. Severe cyst formation and cortex atrophy were found in the kidney of the transgenic animals (Frank et al. 2000).

MAL was suggested to be involved in apical transport in epithelial cells, since it was largely localized in vesicular structures of the trans-golgi network and in transport vesicles (Zacchetti et al. 1995; Millan et al. 1997a; Millan et al. 1997b). It was also shown that MAL cycles between the trans-golgi network and apical membranes (Puertollano et al. 1999). Recently, two groups provided evidence that MAL is involved in the transport of apically destined proteins. Both groups blocked MAL expression in MDCK cells by different antisense techniques and studied the transport of molecules that are known to be lipid-raft-associated and apically transported, such as HA (influenza virus protein Haemagglutinin) and YFP-GPI (yellow fluorescent protein fused to a GPI-anchor; (Cheong et al. 1999; Puertollano et al. 1999; Martin-Belmonte et al. 2000). The transport of all considered proteins to the apical membrane was reduced, suggesting an involvement of MAL in raft-associated trafficking. The fact that the decreased MAL expression in MDCK cells leads to a decrease in the solubility of HA, which is coupled to a decrease in surface transport of HA in these cells, suggests that MAL might stabilize the association of transport cargo within rafts in the trans-golgi network as a prerequisite for apical sorting (Puertollano et al. 1999; Puertollano et al. 2001). Interestingly in this context is the observation that non-transported proteins remained in the golgi (Cheong et al. 1999). However, a role for MAL

in vesicle formation cannot be excluded since ectopic expression of MAL in insect cells induced vesicle formation (Puertollano et al. 1997). MAL seems to be a rate-limiting component in the process of apical transport since overexpression of MAL in MDCK cells leads to an increased apical surface delivery of HA and YFP-GPI (Cheong et al. 1999). These studies also revealed that detergent-soluble proteins, such as p75 (neurotrophin receptor) and gp114 (an endogenous membrane protein of MDCK cells), are also impaired in their apical sorting and trafficking upon MAL depletion, suggesting a general role for MAL in apical transport (Cheong et al. 1999; Martin-Belmonte et al. 2000). To date, it is not clear whether the transport of raft-associated and non-raft proteins occur *via* the same, or different vesicles.

4.3. Proteolipid Protein - PLP

Proteolipid protein PLP is the most abundant protein of the CNS white matter. PLP comprises four hydrophobic α -helices spanning the whole thickness of the lipid bilayer at the intraperiod and major dense line of compact myelin (Weimbs and Stoffel 1992). Alternative splicing of the PLP gene gives rise to a minor isoform known as DM20. PLP and DM20 share complete sequence identity, except for a 35 amino acid intracellular segment, while the full-length gene encodes the PLP isoform with a length of 276 amino acids and a molecular mass of 30 kDa. During development, DM20 is the predominant isoform, which can already be detected in oligodendrocyte precursor cells (Dickinson et al. 1996). PLP and DM20 are synthesized by oligodendrocytes on membrane-bound polysomes directly as the mature protein, and are transported through the Golgi to the cell surface where they are incorporated into compact myelin. The half-life of PLP in myelin is approximately 90 days (Messier and Bizzozero 2000). Despite its net basic charge, PLP is a highly hydrophobic protein. Its hydrophobic character is further increased by the presence of covalently bound long-chain fatty acids, predominantly palmitic acid (Messier and Bizzozero 2000).

Numerous functions have been proposed for PLP and DM20 in the CNS, including membrane adhesion and compaction of myelin, formation of the myelin intraperiod line, maturation of oligodendrocytes, involvement in early stages of oligodendrocyte/axon interactions and wrapping of the axon, and maintenance and survival of axons. PLP-null mice have oligodendrocytes that can assemble compacted myelin sheaths, but with a condensation of the intraperiod line and a decreased physical stability, confirming a likely role for PLP in compaction and stabilization of myelin sheaths (Boison and Stoffel 1994; Klugmann et al. 1997).

4.4. Myelin Basic Protein - MBP

The 'classic' Myelin Basic Proteins (MBP) are major protein components of myelin, comprising ~30% of CNS myelin protein and ~18% of PNS myelin protein. The 'classic' MBP gene comprises seven exons, of which three (exons II, III and VI) are alternatively spliced, accounting for all four major isoforms of mouse MBPs (Figure 9; Zeller et al. 1984; Roach et al. 1985; Takahashi et al. 1985; Mentaberry et al. 1986; Newman et al. 1987).

The transcript corresponding to the 21.5-kDa isoform contains the sequences encoded by all seven exons, the transcript for the 18.5-kDa isoform results from the splicing out of exon II, the transcript for the 17-kDa isoform results from the splicing out of exon III and VI, and the transcript for the 14.5-kDa isoform results from the splicing out of exon II and VI. In the CNS, the 21.5-kDa and the 17-kDa isoforms are expressed during myelination, whereas the 14.5-kDa and the 18.5-kDa isoforms are expressed in mature myelin (Carson et al. 1983).

The MBP proteins contain an unusually high percentage (25%) of basic residues evenly distributed throughout the polypeptide chain. These residues are thought to interact with the negatively charged phospholipids of the lipid bilayer. Therefore, MBPs are believed to participate in the compaction and maintenance of the myelin sheath by holding together the inner leaflets of the myelin membranes (see Figure 6; Omlin et al. 1982).

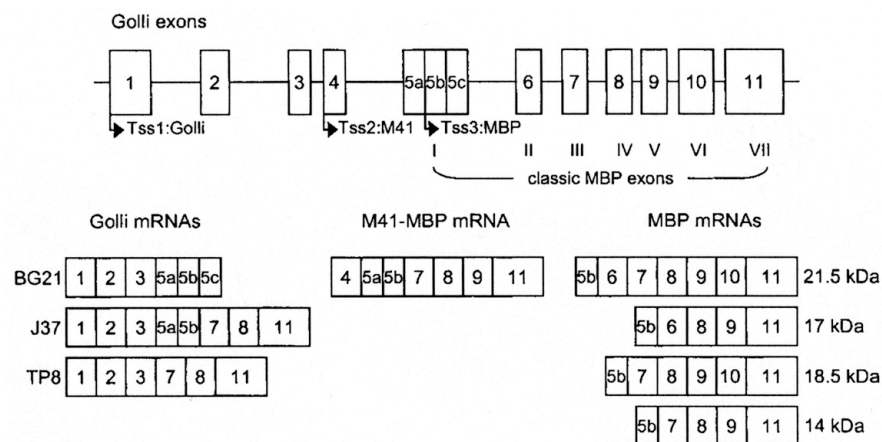


Figure 9 Structure of the myelin basic protein (MBP) gene.

The arrangement of the mouse MBP gene is illustrated. The 'classic' MBP exons are shown in roman numbers while golli exons are shown in arabic numbers. The three transcription start sites (Tss) are indicated with arrows. Exonic structures of BG21, J37 and TP8 golli isoforms, the four main isoforms of MBP and M41-MBP are shown (according to Givogri et al. 2000).

However, the picture was recently complicated by the demonstration that, in both mice and man, the MBP gene is contained within a large genetic locus of 105-180 kbp, which has been called the golli-MBP transcription unit (Campagnoni et al. 1993; Pribyl et al. 1993). The two major transcription start sites present in this complex give rise to two families of transcripts: those that encode the 'classic' MBPs, which are expressed only in myelin-forming cells, and those derived from a distal, upstream promoter, that encode the structurally and immunologically related golli proteins (Figure 8). Indeed the two major golli proteins contain MBP peptide sequences in their C-terminal region. While they may be involved in the early development and maintenance of neurons in the PNS, the golli proteins are not myelin proteins (Landry et al. 1997).

MBP mRNAs are targeted to the developing myelin sheath, where they are translated on free polysomes (Colman et al. 1982; Verity and Campagnoni 1988). The subcellular trafficking pathway for MBP mRNA in the oligodendrocyte involves three distinct sorting steps: (a) assembly into granules, (b) transport along the processes, and (c) localization to the myelin compartment. Specific regions in the 3' untranslated regions (UTR) of MBP mRNA are required for the last two of these steps. The RNA transport sequence (RTS) is necessary and sufficient for the transport of mRNA along oligodendrocyte processes.

Homologous sequences are found in other transported mRNAs, suggesting that the RTS represents a general signal to direct RNAs to the transport apparatus of the cell. The second is a RNA localization region (RLR) with a predicted stable secondary structure, which is required for localization of MBP mRNA to myelin. The RLR may be involved in anchoring or stabilizing MBP mRNA in the myelin compartment of the oligodendrocyte (Ainger et al. 1997). A transgene consisting of a truncated cDNA fragment encoding the 14-kDa MBP isoform and containing the RTS and RLR of mouse, was able to completely rescue the shiverer mutation (see below), consisting of a deletion of the endogenous MBP gene (Kimura et al. 1989), suggesting that these regions are sufficient for normal targeting of MBP expression *in vivo*.

The shiverer mutation comprises a 20-kbp deletion of the 'classic' MBP gene, that results in the absence of MBPs (Roach et al. 1983; Roach et al. 1985; Molineaux et al. 1986). The shiverer mutant, first observed in 1973, is deficient in CNS myelin. Homozygous mice exhibit a distinct behavioural pattern, including a generalized action tremor (shivering), appearing around postnatal day 12, convulsions and early death. Morphological analysis of the CNS revealed an almost total lack of myelin in the brains of affected mice (Bird et al. 1978) with few thinly myelinated axons. The existing myelin was abnormal, presenting no major dense line (Privat et al. 1979). It was thus concluded that the MBPs are necessary for the formation of the major dense line in the CNS myelin. In contrast, the PNS myelin of the shiverer mouse appears to be both qualitatively and quantitatively normal, with normal thickness, lamellar structure, and periodicity (Privat et al. 1979; Rosenbluth 1980). Only relatively minor abnormalities were reported, such as cytoplasmic invaginations of the innermost and outermost layers and aberrant terminations of lamellae in the internodes (Rosenbluth 1980; Inouye et al. 1985). Biochemical studies of shiverer PNS myelin revealed changes in the proportions of some lipids, including an increased amount (+20%) of negatively charged sulfatide (Inouye et al. 1985). Nevertheless, the absence of MBP does not prevent the formation of compact myelin in the PNS. Its absence is possibly compensated by another PNS myelin protein, probably P0 (Martini et al. 1995).

4.5. Myelin/Oligodendrocyte Glycoprotein - MOG

MOG is a 26–28-kDa glycoprotein specifically expressed in oligodendrocytes (Linnington et al. 1984). Like MAG, MOG is a member of the Ig superfamily, is a quantitatively minor component of the myelin sheaths and is localized in membranes distinct from compact myelin. However, unlike MAG, MOG is not expressed in the PNS and is not localized in the adaxonal/periaxonal membranes, but in the abaxonal myelin membrane and on oligodendrocytes. Therefore, MOG is well situated to interact with components in the extracellular environment. MOG has a single Ig-like variable region domain, one site for N-linked glycosylation, and two hydrophobic, potential transmembrane domains. However, topographical studies of MOG have indicated that the second hydrophobic domain does not transverse the membrane completely, but is located within the membrane, so the carboxy terminus of MOG is in the oligodendroglial cytoplasm (Kroepfl et al. 1996). It is of interest that the cytoplasmic domain of MOG contains targeting signals that direct it to the basolateral domain of MDCK cells and presumably account for its selective localization on the surface of oligodendrocytes and myelin sheaths (Kroepfl and Gardinier 2001). Several experiments performed by Dyer and colleagues (Dyer et al. 1994) have identified another

possible function for MOG. They showed that the addition of monoclonal anti-MOG antibodies to oligodendrocytes in culture causes the MOG/anti-MOG complex to redistribute over internal domains of MBP and a subsequent depolymerization of microtubules. As microtubules are stabilized by the cytoplasmic domains of MBP (Pirrollet et al. 1992), they suggested that MBP might have an important role in this process. A similar depolymerization of microtubules in oligodendrocytes was provoked by the addition of antibodies to GalC (Dyer 1993). Thus, it appears that MOG and GalC may share at least one function in common: regulation of microtubule stability through local degradation of MBP. The common mechanism of the glycoprotein MOG and the galactolipid GalC may be explained by an interaction of the lipid-bilayer-associated second hydrophobic domain of MOG, *via* its two palmitoylated cysteine residues, with the fatty acid portion of GalC. Furthermore, MOG is highly immunogenic and immunization with this protein alone can induce severe experimental allergic encephalomyelitis (EAE) in rodents and primates. EAE has often been used as an animal model for MS.

5. Myelin Lipids

5.1. General

All the major lipid classes (phospholipids, glycolipids and cholesterol) and their respective subclasses encountered in other membranes, are also represented in the myelin membrane and thus, strictly speaking, there are no myelin-specific lipids. But one of the major biochemical characteristics that distinguishes myelin from other biological membranes is its high lipid-to-protein ratio. Myelin contains 70-80% lipids and 20-30% proteins. Perhaps the most striking feature of the myelin lipid composition when compared to that of other biological membranes, is the high content in galactolipids (GalC: ~25% and sulfatides: ~5%) and cholesterol (~25%, for review, see Norton and Cammer 1984). The myelin lipids are asymmetrically arranged within the myelin lipid bilayer with glycolipids and cholesterol found in the outer leaflet and phospholipids in the inner leaflet. Myelin also contains gangliosides (sphingolipids with an oligosaccharide head-group including one, or more sialic acid residues; Fong et al. 1976). About 90% of the total gangliosides are monosialogangliosides, such as sialosyllactoneotetraosylceramide (LM1, GM1, GM3 and GM4; Chou et al. 1982). Interestingly, mice lacking complex gangliosides (GM2 and GD2) develop both CNS and PNS pathologies, the latter being characterized by demyelination and axonal degeneration (Sheikh et al. 1999).

5.2. Cholesterol

Cholesterol accumulates continuously throughout the period of neo-myelinogenesis and during the subsequent period of myelin maturation (Yates and Wherrett 1974; Juguelin et al. 1986). This accumulation pattern is consistent with the role proposed for this lipid in the stabilization and the compaction of the multilamellar myelin membrane (Nussbaum et al. 1969; Detering and Wells 1976). Disturbed cholesterol synthesis in young weanling rats

through the inclusion of tellurium in their diet, produces a severe peripheral neuropathy, which is manifested clinically by a hind limb paralysis (Lampert et al. 1970). Tellurium intoxication predominantly damages the myelinating Schwann cells (Lampert and Garrett 1971; Hammang et al. 1986). The process of demyelination stops about one week after the onset of the exposure, and a period of rapid remyelination begins, even if the exposure to tellurium continues (Said and Duckett 1981; Takahashi 1981; Wiley-Livingston and Ellisman 1982). Remyelination is complete within 30 days after starting the exposure to tellurium (Lampert and Garrett 1971; Duckett et al. 1979; Takahashi 1981; Hammang et al. 1986). Thus, the lack of cholesterol required for the formation of new myelin and the maintenance of pre-existing myelin leads to a highly synchronous demyelination. Importantly, the cholesterol deficit also leads to a coordinate down-regulation of the mRNAs coding for myelin-related proteins, indicating that there is a coordinated regulation of the entire program for myelin synthesis and assembly in Schwann cells (Toews et al. 1990; Toews et al. 1996; Toews et al. 1997).

5.3. Myelin Glycolipids

GalC (15-25% of myelin lipids) and its sulphated derivative sulfatide (5-10% of myelin lipids) are the major glycolipid lipid components characteristic of myelin (Garbay et al. 2000). GalC is synthesized by the addition of activated galactose to a ceramide molecule by the enzyme UDP-galactose:ceramide galactosyl transferase (CGT). Further addition of a sulfate group that derives from 3'phosphoadenosyl-5'phosphosulfate (PAPS) by the enzyme 3'phosphoadenylylsulfate:GalC 3'sulfotransferase (CST) leads to the formation of sulfatide. Despite the fact that the myelin membrane is continuous with the plasma membrane surrounding the cell body of an oligodendrocyte, GalC and sulfatide are only present within the myelin-forming membrane (Abe and Norton 1979). During development GalC and sulfatide start to be expressed in immature oligodendrocytes with a peak synthesis during postnatal development paralleling the period of myelination. After myelination is complete, they remain expressed at high levels throughout life (Burkart et al. 1983). Application of the monoclonal anti-sulfatide (O4) and anti-GalC (O1) antibodies reversibly inhibit the onset of terminal differentiation at the pre-GalC immature OL interface into mature oligodendrocytes (Bansal et al. 1999). These data suggest that these anti-galactolipid antibodies mimic a lipid-binding ligand and initiate a constitutive inhibitory signal across the plasma membrane *via* interaction with GalC and/or sulfatide.

Further, interaction of sulfatide in the oligodendrocyte membrane with the extracellular matrix molecule tenascin-R suggests a function in cell recognition and adhesion (Pesheva et al. 1997).

The formation of subcellular microdomains by glycolipids, so-called 'lipid-rafts', is thought to be associated with protein trafficking and signalling in various cell types. GalC has been characterized as a transmembrane signal transducer, since cultured oligodendrocytes treated with an anti-GalC antibody exhibit distorted membrane morphology, calcium flux and cytoplasmic microtubule networks (Dyer and Benjamins 1989, 1990). Similar conclusions were drawn from a study that examined the effects of GalC/sulfatide-containing liposomes on cultured oligodendrocytes (Boggs and Wang 2001). The liposome–cell membrane interaction causes depolymerization of microtubules and actin filaments, along with the redistribution of membrane GalC and MBP.

Despite the *in vitro* work describing the necessity of galactolipids for normal oligodendrocyte differentiation and myelin formation, CGT-null mutant mice are capable to myelinate axons in the CNS and PNS. Overall, the myelin sheaths appears normal but the mice develop a tremor, starting around 2 weeks of age, and exhibit splayed hind limbs in conjunction with an uncoordinated gait. As the mutants age, the hind limbs develop paralysis and the mice rapidly lose mobility. The CGT mutants die prematurely, with few surviving beyond 90 days (Dupree et al. 1998a). Despite the formation of myelin, the abnormal CGT^{-/-} behavioural phenotype was strongly suggestive of dysmyelinated fibre profiles. Although myelin is able to form in the absence of galactolipids, there are a number of more subtle ultra structural abnormalities that are associated with myelination in the mutant CNS. Spinal chord axons display thinner myelin sheaths, with myelin thickness being reduced by about 30% relative to age-matched controls (Coetzee et al. 1996). Schmidt–Lanterman incisures are also abnormally found in the mature mutant CNS (Coetzee et al. 1996; Dupree et al. 1998b). These cytoplasm-filled clefts normally occur in PNS myelin, but their persistence in the mutant CNS might reflect a compensatory structure for compromised sheath integrity. There is an increase in mutant axons that are abnormally myelinated by multiple oligodendrocytic processes, suggesting defective axon–glial, or glial–glial contacts. Galactolipid-deficient myelin can also bear an immature morphology, such as cytoplasm retention within myelin lamellae and redundant myelin profiles (Bosio et al. 1998; Dupree et al. 1998b). Significant alterations in myelin ultrastructure are not seen in the PNS of CGT mutants, indicating that galactolipids are not absolutely essential for peripheral myelin formation (Dupree et al. 1998b). Interestingly, the CGT^{-/-} and the MAG^{-/-} single mutant mice produce abnormal myelin containing similar ultra structural abnormalities. The absence of the galactolipids results in a disruption in paranodal axon-glia and/or glial-glia interactions, which exist, albeit less severe, also in the developing MAG mutant. In the double-mutant mice, maintenance of glial-glia adhesion is significantly more affected than in the single mutants. Nodes of Ranvier form normally in the absence of both MAG and the galactolipids, but they rapidly destabilize thereafter (for more details about the MAG/CGT mutant, see above in section 4.1.).

6. Lipid-Rafts

In the prevailing view of cellular membrane structure, lipids in the bilayer function mainly as a solvent for membrane proteins (Singer and Nicolson 1972). But in the fluid bilayer, different lipid species are asymmetrically distributed over the exoplasmic and cytoplasmic leaflets of the membrane (van Meer 1989). The lipids are also organized in the lateral dimension and impose more short- and long-range order than was previously recognized (Kusumi and Sako 1996). This lateral organization probably results from preferential packing of sphingolipids and cholesterol into moving platforms, or rafts, onto which specific proteins attach within the bilayer. Simons and Ikonen (Simons and Ikonen 1997) proposed a new model for membrane structure that describes the organization of these lipid microdomains and presented evidence that proteins can selectively be included or excluded from these microdomains. They concluded that the function of these microdomains is to serve as rafts for the transport of selected membranes or as relay stations in intracellular signalling.

Simons and Ikonen (1997) based their lipid-raft concept on earlier studies on the delivery

of newly synthesized sphingolipids in epithelial MDCK cells that had showed that a simple glycosphingolipid, glucosylceramide, was preferentially transported to the apical membrane (Simons and van Meer 1988; van Helvoort et al. 1996). To explain delivery to the apical domain, it was proposed that glycosphingolipid clusters formed within the exoplasmic leaflet of the Golgi membrane (Simons and van Meer 1988): these microdomains were considered to be sorting centres for proteins destined for delivery to the apical plasma membrane. In support of this model, glycosylphosphatidylinositol (GPI)-anchored proteins use glycolipid anchors as apical sorting determinants (Brown and Rose 1992). Moreover, caveolae, small invaginations of the plasma membrane that are devoid of clathrin coats and are present in many cell types (Parton 1996), contain clusters of glycosphingolipids (Tran et al. 1987), and need cholesterol to function (Rothberg et al. 1990). As caveolae may be involved in endocytosis (Tran et al. 1987), and transcytosis (Ghitescu et al. 1986) a function for sphingolipid-rafts in membrane trafficking was plausible (Dupree et al. 1993).

Sphingolipid-cholesterol rafts are insoluble in the detergent TritonX-100 at 4°C, in which they form glycolipid-enriched complexes (Brown and Rose 1992; Parton and Simons 1995). Because of their high lipid content, these detergent-insoluble, glycolipid-enriched complexes (DIGs) float to a low density during sucrose gradient centrifugation (Brown and Rose 1992), which enables any associated proteins to be identified and distinguishes DIGs from other detergent insoluble complexes. Milder detergents such as octylglucoside will solubilize lipid-rafts (Schroeder et al. 1994). Glycosphingolipids are insoluble by themselves, and sphingomyelin is resistant to detergent extraction in the presence of cholesterol (Schroeder et al. 1994). One problem with TritonX-100 extraction is that the original subcellular locations of DIGs are unknown. Confusion has been created because sphingolipid-rafts in apical transport vesicles, in caveolae, and even in plasma membranes from cells devoid of morphologically recognizable caveolae, all form DIGs after Triton X-100 extraction (Skibbens et al. 1989; Sargiacomo et al. 1993; Fra et al. 1994). Only by isolating specific organelles before detergent extraction can the origin of DIGs be determined; neither can it be assumed that two proteins are in contact with each other on the basis of their partitioning into DIGs.

The raft model of protein sorting and trafficking and signalling has also been applied to the myelinating cells of the peripheral and central nervous system. Along this line, TritonX100-resistant membrane domains have been isolated from primary oligodendrocytes and myelin that are enriched in GalC, sulfatide, and the GPI-linked adhesion molecules NCAM120 and F3/contactin as well as src-family kinases Fyn and Lyn (Kramer et al. 1997). These raft complexes are proposed to be functionally involved in axon-glia recognition and in the compartmentalisation of signalling cascades, one of which utilises the tyrosine kinase Fyn in the initial phase of myelination (Kramer et al. 1999; Trotter et al. 2000). The non-compact myelin proteins CNPase and MOG were also shown to fulfil criteria for raft association when solubilized from purified myelin and a role of these rafts in signalling processes along non-compact myelin regions was suggested (Kim and Pfeiffer 1999). The advantage of utilising rafts for the generation of myelin could be the efficiency of a self-driven assembly of the specific myelin lipids. These form a membrane of specific biophysical characteristics (liquid-ordered phase, high melting temperature, low fluidity) that facilitates electric insulation of the axon. The myelin and lymphocyte protein (MAL) is a component of glycosphingolipid-rafts in myelinating glial cells (for more aspects about MAL and rafts, see section 4.2.; Schaeren-Wiemers et al. 1995b; Frank et al. 1998; Frank 2000).

Motivation and Aim of the Work

Myelin is generated during a relatively short time during development and must be maintained throughout life. To meet the requirements imposed by its different functions, the structure of myelin is unique and comprises several compartments. We do know only little about the signals involved in myelination initiation, the interplay of the different molecular components to achieve myelin wrapping, formation and maintenance and how myelin components, which are synthesized in the cytoplasm, are sorted and targeted to their respective sites of assembly.

The myelin-associated glycoprotein isoforms L- and S-MAG are believed to be multifunctional proteins intervening at several levels of the myelination process. As such, they constitute key components of the myelin sheath and the elucidation of their function emerges as an important step towards understanding myelin formation, maintenance and disease. We planned to generate transgenic mice expressing both MAG isoforms as individually fluorescent protein-tagged fusion proteins, since the generation of antibodies specifically recognizing the two mouse isoforms had failed. These mouse lines were planned to be used, for instance, to investigate the isoform-specific expression pattern within the different structures of the brain, within the different domains of the myelin sheath during development and in the adult and in mouse models for primary demyelinating neuropathies.

Investigations of L- and S-MAG expression in sural nerve biopsies from patients with primary demyelinating hereditary peripheral neuropathies (CMT1A and HNPP) had revealed a significant increase of L-MAG-positive fibres compared to control autoptic sural nerves (Lützel Schwab 1998; Schaeren-Wiemers et al. 1999). The analysis of the L- and S-MAG-specific mRNAs in the corresponding mouse models, however, showed a significant up-regulation of S-MAG, but not L-MAG (Adlkofer et al. 1995; Adlkofer et al. 1997; Lützel Schwab 1998; Schaeren-Wiemers et al. 1999). The cross-breeding of these animal models with the fluorescent protein-tagged MAG mice should have allowed to verify whether these mice also up-regulate S-MAG at the protein level, as suggested by the mRNA, or if the L-MAG protein is up-regulated in a manner similar to that observed in the human sural nerve biopsies.

Materials and Methods

1. Molecular Biology

1.1. RNA Isolation and cDNA Synthesis

RNA was isolated from 2×10^6 Oli-neu cells with the SV Total RNA Isolation kit (including a DNase treatment, Promega Corporation, Madison, USA) or from whole mouse brains with the RNeasy Mini Kit (Qiagen). About 10 μ g total RNA could be isolated from 10^6 Oli-neu cells. cDNA synthesis was performed with 5 μ g total RNA using the Oligo(dT)₁₅ Primer and the M-MLV Reverse Transcriptase (Promega Corporation, Madison, USA). A typical cDNA synthesis reaction contained: 5 μ g total RNA, 1 μ g Oligo(dT)₁₅ Primer, 25 units rRNasin Ribonuclease Inhibitor (Promega), 200 units M-MLV Reverse Transcriptase (Promega), 0.5 mM dNTP, 1 x reaction buffer, in a final volume of 25 μ l. The RNA was incubated together with the primer for 5' at 70°C and cooled on ice thereafter. The other reagents were then added and the synthesis was carried out at 42°C for one hour.

1.2. Primer List

The following Table 1 lists all primers used in PCR amplifications for semi-quantitative and quantitative RT-PCR and for cloning.

Primer	Sequence (5' to 3')
3'13a-BamHI	CACGGATCCCTTGACTCGGATTTCTGCATA
3'13b-BgIII-SacII	GAGCCGCGGAGATCTGATGGTCTCTTCTGGCTCTT
3'amusL	TGCTTCTCACTCTCATACTTA
3'DsRed-HindIII	CACAAGCTTCTACAGGAACAGGTGGTGG
3'exon13-A	TCTCCATGGCCTTGACTCGGATTTCTGCATAC
3'exon13-B	ATGTAGGCAAGGAATGTTG
3'GFP-NarI	CTCGGCGCCTTACTTGTACAGCTCGTCCAT
3'GFP-SmaI	ACACCCGGGACCTACCTCCTGGGCTCTCACTTGTACAGC
3'GFP-SpeI	GAGACTAGTCACTTGTACAGCTCGTCCATG
3'Ig κ SP-StuI	CACAGGCCTAGCAGGAGACTGTGTCAGC
3'L-MAG-NcoI	TCTCCATGGCCTTGACTCGGATTTCTGCATAC
3'L-MAG-XbaI	CGCTCTAGACTCACTTGA CT CGGATTTCTG
3'MAG-NdeI-HindIII	CTCAAGCTTCATATGTTTAGCAAGTGATTGAGCTA
3'MAG-SalI	CTCGTCGACTTTTCAGCGGGTATATAAATG
3'mGAPDHrpaXbaI	TGGTTCACACCCATCACAAAC
3'mMAG-LC	TCCCTCTCCGTCTCATTACAGTC
3'mMAL-537	CCACTGCGGCGATGTTTTTC

3'mPLP/DM20-960	GCGAAGTTGTAAGTGGCAGCAATC
3'S-MAG-BamHI	CACGGATCCGTGACAATCCCGGGTAGAG
3'S-MAG-NcoI	TCTCCATGGCGTGACAATCCCGGGTAGAG
3'S-MAG-VSVG-XbaI	CGCTCTAGATCACTTGCCCAGGCGGTTTCATCTCGATGTCGGTG TAGCCGTGACAATCCCGGGTAGAG
3'S-MAG-XbaI	CGCTCTAGACTCAGTGACAATCCCGGG
3'VSVG-SmaI	GCGCCCGGGACCTACCTCCTGGGG
5'13b-SpeI	GAGACTAGTGGGGGCTGGCCCTGTG
5'DsRed-BamHI	CACGGATCCGGTAGTACCATGGTGCGCTCCTCC
5'exon10	CACCTCGAGTCGCCTTTGCCATCCTGATT
5'exon11/13	TGATAAGTATGAGAGTGAGAAG
5'exon12	TCCAGAGAGGTCTCTACCC
5'GFP-BamHI	CACGGATCCATGGTGAGCAAGGGCGAG
5'GFP-SmaI	ACACCCGGGATTGTCACGCCATGGTGAGCAAGGGCGAGG
5'Ig α SP-HindIII	CACAAGCTTATCCACCATGGAGACAGAC
5'MAG16760	CACAAGCTTCCAAAAGGGTGGTCCAACC
5'MAG-gs-RsrII	CACCGGACCGGTAGTGGAAGTGGAGGGGGCCACTGGGGT
5'MAG-HindIII-NarI	GAGAAGCTTGGCGCCTGGGGGCTGGCCCTGTG
5'MAG-NdeI	GAGCATATGATATTCCTCGCCACCC
5'MAG-NotI	GAGGCGGCCGCGATCCACTCCCCGGTCTAA
5'MAGrpaXhoI	GTCGCCTTTGCCATCCTGATT
5'MAG-StuI	CACAGGCCTACCATGATATTCCTCGCCACCC
5'MAG-XbaI	CACTCTAGAAGATGATATTCCTCGCCACC
5'mGAPDHrpaXhoI	GACCCCTTCATTGACCTCAA
5'mMAG-LC	GTTTGCCCCCATAATCCTTCTG
5'mMAL-208	CCACCTTCCCTGACTTGCTCTTC
5'mPLP/DM20-641	ACTGTTGTATGGCTCCTGGTGTGG
5'S-MAG-HindIII	CACAAGCTTGATCGTCCAAGGTTGAAAGG
5'VSVG-SmaI	CTACCCGGGATTGTCACGGCTACAC

Table 1 List of Primers

All primers used for PCR amplifications are listed in alphabetical order. The primer sequences are written from 5' to 3'. The names of so-called 'forward' (hybridizing to the antisense DNA strand) and 'reverse' (hybridizing to the sense DNA strand) primers begin with the 5'- and 3'-nucleotides, respectively.

1.3. Semi-Quantitative RT-PCR

To amplify the MAG mRNA region of exons 10 to 13, we used the primer pair 5'exon10 and 3'exon13-A. This primer pair amplifies a L-MAG-specific product of 338 bp and a S-MAG-specific product of 383 bp. L-MAG-specific mRNAs were amplified with the 5'exon11/13 and 3'exon13-B primer pair, whereas S-MAG specific mRNAs were amplified with the 5'exon12 and 3'exon13-B primer pair. The 5'exon11/13 primer is L-MAG-specific, because its sequence is homologous to the exon 11/exon 13 junction. The 5'exon12 primer is S-MAG specific, because its sequence is homologous to the S-MAG specific exon 12. For detailed localization of the primers see Figure 22A. Transcripts for

glyceraldehyde-3-phosphate dehydrogenase (GAPDH), employed as an internal standard, were amplified with the primer 5'GAPDHrpaXhoI and 3'GAPDHrpaXbaI.

1.4. Quantitative RT-PCR

The analysis was carried out using the Roche LightCycler with the FastStartDNA Master SybrGreenI. The following primer pairs were used: GAPDH: 5'GAPDHrpaXhoI x 3'GAPDHrpaXbaI; MAL: 5'mMAL-208 x 3'mMAL-537; total MAG: 5'mMAG-LC x 3'mMAG-LC; L-MAG: 5'MAGrpaXhoI x 3'amusL; PLP/DM20: 5'mPLP/DM20-641 x 3'mPLP/DM20-960. The following plasmids were used as internal standards: pBlue-GAPDH (insert: 5'GAPDHrpaXhoI x 3'GAPDHrpaXbaI; clone IV.1 04/11/99); pBlue-MAL (insert: cDNA library clone (gift from the Suter lab, Zürich); clone: 1.1 19/09/01); pBlue-L-MAG (insert: clone 3a1 13/08/99); pPCR-Topo-PLP/DM20 (insert: 5'mPLP/DM20-641 x 3'mPLP/DM20-960; clone 3 22/08/02). The standard curve was created by the analysis of the following plasmid copy numbers: 10^9 , 10^8 , ..., 10^3 , 10^2 . The primers, the plasmid DNA and the cDNA were diluted in 5 mM Tris pH 8,5. A 20- μ l reaction had a final concentration of 4 mM MgCl₂ and contained the following ingredients: 8.6 μ l H₂O, 2.4 μ l MgCl₂, 2 μ l SybrGreenMix, 1 μ l 5'primer 5 μ M, 1 μ l 3'primer 5 μ M and 5 μ l template. The annealing temperature was set to 57°C for all reactions. In each analysis, two internal standards (10^6 and 10^5 copies) were included to connect the values of the samples with the standard curve.

1.5. Cloning of The cDNA Expression Constructs

The cloning of the native MAG and the different fusion protein cDNA expression constructs described below are schematically represented in Figure 15. Primers with incorporated restriction sites were used for subcloning of PCR products. The mouse L- and S-MAG open reading-frames were cloned from adult mouse brain by RT-PCR.

1.5.1. Cloning of the L-/S-MAG Expression Vectors

For the L- and S-MAG expression constructs, the primer 5'MAG-StuI and 3'L-MAG-XbaI, for L-MAG, and 3'S-MAG-XbaI, for S-MAG, were used. The products were subcloned at the position of GFP into the β -actin-GFP expression vector (kindly provided by Prof. A. Matus, FMI, Basel, Switzerland).

1.5.2. Cloning of the L-/S-MAG-GFP Expression Vectors

For the L- and S-MAG-GFP fusion protein constructs, the primers 5'MAG-StuI and 3'L-MAG-NcoI and 3'S-MAG-NcoI were used, respectively. The products were cloned into the β -actin-GFP vector upstream of, and in frame with, the GFP sequence.

1.5.3. Cloning of the S-MAG-DsRed1 Expression Vector

For the S-MAG-DsRed1 construct, the DsRed1 sequence (Clontech, Heidelberg, Germany) was amplified with the primers 5'DsRed1-BamHI and 3'DsRed1-HindIII. This product was subcloned into the pcDNA3.1 expression vector (Invitrogen AG, Basel, Switzerland), resulting in the cmv-DsRed1 expression vector. In a second step, S-MAG was amplified with the primers 5'MAG-XbaI and 3'S-MAG-BamHI and subcloned in front of, and in frame with, the DsRed1 sequence.

1.5.4. Cloning of the S-MAG-VSVG Expression Vector

For the S-MAG-VSVG construct, S-MAG was amplified with the primers 5'S-MAG-HindIII and 3'S-MAG-VSVG-XbaI and subcloned into pcDNA3.1. The antisense primer introduced a 3' extension encoding the VSVG-tag (Vesicular Stomatitis Virus Glycoprotein).

1.5.5. Cloning of the GFP-L-MAG/GFP-S-MAG Expression Vectors

For GFP-MAG fusion protein constructs, the Igk light chain signal peptide and cleavage site sequence was amplified from mouse spleen with the primers 5'IgkSP-HindIII and 3'IgkSP-StuI and subcloned into the β -actin-GFP vector upstream of, and in frame with, the GFP sequence. In a second step, L- and S-MAG were amplified with the primers 5'MAG-gs-RsrII and 3'L-MAG-XbaI and 3'S-MAG-XbaI, respectively. The 5'MAG-gs-RsrII primer replaced the MAG signal peptide by a sequence coding for a five amino acid glycine/serine stretch. These products were subcloned downstream of the IgkSP-GFP sequence.

1.6. Cloning of the Genomic Mouse MAG Expression Constructs

Genomic constructs encoding MAG-GFP fusion proteins were generated from the intact 19 kb C57Bl mouse MAG gene, including the 1.8-kb promoter and all exons that were included on a cosmid (cos301). The MAG gene was subcloned into Bluescript pBSKS. The plasmid used for further cloning (*pmag*-MAG) is schematically shown in Figure 18.

1.6.1. Cloning of the *pmag*-MAG-e13GFP Construct

The *pmag*-MAG-e13GFP genomic expression construct was generated by the insertion of the GFP sequence before the stop codon within the mag exon 13 (Figure 10 and 18B: 2). This insertion required three sequential and reversible subcloning steps. In a first step, the HindIII fragment (\square HindIII-F) of the *pmag*-MAG plasmid was excised (HindIII sites: 10316 and 16756 bp) and the vector was ligated to yield: *pmag*-MAG \ominus HindIII fragment (\square NotI-Sall-F). In a second step, the 2315 bp HindIII-Sall fragment (HindIII site: 16756 bp and Sall site: 19070 bp) from this plasmid was isolated and subcloned into pBluescript II KS+ (\square HindIII-Sall-F). In a third step, the HindIII-BglII fragment (HindIII site 16756 bp and BglII site 17867) of the HindIII-Sall-F was replaced with a HindIII-e13GFP-BglII fragment. This HindIII-e13GFP-BglII fragment was generated by sequential ligation of three PCR products. The 5' part was amplified from the *pmag*-MAG with the primers 5'MAG16760 and 3'13aBamHI (\square 13-A), the middle part from the b-actin-GFP vector with 5'GFP-BamHI and 3'GFP-SpeI (\square EGFP), and the 3' part (\square 13-B) from the *pmag*-MAG with 5'13b-SpeI and 3'13b-BglII-SacII. This HindIII-e13GFP-Sall fragment was cloned into the *pmag*-MAG \ominus HindIII fragment by replacing the wild-type HindIII-Sall fragment. The cloning of the HindIII fragment into *pmag*-MAG \ominus HindIII fragment-e13GFP resulted in the *pmag*-MAG-e13GFP construct.

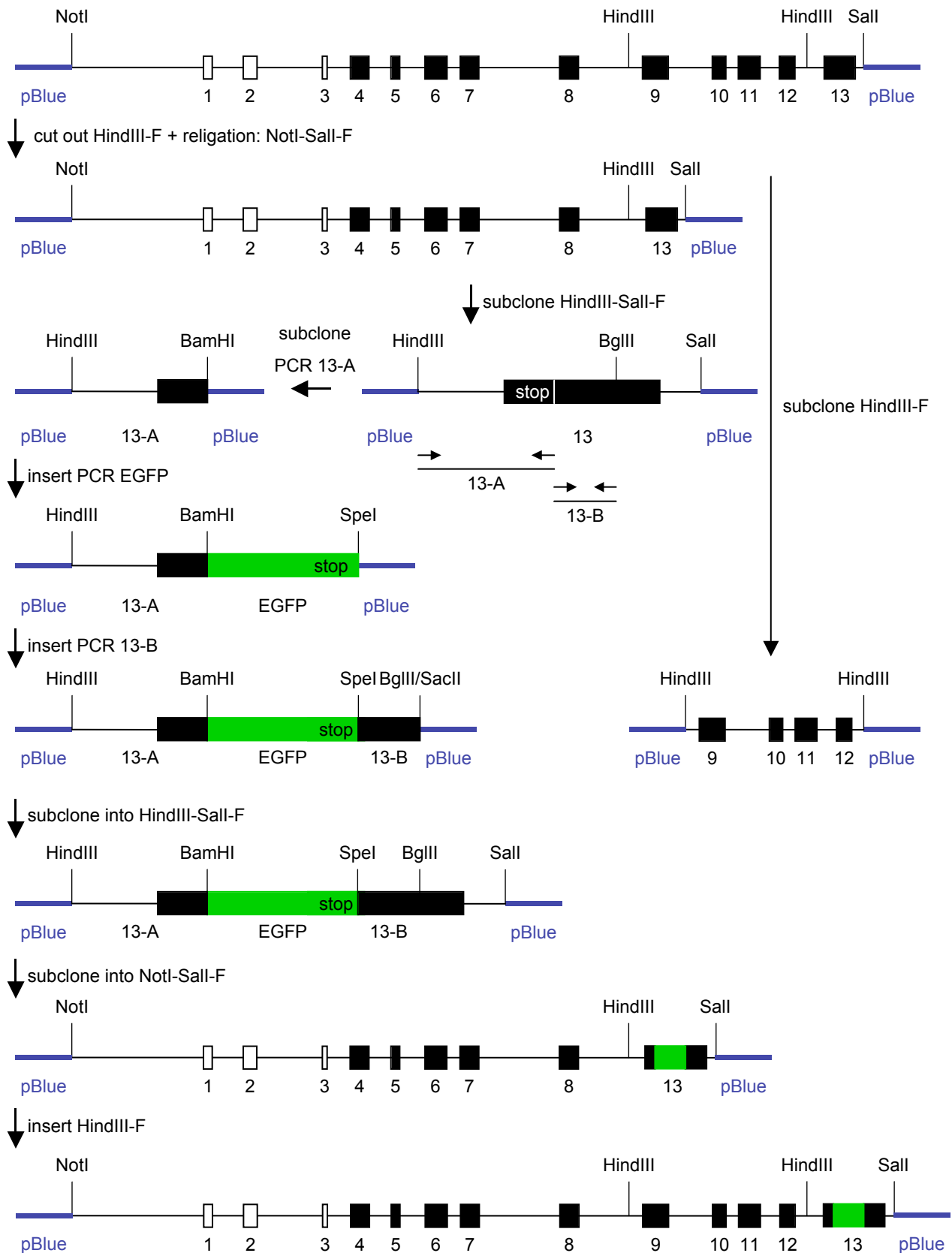


Figure 10 Cloning of the *pmag-MAG-e13GFP* genomic expression construct. top: wild-type *pmag-MAG* mouse MAG genomic clone (size 19 kb); bottom: *pmag-MAG-e13GFP* clone containing the EGFP-encoding DNA sequence before the stop codon of mag exon 13; white boxes: non-coding exons; black boxes: coding exons; green boxes: EGFP DNA sequence; F: DNA fragment.

1.6.2. Cloning of the *pmag*-MAG-e12GFP Construct

The *pmag*-MAG-e12GFP genomic expression construct was generated by the insertion of the GFP sequence before the stop codon within the mag exon 12 (Figure 11 and 18B: 3). The HindIII fragment was excised from *pmag*-MAG and subcloned into the pSP70 cloning vector (□ HindIII-F; pSP70 from Promega Corporation, Madison, USA). The SmaI fragment (SmaI-F; restriction sites: 16395 and 16430 bp) within the HindIII fragment contained the stop codon of exon 12 and was replaced by a SmaI-e12GFP-SmaI fragment. This was amplified by PCR from the p□actin-EGFP vector with the primer 5'GFP-SmaI and 3'GFP-SmaI. The resulting HindIII-e12GFP fragment was cloned back into *pmag*-MAG by replacing the wild-type HindIII fragment.

1.6.3. Cloning of the *pmag*-MAG-e12VSVG Construct

The *pmag*-MAG-e12VSVG genomic expression construct was generated by the same approach as that used for *pmag*-MAG-e12GFP. However, the SmaI fragment was replaced by a SmaI-e12VSVG-SmaI fragment. This was amplified by PCR from the cmv-S-MAG-VSVG vector with the primers 5'VSVG-SmaI and 3'VSVG-SmaI.

1.6.4. Cloning of the *pmag*-MAG-e12VSVG-e13GFP Construct

The *pmag*-MAG-e12VSVG-e13GFP genomic expression construct was generated by cloning of the HindIII-e12VSVG fragment (from the *pmag*-MAG-e12VSVG cloning) into the *pmag*-MAG□HindIII fragment-e13GFP vector (from the *pmag*-MAG-e13GFP cloning) (Figure 18B: 4).

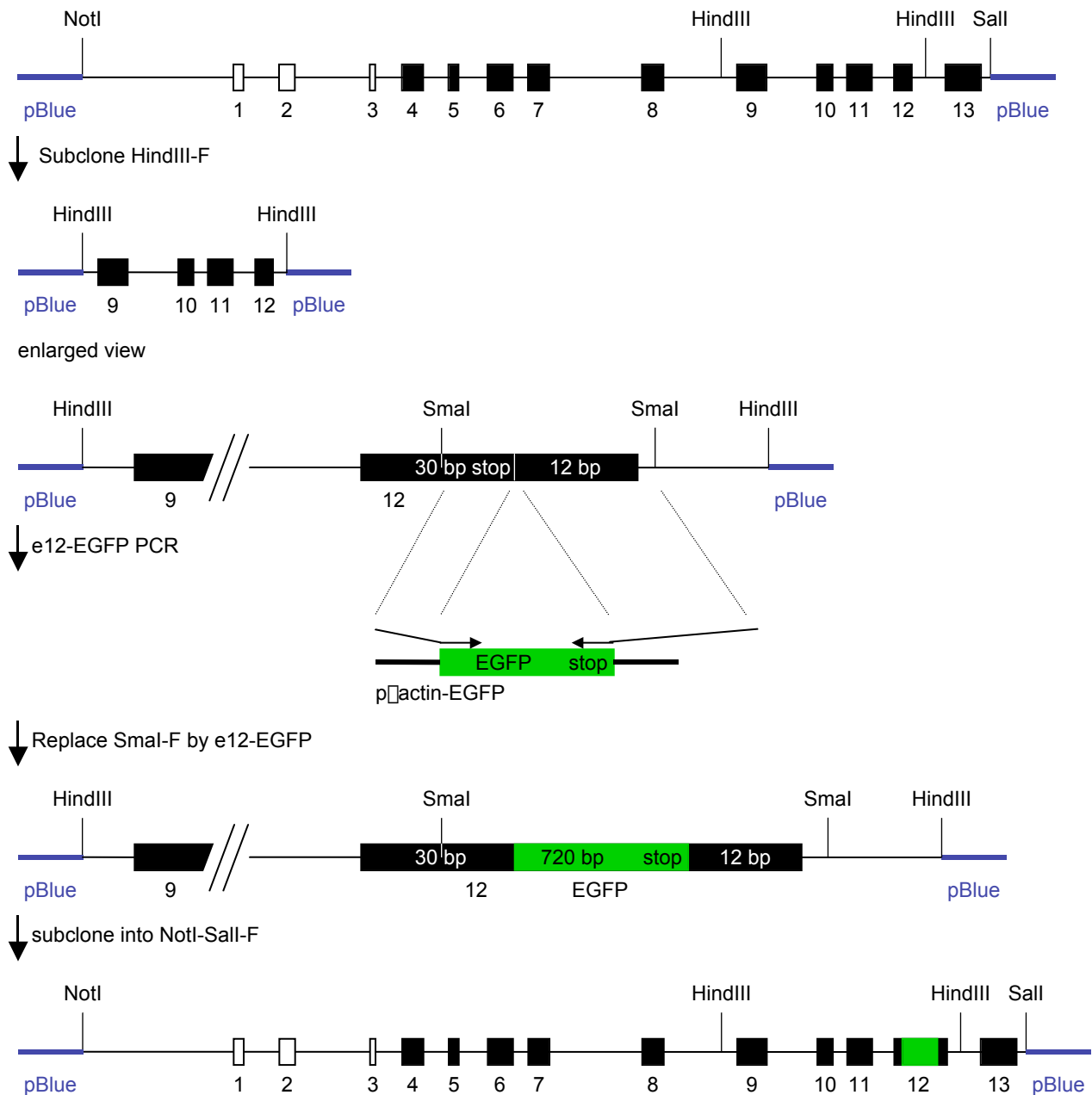


Figure 11 Cloning of the *pmag*-MAG-e12GFP genomic expression construct.

top: wild-type *pmag*-MAG mouse MAG genomic clone (size 19 kb); bottom: *pmag*-MAG-e12GFP clone containing the EGFP encoding-DNA sequence before the stop codon of the mag exon 12; white boxes: non-coding exons; black boxes: coding exons; green boxes: EGFP DNA sequence; F: DNA fragment.

1.6.5. Cloning of the *pmag*-L-MAG-GFP Construct

The *pmag*-L-MAG-GFP expression construct was generated by a sequential cloning of the *pmag*-MAG 5'-region upstream of the start codon within mag exon 4, the L-MAG-GFP coding sequence and the *pmag*-MAG 3'-region downstream of the stop codon within mag exon 13 (Figure 12 and 18B: 5). In detail, the 3'-region of *pmag*-MAG was amplified by PCR with 5'MAG-HindIII-NarI and 3'MAG-Sall and subcloned into pBluescript. In a second step the 5'-region of *pmag*-MAG was amplified by PCR with 5'MAG-NotI and 3'MAG-NdeI-

HindIII, and subcloned into pBluescript upstream of the 3'-region. In the last step, the L-MAG-GFP open reading frame was amplified with 5'MAG-NdeI and 3'GFP-NarI from p α actin-L-MAG-GFP and subcloned into pBluescript between the *pmag*-MAG 5'- and 3'-region, resulting in the *pmag*-L-MAG-GFP construct.

PCR amplifications were carried out with the Expand High Fidelity PCR System (Roche, Diagnostics GmbH, Mannheim, Germany). Recombinant plasmids were grown in *Escherichia coli* DH5a cells. The orientations of all inserts were analysed by restriction mapping and PCR analysis. Sequence analysis for verification of the correct sequence was performed after all PCR amplification steps (Microsynth, Balgach, Switzerland).

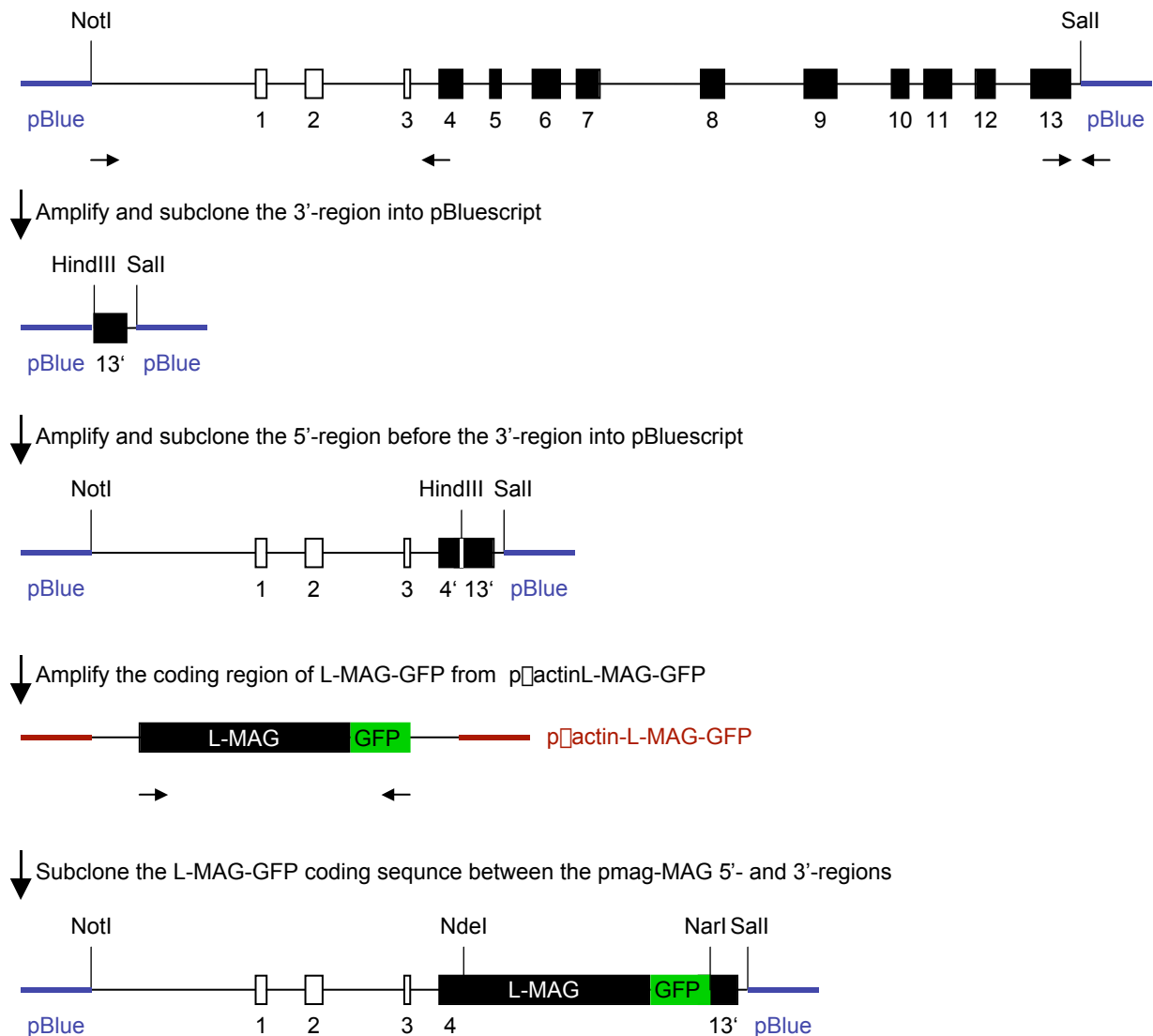


Figure 12 Cloning of the *pmag*-L-MAG-GFP expression construct. top: wild-type *pmag*-MAG mouse MAG genomic clone (size 19 kb); bottom: *pmag*-L-MAG-GFP clone having the sequence between the start codon within exon 4 and the stop codon within exon 13 replaced by the L-MAG-GFP coding sequence; white boxes: non-coding exons; black boxes: coding exons; green boxes: EGFP DNA sequence; horizontal arrows: position of primers used for amplification and subcloning.

2. Generation of Transgenic Mice

All three plasmids were treated with the restriction enzymes Sall and NotI to cut out the inserts from the pBluescript cloning vector. The inserts were separated from the cloning vectors by agarose gel electrophoresis using TAE buffer at 4°C. The DNAs were purified from the agarose gel using the GENECLEAN SPIN Kit (Q-BIO gene/Bio 101) and were further purified using the ELUTIP-D-COLUMN-SET (Schleicher & Schuell).

The transgenic mice were generated by Dr. Cécile Goujet-Zalc at the CNRS, UPS 44, Villejuif, Paris, France. The linearized DNA was injected into C56BL/6+DBA2 oocytes. About 1 pg of linearized DNA was injected per oocyte. For the *pmag*-MAG-e12GFP DNA, 153 oocytes were injected, of which 80 were implanted into 4 females. From the two born mice, one was transgenic. For the *pmag*-MAG-e13GFP DNA, 220 oocytes were injected, of which 160 were implanted into 4 females. From the 13 born mice, one was transgenic. For the *pmag*-L-MAG-GFP DNA 210 oocytes were injected, of which 117 were implanted into 7 females. From the 19 born mice, 7 were transgenic.

3. Cell Culture

The mouse oligodendrocyte precursor cell line Oli-neu (Jung et al., 1995; kindly provided by Prof. J. Trotter, Heidelberg, Germany) was cultured in Sato medium containing 1% horse serum, on poly-L-lysine coated culture dishes (Dulbecco's modified Eagle's Medium DMEM from Gibco BRL/Invitrogen; medium additives and poly L-lysine from Sigma Chemical CO., St. Louis, USA). Cells were plated at a density of 2500 to 6000 cells per cm². For differentiation, Oli-neu cells were cultured in the presence of 1 mM dbcAMP (Sigma) for up to 12 days, as described previously (Jung et al. 1995). COS7 monkey kidney cells (Gluzman 1981) were cultured in DMEM containing 10% foetal calf serum (Gibco BRL/Invitrogen). COS7 cells were plated at a density of 2500 cells per cm². Oli-neu and COS7 cells were cultured at 37°C and 5% CO₂. Transfection was carried out one day after plating with Fugene6 (Roche Diagnostics GmbH, Mannheim, Germany), according to the manufacturer's protocol. Briefly, 3 μ l Fugene6 were mixed with 100 μ l DMEM (37°C) before 2 μ g plasmid DNA was added. After 30 minutes incubation at room temperature, the transfection mix was added to the cells. Routinely, transfection efficiency of COS7 cells was about 50% and of Oli-neu cells about 40 to 50%.

4. Biochemical Methods

4.1. Generation and purification of an anti-L-MAG polyclonal antibody

To generate a polyclonal anti-L-MAG-specific polyclonal antibody, a 19-amino-acid peptide corresponding to the mouse L-MAG-specific C-terminus: (KDSYTLTEELAEYAEIRVK) was synthesized (nanoTOOLS, Denzlingen, Germany). The KLH-coupled peptide was used for the immunization of two rabbits (NZW). For the immunisation, about 100 μ g of the peptide

were dissolved in 0.5 ml PBS and emulsified with an equal volume of Complete Freund's Adjuvant. About 20 sites of the back of the rabbit were injected subcutaneous with about 0.05 ml of emulsified antigen. The first and second boosts were done with the same emulsion that was prepared with Incomplete Freund's Adjuvant. The first boost was done 4 weeks after the first immunisation, while the second boost was done 3 weeks after the first boost. The blood was taken 10 days after the second boost.

Affinity purification: the column (KDSYTLTEELAEYAEIRVK peptide coupled to matrix, made by nanoTools) was washed for 1 h with PBS 0.05% Tween20 (PBST), for 30 min with 100 mM glycine, pH 2.5, and again for 1 h with PBST. 500 μ l rabbit serum (L1 12 Wo 1. 2.Boost 725716) were mixed with 1.5 ml PBST and applied five times to the column. Unbound antibodies were washed away for 2 h with PBST. Specifically bound antibodies were eluted with 100 mM glycine pH 2.5. 1.3-ml fractions of the eluate were collected in 1.5-ml tubes containing 150 μ l 1 M Tris pH 8 on ice. The eluate was ultrafiltrated and washed with PBS four times using Centricon YM-10 tubes for 45 min with 600 g at 4°C. The following protein measurement revealed a total amount of about 100 μ g antibodies per 0,5 ml serum.

4.2. Immunocytochemistry

Cells were fixed in ice-cold paraformaldehyde (4%) for 10 min and rinsed twice with Hank's Balanced Salts (HBSS Gibco BRL/Invitrogen). Subsequently, cells were incubated with blocking buffer (1% normal goat serum, 2% Teleostean gelatine (Sigma Chemicals CO., St. Louis, USA) and 0.02% Triton X-100 (Fluka Chemie GmbH, Buchs, Switzerland) in PBS) for 1 hour at room temperature and thereby permeabilized. Primary antibodies were incubated in blocking buffer for 1 hour at room temperature. After rinsing with PBS, the secondary antibodies were incubated in blocking buffer for 30 minutes. Cells were rinsed three times with PBS and once with water and embedded with FluorSaveTM Reagent (Calbiochem/Merck KGaA, Darmstadt, Germany). To specifically analyse the extracellular localization of MAG and/or GFP, living cells were rinsed with Hank's Balanced Salts and incubated with 5% FCS/HBSS for 5 minutes at room temperature. The primary antibodies were diluted in 5% FCS/HBSS and added to the cells for 10 minutes. Then the cells were washed twice with HBSS for 5 minutes. After rinsing once with ice-cold HBSS, the cells were fixed and processed as described above.

Primary antibodies used: polyclonal anti-L-MAG (own production; dilution 1: 3'000), monoclonal anti-VSVG (kindly provided by Prof. A. Matus, FMI, Basel, Switzerland; dilution 1:50), polyclonal anti-MAG (kindly provided by Dr. A. Heape, Oulu, Finland; dilution 1:5000) and monoclonal anti-MAG (clone 513, Roche; dilution 1:500). Secondary antibodies used: Cy2-, Cy3- or Cy5-coupled anti-rabbit or anti-mouse IgG antibodies (Jackson ImmunoResearch Laboratories, Inc., West Grove, USA; dilution 1:500). A Zeiss LSM510 confocal scanning microscope was used. An optical slice of 10 μ m was used, if no other value is stated.

4.3. Myelin Purification

Fresh frozen brain samples (stored at -80°C) were thawed on ice and homogenized, with a 12- mm polytron, for about 10 seconds in 4 ml 250 mM sucrose/10 mM Hepes/2 mM EGTA pH 7.4 (buffer A containing 1 $\mu\text{g/ml}$ aprotinin, 2 $\mu\text{g/ml}$ leupeptin, 1 $\mu\text{g/ml}$ pepstatin and 100 $\mu\text{g/ml}$ PMSF) and cooled on ice for 5 min, before a second homogenisation step. Non-homogenized tissue was pelleted by a centrifugation step with 2000 rpm for 3 min at 4°C , in a SW rotor. The supernatant was poured into a new 15-ml tube and adjusted to 3.7 ml with buffer A. Furthermore, 6.7 ml 2 M sucrose/10 mM Hepes/2 mM EGTA pH 7.4 (buffer C) was added and mixed by rotation for 5 min, to reach an sucrose concentration of 1.4 M. Thereafter the sucrose gradient was set up in a 14 ml Beckmann 14x95 mm Polyallomer tube starting with 1.1 ml buffer C (2 M sucrose), followed by the 10 ml homogenate (1.4 M sucrose), 2.2 ml buffer B (850 mM sucrose) and 0.75 ml buffer A (250 mM sucrose). The gradient was centrifuged for 20 h with 25'000 rpm at 4°C in a TST-41-14 swing-out with a Centrikon T-1055 ultracentrifuge. The myelin and plasma membrane phases, that accumulated in the 250 mM and 850 mM sucrose layers, respectively, were transferred to a new 15-ml tube using a spatula or by a pipette. The samples were homogenized once in 4 ml 10 mM Hepes/2 mM EGTA, pH 7.4, with the 12-mm polytron and the volume was adjusted to 14 ml. These homogenates were pelleted at 25'000 rpm, for 3 h at 4°C . The supernatant was discarded and the pellets were resuspended in 200 - 500 μl water by intensive vortexing using a yellow micropipette tip. The samples were stored at -80°C .

4.4. Myelin Protein Quantification

Proteins were quantified by the Bradford assay. A protein dilution series was done, creating a standard curve with 100, 200, 400, 600 and 800 ng/ μl BSA (in water). Two dilution series, with water, were done for each myelin sample to reach the following dilutions: 1:5, 1:10, 1:20, 1:40 and 1:80. The Bradford reagent was diluted 1:5 in water before 20 μl sample, or standard, were mixed with 200 μl diluted Bradford reagent. For the creation of the linear standard curve, only those samples, which were within the linear range ($\text{OD}_{590\text{nm}}$ relative to protein concentration), were included. The same criteria were applied to the measured sample dilutions.

4.5. DIGs Isolation

600 μg membrane protein were suspended in a final volume of 1.5 ml containing 2% CHAPS or TritonX-100, 10 mM Tris, 150 mM NaCl, 5 mM EDTA, pH 8, and 1 mM PMSF, in a 2 ml tube, on ice in the cold-room. This was done by mixing together 600 μg protein (dissolved in water) with 500 μl 6% CHAPS, or TritonX-100, in 3xTNE (30 mM Tris, 450 mM NaCl, 15 mM EDTA, pH 8), 15 μl 100mM PMSF and water up to 1,5 ml. Then the samples were sonicated 2 times for 15 seconds on ice and incubated on a rotating wheel at 4°C for 30 minutes. Afterwards, 1.5 ml 80% sucrose in 1xTNE were added to the 1.5 ml

sample and mixed on the wheel for several minutes. To set up the gradient, 2 ml of the sample (containing 400 μ g protein) was poured into a 14-ml ultracentrifuge tube and carefully overlaid with 5 ml 30% sucrose in 1xTNE and 5 ml 5% sucrose in 1xTNE. After 21 hrs of ultra centrifugation at 4°C and with 36'000 rpm, the 12 ml of the gradient were collected, starting from the top, as 1-ml fractions with a syringe, and stored at -80°C.

4.6. SDS-PAGE and Western Blot Analysis

The gels were prepared according to Laemmli (Laemmli 1970) with some modifications. The resolving gel contained 8, or 15% Acrylamide/Bis, 375 mM Tris, pH 8.8, and 0.1 % SDS, and was polymerised with 50 μ l 10 % APS and 5 μ l Temed per 10 ml gel. The stacking gel contained 5% Acrylamide/Bis, 125 mM Tris, pH 6.8, and 0.1 % SDS, and was polymerised with 50 μ l 10 % APS and 10 μ l Temed per 10 ml gel. The 4x sample buffer contained 40% glycerol, 8 % SDS, 0.5 % bromophenol blue, 80 mM Tris, pH 6.8, and 20% β -mercaptoethanol (added just before use). The samples were denatured for 1 h at 37°C. The separation buffer contained 25 mM Tris-base, 14.4 % glycine and 1 % SDS. The gels were run overnight with 15 V. Before the protein transfer, the gels were washed once in running buffer and once in transfer buffer (25 mM Tris-base, 14.4 % glycine). The proteins were blotted to Immun-Blot PVDF Membrane (Biorad) using the Mini Trans-Blot Electrophoretic Transfer Cell (Biorad) with 50 V for 90 minutes. The blots were washed once in TBST (500 mM NaCl, 20 mM, Tris pH 7.5, and 0.05 % Tween20) before they were blocked in 3 % TopBlock (JuroSupply GmbH) in TBST for 3 h at room temperature. The primary antibody (see below) was incubated in 1 % TopBlock (TBST) overnight at 4°C. The primary antibody was washed away 3 times in TBST for 20 minutes before the secondary antibody (see below) was incubated in 1 % TopBlock (TBST) for 1 h at RT. After washing three times with TBST and once with TBS, the protein bands were detected with the ECL Western Blotting Detection Reagents (Amersham Pharmacia) and exposed to Hyperfilm ECL (Amersham Pharmacia).

4.7. Antibodies used for brain myelin Western blot analysis

Primary Antibodies	Source	Dilution
pAb L-MAG	Own production (see section 3.1.)	500
pAb total MAG	Anthony Heape, Oulu, Finland	5000
mAb MOG	Richard Reynolds, London, England	2000
mAb MBP (Nr.1118099)	Boeringer Mannheim, Germany	1000
pAb PLP/DM20	Klaus Nave, Goettingen, Germany	1000
pAb F3/contactin	Jacky Trotter, Heidelberg, Germany	500
pAb Caspr	Ori Peles/Ivo Spiegel, Rehovot, Israel	1000
Secondary Antibodies	Source	Dilution
goat-anti-rabbit IgG	Jackson Laboratories	5000
peroxidase-coupled goat-anti-mouse IgG	Jackson Laboratories	5000
peroxidase-coupled		

4.8. Densitometric quantification of Western blot results

For this quantification, equal amounts of myelin protein from the three MAL wild-type and knock-out brain myelin samples were pooled for further Western blot analysis. In one Western blot experiment, 5 different protein amounts from both pools were analysed in parallel. For example, 5 μ g (100%), 4 μ g (80%), 3 μ g (60%), 2 μ g (40%) and 1 μ g (20%) myelin protein of each genotype (myelin protein pool) were separated on one gel, blotted and analysed with the MBP antibody. Different amounts of protein were set to 100% for the different antibodies used, to achieve an optimal relation between the analysed protein amount and the signal intensity. Therefore, for the analysis of MBP, MAL, F3/contactin and Caspr, 5 μ g myelin proteins were set to 100%, whereas for the analysis of total MAG, L-MAG, PLP und MOG 1 μ g of myelin proteins were set to 100%. For the analysis of DIGs, equal volumes of fraction number 6 from the three sucrose gradient fractions of both genotypes were pooled and 37.5 μ l and 5 μ l were set as 100% for e.g. MBP and e.g. total MAG, respectively. To quantify the resulting bands on the film after a short exposure, the films were read with the AlphaInnotech Corporation Multimage Cabinet and Camera and analysed with the 'Spot Denso' module of the Chemilmager v5.5 software. The background, estimated above the specific band in each lane, was subtracted. The signal intensities were plotted against the amount of analyzed myelin protein and trend lines through the values obtained for the wild-type and the knock-out samples were added. The ratio of the slopes of the knock-out and the wild-type trend lines was the value that directly reflected the amount of the analysed myelin protein in the MAL knock-out relative to the wild-type. As an example, the analysis of the MBP levels in brain myelin is shown in Figure 13.

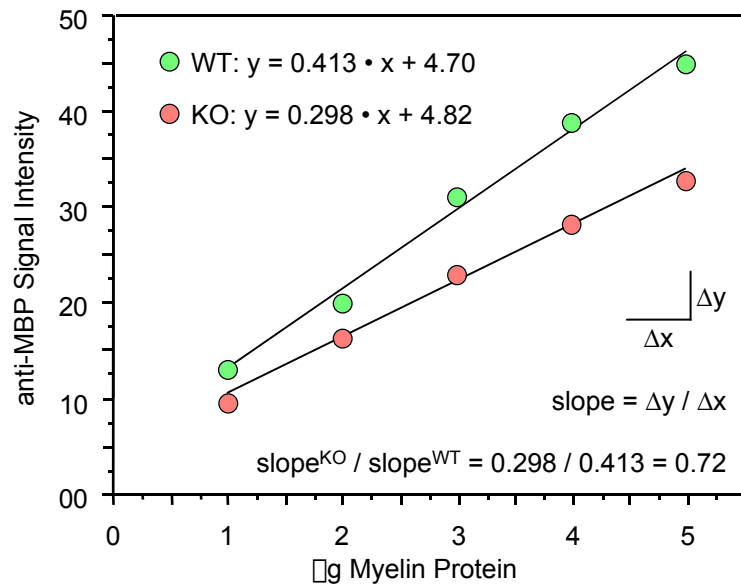


Figure 13 Illustration of the method for the quantification of a Western blot analysis.

For the analysis of the MBP levels in the MAL knock-out relative to wild-type mouse brain myelin samples, five different myelin protein amounts of both genotypes were analysed in a single Western blot analysis. The signal intensities from the densitometric analysis of the bands were plotted against the corresponding amount of analysed myelin protein. The calculated equations of the trendlines of both genotypes are indicated in the top left of the graph. The ratio of their slopes indicates the MBP levels in the knock-out samples relative to the wild-type samples (0.72; shown in the bottom right of the graph). The knock-out myelin contains 72% of the MBP protein level observed in the wild-type myelin.

Results

1. Characterization of the L- and S-MAG mRNA Levels in Oli-neu Cells upon cyclicAMP Stimulation

To investigate the regulation of MAG transcription and its alternative splicing into L- and S-MAG, we characterized which MAG isoforms are expressed by the oligodendroglial cell line Oli-neu and whether they are differentially expressed upon cAMP stimulation. Oli-neu cells grown in SATO medium proliferate and most of them have a bipolar shape. Grown under the influence of cAMP Oli-neu cells stop their proliferation, develop a radial morphology and up-regulate the expression of MAG (Jung et al. 1995). Analysis of the endogenous MAG expression revealed that about 10% of the cells express MAG, whereas upon stimulation with cAMP for 10 days about 35% of the cells express MAG. We performed an RT-PCR analysis to determine the endogenous L- and S-MAG expression levels in Oli-neu cells stimulated with cAMP for 0, 4, or 12 days (Figure 14). We used a single set of primers, which amplified the exon 10 – 13 region (5'exon10 and 3'exon13-A) leading to L- and S-MAG-specific products. The L-MAG-specific product was, due to the absence of exon 12, 45 bp shorter than the exon 12 containing S-MAG product. Our results show that in unstimulated Oli-neu cells, most of the primary transcripts were spliced into the L-MAG variant, whereas stimulation with cAMP for 4 days revealed an up-regulation of S-MAG. Stimulation for 12 days led to a strong expression of S-MAG as the main expressed isoform, while L-MAG was expressed at a lower level.

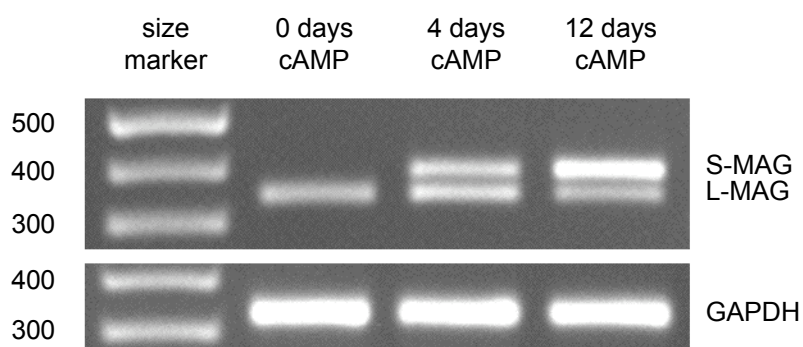


Figure 14 Effects of cAMP treatment on L- and S-MAG mRNA levels in Oli-neu cells

Oli-neu cells were grown in Sato medium containing 1 mM dbcAMP (dibutyryl-cyclicAMP) for 0, 4 and 12 days. The alternative splicing of exon 12 was analysed by the amplification of the region of exon 10 to 13 using a single primer pair (5'exon10 and 3'exon13-A, see Figure 22A). This reaction produced a L-MAG specific product of 338 bp and a S-MAG specific product of 383 bp in length. In unstimulated Oli-neu cells, L-MAG was the predominant splice variant, whereas after 12 days of cAMP stimulation more S- than L-MAG was detected. As an internal standard, GAPDH mRNA was amplified in parallel. The molecular standard bands (M) are indicated in bp.

2. MAG-GFP Fusion Proteins show normal Biosynthesis and Membrane Incorporation

To determine whether cAMP treatment leads to an S-MAG up-regulation in all MAG-expressing Oli-neu cells independently of their extent of morphological differentiation, we investigated the isoform-specific protein expression at the cellular level. To differentiate between the two isoforms, L- and S-MAG were expressed as individually tagged isoforms under the control of their promoter and regulatory region. To first study the expression and unimpaired export of these gene products, we generated cDNA expression constructs encoding L- and S-MAG fusion proteins with N- or C-terminal tags (Figure 15).

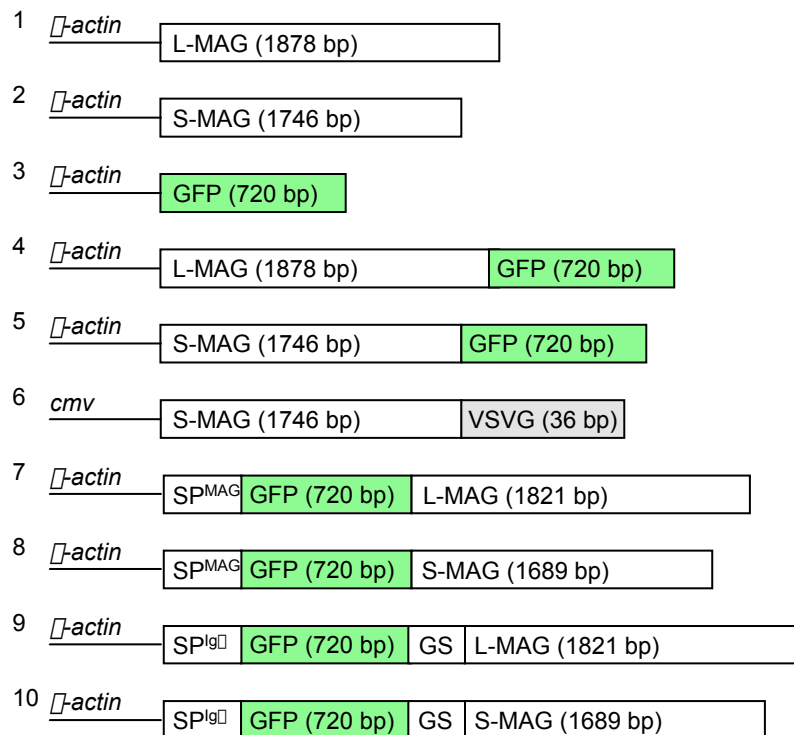


Figure 15 Schematic drawing of the different cDNA MAG fusion protein expression constructs. The promoters are drawn as a line: mouse β -actin-promoter (1-5, 7-10) and cmv-promoter (6). The open boxes of the cDNA expression constructs represent the open reading-frames. In the β -actin-magSP-GFP-MAG constructs (7,8), the GFP sequence is preceded by the MAG signal peptide sequence, whereas in the β -actin-IgkSP-GFP-MAG constructs (9,10), the GFP sequence is preceded by the signal peptide sequence of the Igk-light-chain κ and the sequences of GFP and mature MAG are linked with a DNA stretch encoding a linker peptide of five Glycine and Serine residues (GS).

2.1. L-MAG-GFP: C-terminal GFP

All experiments described below for L-MAG were also carried out for S-MAG. Since the expression patterns of the two isoforms were indistinguishable, the data for the S-MAG isoform is not shown. The expression pattern of native L-MAG and L-MAG-GFP fusion proteins were analysed in COS7 cells (Figure 16). Native L-MAG and L-MAG-GFP (Figure 15-1, 15-4) were both detected in the endoplasmic reticulum (ER), the Golgi apparatus (Figure 16A,C arrow), and in the plasma membrane, including cellular processes (Figure 16A,C arrowhead). The incorporation of L-MAG and L-MAG-GFP into the plasma membrane was confirmed by surface staining with a monoclonal antibody recognizing an extracellular MAG epitope (Figure 16B,D). L-MAG-GFP showed a distinct expression pattern when compared to soluble GFP in living cells. L-MAG-GFP was detected by its autofluorescent signal mainly in the rER and Golgi (Figure 16F, arrow) and in the plasma membrane (Figure 16F, arrowhead). Soluble GFP, however, was mainly detected in the nuclear region (Figure 16E, asterisk) and in the surrounding ER (Figure 16E, arrow), but not in the plasma membrane.

2.2. GFP-L- and GFP-S-MAG: N-terminal GFP

In parallel to the C-terminal fusion constructs, we also investigated whether fusion of GFP to the extracellular N-terminus of MAG interferes with the latter's biosynthesis and membrane incorporation. These constructs would have been required in case the C-terminal fusion proteins proved to interfere with cell viability, as seen for other C-terminal tagged GFP fusions (Caduff et al. 2001). To direct the GFP-MAG fusion protein into the secretory pathway, as seen for native MAG, the MAG signal peptide (amino acids 1-26, including 7 amino acids following the putative cleavage site) was cloned into the N-terminus of GFP. The L-MAG open reading-frame (amino acids 20-627, missing its signal peptide) was cloned into the C-terminus of GFP resulting in the β actin-magSP-GFP-L-MAG construct (Figure 15-7, 15-8). COS7 cells transfected with this construct showed no GFP autofluorescence, nor an anti-GFP or anti-MAG immunosignal (data not shown). In a second expression construct, the MAG signal peptide sequence was replaced with that of the mouse Ig κ light chain. Additionally, the GFP and the L-MAG sequences were linked with a DNA sequence encoding a five-amino-acid linker peptide consisting of glycine and serine residues. This β actin-Ig κ SP-GFP-gs-L-MAG construct (Figure 15-9, 15-10) led to the expression of GFP-gs-L-MAG in COS7 cells (Figure 16G,H). The expression pattern was comparable to that observed for L-MAG or L-MAG-GFP (Figure 16A-D). The immunofluorescent surface staining was carried out using either anti-GFP polyclonal (Figure 16H), or the anti-MAG monoclonal antibodies (data not shown). Both surface stainings showed a homogeneous distribution of GFP-gs-L-MAG, comparable to L-MAG or to that of L-MAG-GFP on the plasma membrane. The GFP autofluorescence signal intensity in living COS7 cells expressing L-MAG-GFP or GFP-gs-L-MAG fusion proteins were comparable. It is note worthy that paraformaldehyde fixation did not remarkably alter the GFP autofluorescence intensity of L-MAG-GFP, while the GFP autofluorescence intensity of GFP-gs-L-MAG, with GFP located extracellularly, was clearly reduced (data not shown).

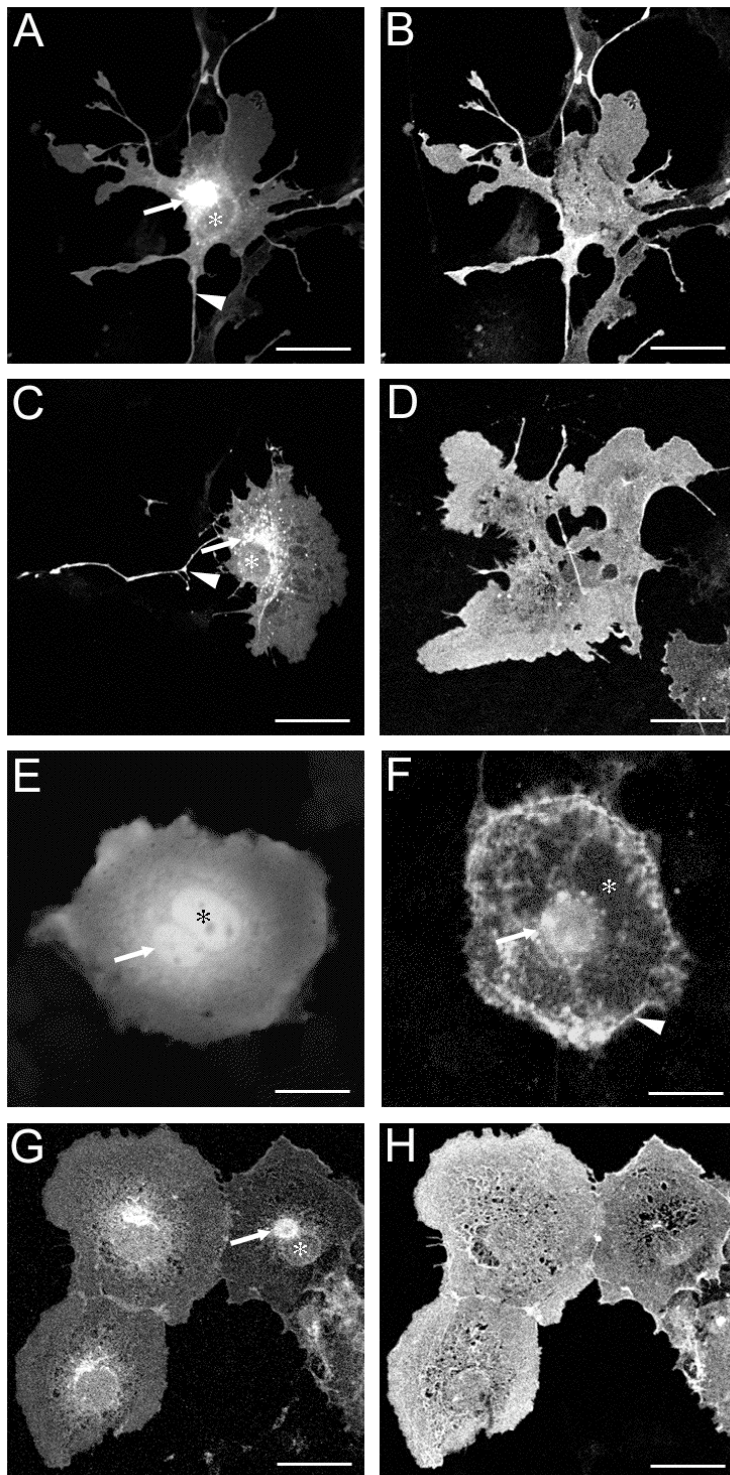


Figure 16 L-MAG-GFP and GFP-gs-L-MAG fusion protein expression patterns in COS7 cells. Laser scanning confocal microscopy was performed on COS7 cells upon transient transfection. To analyse membrane incorporation, living cells were incubated with the anti-MAG monoclonal antibody (B and D), or with a polyclonal anti-GFP antibody (H) before fixation. A, B: L-MAG-expressing cells were stained with an anti-L-MAG antibody (A), recognizing the intracellular C-terminus, or with anti-MAG mAb 513 (B), recognizing an extracellular epitope (“living staining”). C, D: L-MAG-GFP expressing cells were visualized by the GFP autofluorescence (C) or living cells were incubated with the MAG mAb 513 (D). E, F: Living cells expressing soluble GFP (E) or L-MAG-GFP (F) were visualized by the GFP autofluorescence. The rather diffuse GFP signal originates from the analysis of living cells. G, H: GFP-gs-L-MAG-expressing cells (GFP at the extracellular N-terminus of MAG) were visualized by the GFP autofluorescence (G), or living cells were incubated with an anti-GFP antibody (H). Arrows point to the ER and Golgi; arrowheads point to cellular processes (A,C) and plasma membrane (F); asterisks mark the position of the nucleus. Note that COS7 cells show a high degree of heterogeneity within their cellular morphology. MAG and its GFP fusion proteins were detected in all cells irrespective of their morphology. Bar: A, B: 35 μm , C: 38 μm , D: 36 μm , E: 44 μm , F: 26 μm , E, F: 49 μm .

2.3. Comparable Expression Patterns of L-MAG-GFP and S-MAG-VSVG in Oli-neu Cells

To check the correct sorting and transport of the L- and S-MAG fusion proteins in oligodendroglial cells, we analysed their expression pattern in Oli-neu cells (Figure 17). The strong increase in L-, or S-MAG expression levels upon transfection of Oli-neu cells revealed no obvious differences in their subcellular localization (Figure 17A,B). Both

isoforms were detected in the rER and Golgi and the immunofluorescent surface staining revealed a homogeneous distribution of L-MAG (Figure 17A) and S-MAG (Figure 17B) in the Oli-neu plasma membrane, indicating that the two isoforms are not sorted differently in these cells. L-MAG-GFP (Figure 17C,D) and the S-MAG-VSVG fusion proteins (Figure 15-6 and 17E,F) revealed both a subcellular localization in the rER, Golgi (Figure 17C,E arrow) and in the plasma membrane, including cellular processes (Figure 17C,E arrowhead). Their immunofluorescent surface staining illustrated their incorporation into the plasma membrane (Figure 17D and F, respectively). The overall expression patterns of L-MAG-GFP and S-MAG-VSVG, and their distribution within the plasma membrane of Oli-neu cells, are comparable to the patterns of native L- and S-MAG (Figure 17A and B, respectively), indicating that the fusion of GFP to L-MAG and the fusion of the VSVG-tag to S-MAG seem to influence neither their synthesis and transport, nor their distribution within the plasma membrane in Oli-neu cells.

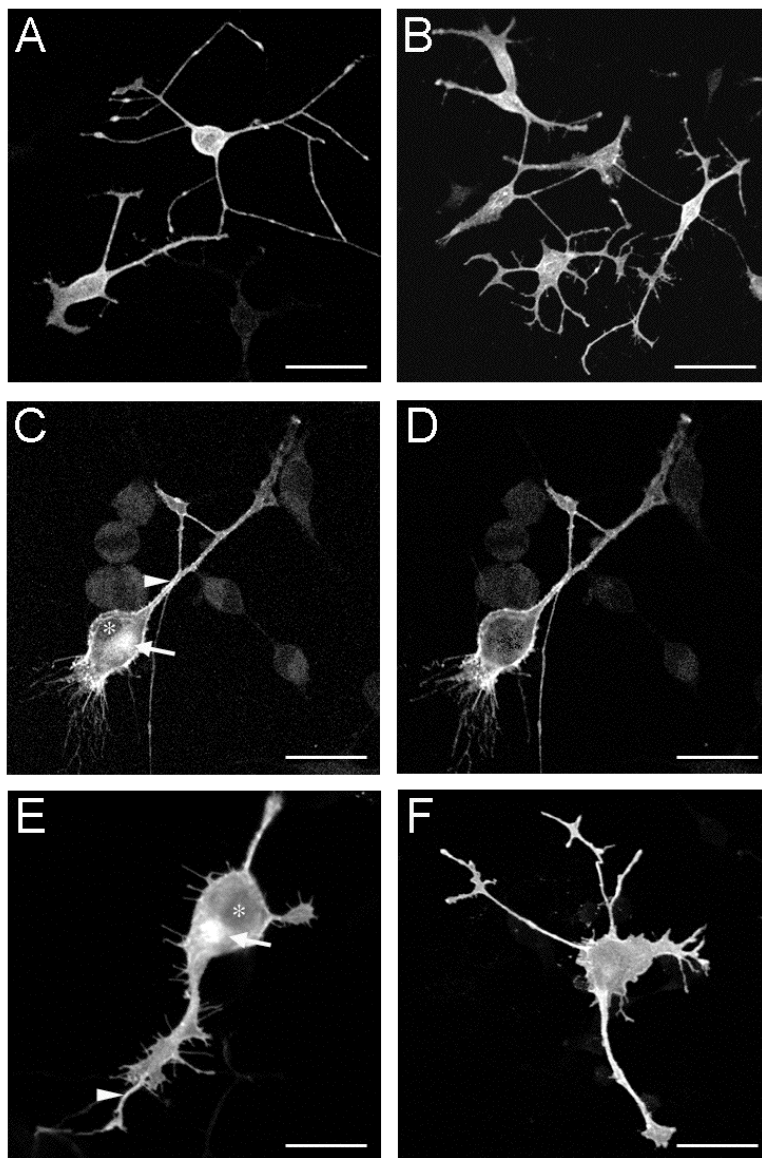


Figure 17 Expression pattern of L-MAG, S-MAG, L-MAG-GFP and S-MAG-VSVG in Oli-neu cells. Laser scanning confocal microscopy was performed on Oli-neu cells upon transient transfection. To analyse membrane incorporation, living cells were incubated with the anti-MAG monoclonal antibody before fixation (A,B,D,F). A,B: L-MAG- (A), or S-MAG- (B) expressing cells were visualized by the anti-MAG mAb before fixation. C,D: A L-MAG-GFP-expressing cell was visualized by its GFP autofluorescence (C) or by the anti-MAG mAb immunofluorescent signal (D) in an optical slice of 4 μm at the position of its nucleus. E,F: S-MAG-VSVG-expressing cells were stained with an anti-VSVG antibody (E), or visualized by the anti-MAG mAb signal before fixation (F). Arrows point to the ER and Golgi; arrowheads point to the cellular processes; asterisks mark the position of the nucleus. Bar: A, B: 36 μm , C, D: 23 μm , E, F: 38 μm .

3. Expression of Individually Tagged MAG Isoforms from Genomic Expression Constructs

3.1 Expression of L- and S-MAG from a Genomic Mouse MAG Clone in Oli-neu Cells

We have used a mouse MAG gene cDNA clone to generate genomic expression constructs encoding individually tagged L- and S-MAG isoforms. This genomic clone has a length of about 19 kb and includes a 1.8 kb promoter sequence and all 13 exons: *pmag*-MAG (Figure 18A, 18B-1).

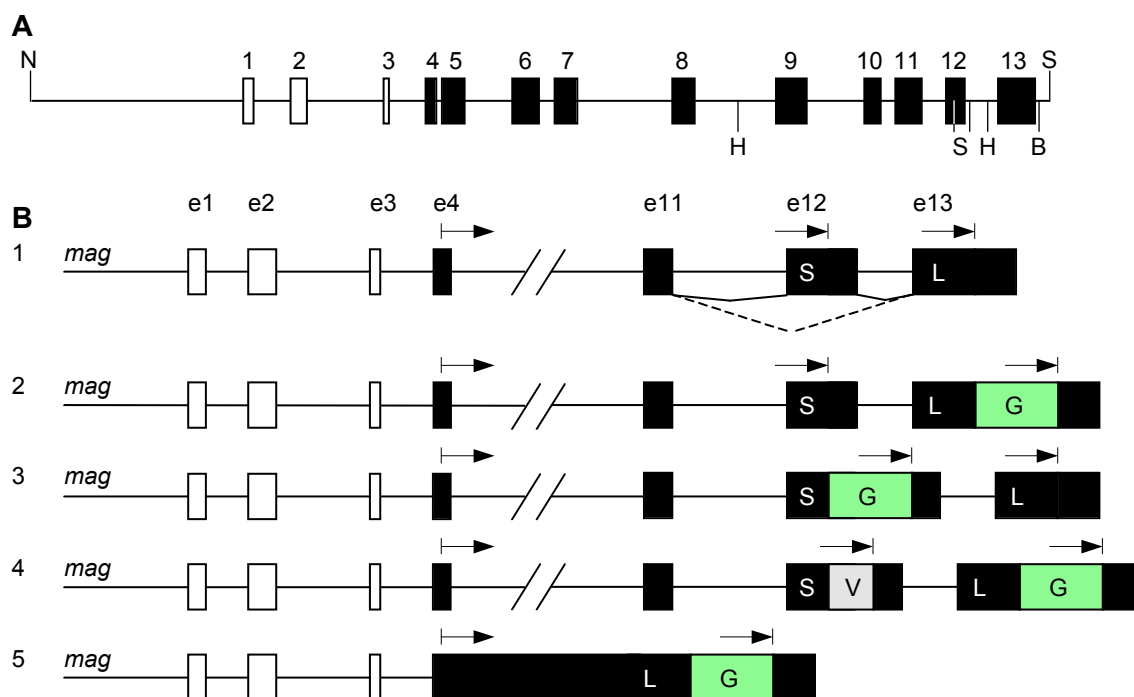


Figure 18 Schematic drawing of the mouse MAG gene clone and the genomic MAG fusion protein expression constructs

The genomic mouse MAG clone (A) has a length of 19 kb, including a 1.8 kb MAG promoter sequence. The 5' non-coding exons are drawn in open boxes while the coding exons are drawn as black boxes. Restriction sites for the subcloning into pBluescript KS- are indicated above the line: NotI (N) and Sall (S), whereas the sites used for the insertions into exon 12 and 13 are indicated below the line: HindIII (H), BglIII (B) and SmaI (S, two neighbouring sites). The alternative splicing of exon 12 is indicated with continuous lines for its inclusion, while its skipping is drawn with a dashed line. The positions of the start and stop codons are indicated (arrows) for all genomic expression constructs (B): 1: *pmag*-MAG (wild-type), 2: *pmag*-MAG-e13GFP, 3: *pmag*-MAG-e12GFP, 4: *pmag*-MAG-e12VSVG-e13GFP, 5: *pmag*-L-MAG-GFP. Abbreviations: S: S-MAG C-terminus; L: L-MAG C-terminus; G: GFP; V: VSVG-tag.

Transfection of Oli-neu cells with *pmag*-MAG and cAMP stimulation led to a significant increase of the MAG expression levels (Figure 19), showing that this genomic MAG clone contains all promoter elements necessary to induce transcription. The percentage of Oli-neu cells expressing surplus MAG following transfection with *pmag*-MAG and cAMP stimulation was around 10%. The transfection efficiency of Oli-neu cells with the 22-kb *pmag*-MAG plasmid DNA could not be determined, since not all transfected cells are expected to express MAG protein from the transfected DNA due to the MAG-specific

promoter. However, given that about 35% of the Oli-neu cells express endogenous MAG (activate the MAG promoter) and the transfection efficiency of Oli-neu cells using the 5-kb p \square actin-EGFP plasmid DNA was around 40-50%, the 10% of Oli-neu cells expressing MAG from the *pmag*-MAG plasmid are in the expected range. Thus, the transfection efficiencies of Oli-neu cells with the 5-kb (p \square actin-EGFP) or the 22-kb (*pmag*-MAG) plasmid DNAs seem to be comparable.

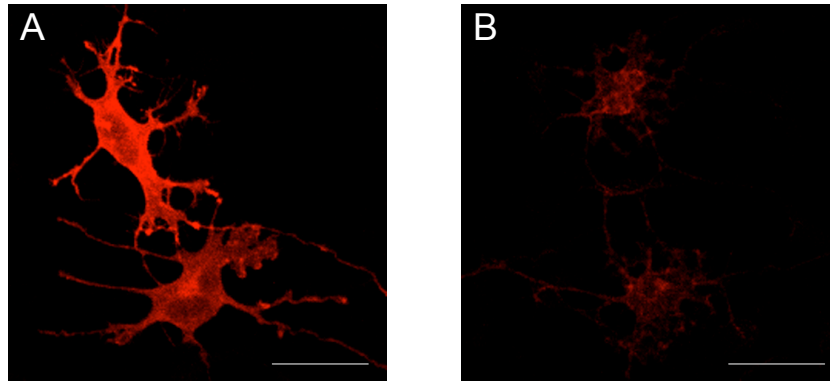


Figure 19 Expression of MAG from the wild-type genomic mouse MAG clone *pmag*-MAG in Oli-neu cells. Laser scanning confocal microscopy was performed on Oli-neu cells upon transient transfection with the wild-type genomic mouse MAG plasmid DNA. *pmag*-MAG-transfected (A) and -untransfected (B) cells after 3 days cAMP treatment were stained with anti-MAG mAb. Transfected cells show a much higher MAG expression compared to the endogenous expression in untransfected cells. Bar: A: 46 μ m, B: 59 μ m.

L-MAG was mainly localized in bipolar cells shown by the specific anti-L-MAG antibody (Figure 20B arrow), whereas immunofluorescence for both MAG isoforms revealed strong staining also of the radial-shaped cells with many processes (Figure 20A arrow), suggesting the expression of the S-MAG isoform. These results indicate that primary MAG transcripts are synthesized from *pmag*-MAG and are alternatively spliced into L- and S-MAG specific mRNAs.

3.2. Expression of L-MAG-GFP in Bipolar Oli-neu Cells from *pmag*-MAG-e13GFP

To generate a single genomic expression construct that encodes L-MAG-GFP and untagged S-MAG, we inserted the GFP DNA sequence directly into the L-MAG specific C-terminus-encoding exon 13 of *pmag*-MAG (Figure 18B-1). This *pmag*-MAG-e13GFP (Figure 18B-2, for the cloning strategy see Figure 10) construct was reintroduced into Oli-neu cells to analyse the alternative splicing of primary transcripts originating from this construct and the corresponding expression of the L-MAG-GFP and S-MAG protein. Both, tagged L-MAG-GFP and untagged S-MAG were expressed from this construct (Figure 20C,D). The expression of L-MAG-GFP could be shown by the overlapping anti-L-MAG immunofluorescence (Figure 20C main picture), GFP-autofluorescence (Figure 20D) and anti-MAG immunofluorescent signal (not shown). The L-MAG-GFP-expressing cells always possessed few processes, independently of the cAMP stimulation time. In contrast, the expression of untagged S-MAG was detected in cells with a radial shape following cAMP stimulation (Figure 20C,D inset). Unexpectedly, the number of L-MAG-GFP

expressing cells following transient transfection with the *pmag*-MAG-e13GFP construct was much lower (beneath 1%) compared to number of cells expressing surplus L-MAG following transfection with the wild-type *pmag*-MAG construct.

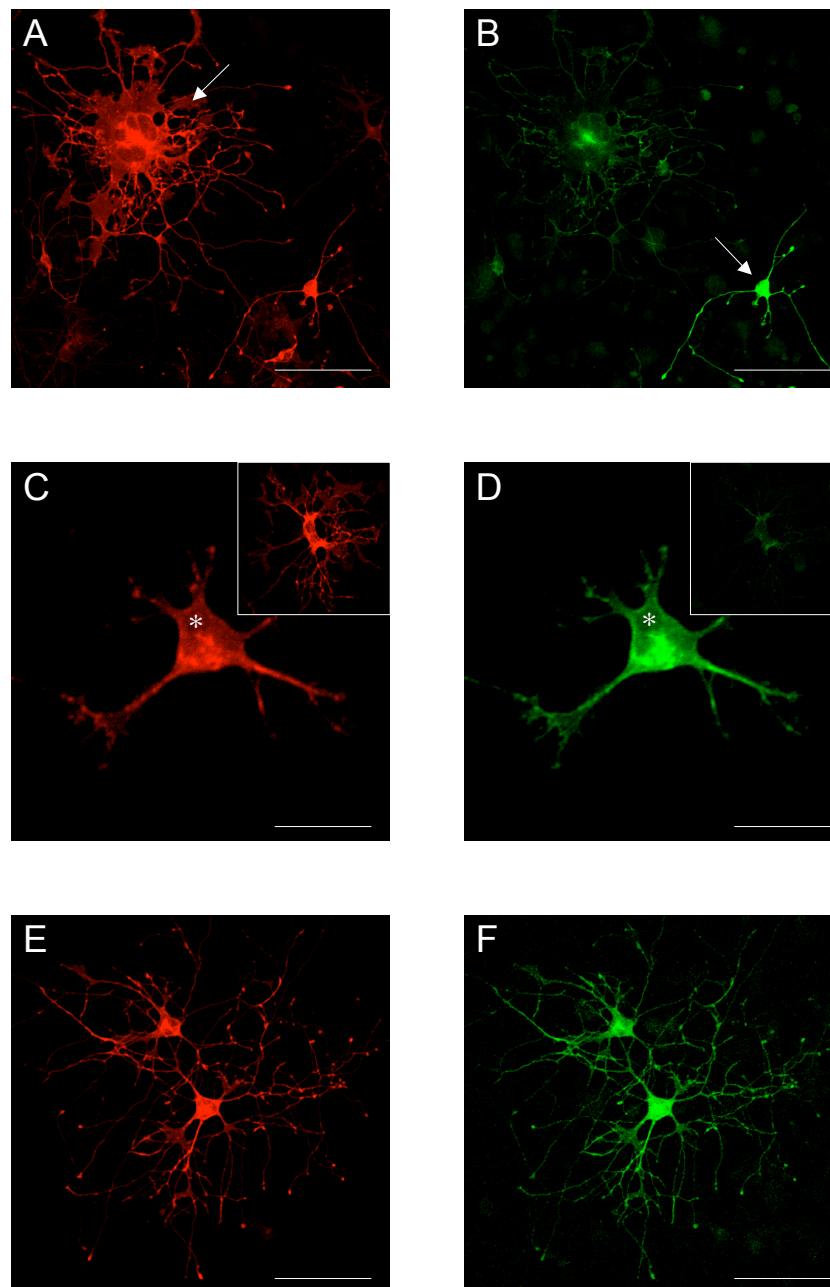


Figure 20 Expression of individually tagged MAG isoforms from genomic constructs in Oli-neu cells
Laser scanning confocal microscopy was performed on Oli-neu cells upon transient transfection with the genomic expression constructs. A,B: *pmag*-MAG-transfected cells after 6 days cAMP treatment were stained with anti-MAG mAb (A) recognizing both isoforms and anti-L-MAG specific antibody (B). C,D: *pmag*-MAG-e13GFP (GFP for L-MAG) transfected, but unstimulated cells were detected with anti-L-MAG antibody (C) or by its GFP autofluorescence (D); the top right inset within C, D: 6 days cAMP-treated cells were stained with anti-MAG mAb (C, inset), or detected by its GFP autofluorescence (D, inset). E,F: *pmag*-MAG-e12GFP (GFP for S-MAG) transfected cells after 6 days cAMP treatment were stained with anti-MAG mAb (E) or detected by its GFP autofluorescence (F). The position of the nucleus is marked by an asterisk (C, D). Bar: A, B: 97 μ m, C, D: 21 μ m, E, F: 61 μ m.

The expression of untagged S-MAG was analysed at the mRNA level. RT-PCR and subsequent sequence analysis showed exon 12 inclusion in stimulated cells, confirming that splicing for S-MAG occurred normally. In conclusion, the *pmag*-MAG-e13GFP construct demonstrated that L-MAG is predominantly expressed in bipolar cells, independently of the cAMP stimulation.

3.3. Expression of S-MAG-GFP, or S-MAG-VSVG in Radial Oli-neu Cells from *pmag*-MAG-e12GFP, or -e12VSVG

To characterize specific S-MAG expression, GFP was introduced into the S-MAG-specific exon 12 of *pmag*-MAG (Figure 18B-1). The analysis of this *pmag*-MAG-e12GFP construct (Figure 18B-3, for the cloning strategy see Figure 11) in Oli-neu cells illustrated S-MAG-GFP expression exclusively in cells with a radial shape and many processes (Figure 20E,F). Immunofluorescence (Figure 20E) and GFP autofluorescence (Figure 20F) shows that S-MAG-GFP is evenly distributed within the plasma membrane of the Oli-neu cells. The number of S-MAG-GFP-expressing cells was strongly increased with prolonged cAMP stimulation, whereas, in untreated cells, S-MAG-GFP-expressing cells were not detected. The overall number of S-MAG-GFP expressing cells was comparable to the number of cells expressing surplus MAG following transfection with the wild-type *pmag*-MAG construct. To detect, whether L-MAG is alternatively spliced from the *pmag*-MAG-e12GFP construct, immunofluorescent analysis for L-MAG was performed. For this, we used the L-MAG specific antibody recognizing the C-terminal epitope lying within exon 13: no specific immunosignal could be detected (data not shown). RT-PCR and subsequent sequence analysis showed that the S-MAG-GFP-encoding mRNA contained all exons, including exon 13, correctly joined together. The L-MAG mRNA originating from the *pmag*-MAG-e12GFP construct could not be analysed, because the transcript derived from the construct cannot be distinguished specifically from the endogenous one.

Our analysis showed that the insertion of the GFP DNA sequence (720 base pairs) into exon 12 (45 bp) did not disturb the generation and regulation of mRNAs including exon 12 and 13, but unexpectedly disturbed the skipping of the elongated exon 12. To check whether this is due to the large size of GFP, we have chosen the shorter VSVG-tag (36 bp). Analysis of the *pmag*-MAG-e12VSVG construct in Oli-neu cells, however, showed the same characteristics as the *pmag*-MAG-e12GFP construct, namely the expression of S-MAG-VSVG exclusively in radial Oli-neu cells following cAMP treatment, and the absence of untagged L-MAG expression (data not shown). These results from the *pmag*-MAG-e12GFP and the *pmag*-MAG-e12VSVG constructs indicate that the length of the DNA inserted in front of the exon 12 stop codon is not critical, but rather the insertion per se seems to disturb the joining of exon 11 to exon 13 necessary for L-MAG expression. However, both constructs revealed that S-MAG is exclusively expressed in cells with a radial morphology following cAMP treatment. In addition, the number of cells expressing either GFP-, or VSVG-tagged S-MAG is comparable to that observed using the wild-type *pmag*-MAG construct.

3.4. Simultaneous Expression of S-MAG-VSVG and ‘Soluble GFP’ from the Genomic Expression Construct *pmag-MAG-e12VSVG-e13GFP*

The construction of a genomic expression vector containing the VSVG-tag in exon 12 (fused to S-MAG) together with GFP in exon 13 (fused to L-MAG) revealed more aspects of the impaired alternative splicing of tagged exon 12.

3.4.1. The Protein Expression Pattern of S-MAG-VSVG and L-MAG-GFP within Single Cells

The analysis of the *pmag-MAG-e12VSVG-e13GFP* construct (Figure 18B-4) in Oli-neu cells displayed both an anti-VSVG signal (Figure 21A) and an GFP autofluorescent signal (Figure 21B). The GFP signal (corresponding to L-MAG-GFP) was detected in cells with a bipolar shape, whereas the VSVG signal (corresponding to S-MAG-VSVG) was detected in more radial cells. Cells with an intermediate process number were positive for both GFP and VSVG (Figure 21). The subcellular distribution of the VSVG signal (Figure 21A) was comparable to that of MAG (Figure 20A,B), or S-MAG-GFP (Figure 20E,F). This pattern includes the rER (Figure 21A, arrow), plasma membrane and processes (Figure 21A arrowheads), but clearly excludes the nuclear region (Figure 21A, asterisk). The GFP signal, however, resembles that of soluble GFP, namely localization in the ER (Figure 21B, arrow), cytoplasm and in the nuclear region (Figure 21B asterisk), but excluding the plasma membrane processes. This pattern was clearly different to the one seen for L-MAG-GFP in Oli-neu cells transfected either with the β -actin-L-MAG-GFP (Figure 17C,D), or *pmag-MAG-e13GFP* constructs (Figure 20C,D).

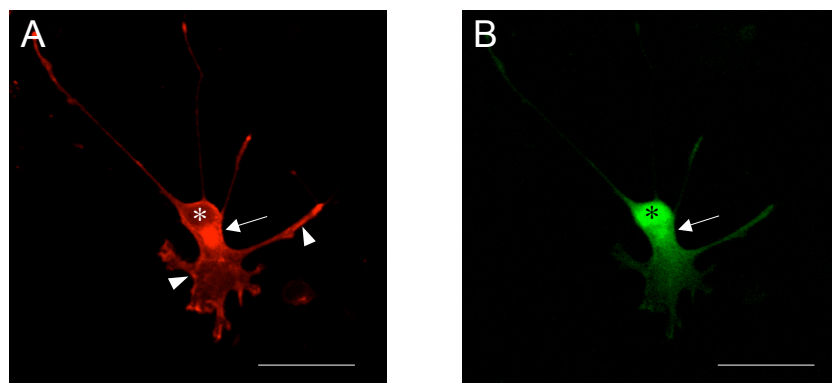


Figure 21 Expression of individually tagged MAG isoforms from a single genomic construct in Oli-neu cells. Laser scanning confocal microscopy was performed on Oli-neu cells upon transient transfection with the *pmag-MAG-e12VSVG-e13GFP* (VSVG for S-MAG, GFP for L-MAG) genomic expression construct. A,B: transfected cells were treated for 4 days with cAMP and were stained with anti-VSVG antibody (A) or detected by its GFP autofluorescence (B). Note that the GFP autofluorescent signal in B mainly highlights the nucleus (asterisk) and the ER (arrow), whereas the anti-VSVG signal detects exclusively the rER, Golgi (arrow) and plasma membrane and cellular processes (arrowhead). The position of the nucleus is marked by an asterisk (A, B). Bar: A, B: 32 μ m.

In addition, the GFP-positive cells, transfected with the *pmag*-MAG-e12VSVG-e13GFP construct, did not show any L-MAG immunosignal, which is in line with our previous observations with the S-MAG-GFP, or S-MAG-VSVG constructs. The number of GFP-, or VSVG-positive cells was comparable to the number observed for the expression of surplus MAG from the wild-type *pmag*-MAG construct. Taken together, the insertion of the VSVG tag-encoding DNA into exon 12 does not seem to disturb the expression of S-MAG-VSVG, but results in a disturbed skipping of exon 12 leading to the translation of GFP instead of L-MAG-GFP. However, the *pmag*-MAG-e12VSVG-e13GFP construct revealed the expression of GFP (skipped exon 12) in bipolar cells and of S-MAG-VSVG (including exon 12) in radial Oli-neu cells, indicating that the regulation of L-/S-MAG mRNA splicing occurred correctly.

3.4.2. L-MAG-GFP and S-MAG-VSVG mRNAs Show Normal Length and Regulation

To obtain further insight into the regulation and splicing of L- and S-MAG-specific transcripts from the *pmag*-MAG-e12VSVG-e13GFP construct, we performed a RT-PCR analysis. The L- and S-MAG mRNA levels were specifically amplified by the use of the L- and S-MAG-specific forward primers 5'exon11/13 and 5'exon12, respectively (Figure 22A). We compared the endogenous L- and S-MAG mRNA levels with those from *pmag*-MAG- and *pmag*-MAG-e12VSVG-e13GFP-transfected Oli-neu cells. The cells were stimulated with cAMP for 6 days to achieve the co-expression of L- and S-MAG mRNAs. Both constructs elevated the L- and S-MAG mRNA levels (Figure 22B1,B2: lane 2,3) in a similar manner compared to the endogenous levels (Figure 22B1,B2: lane 1). The S-MAG-VSVG product (Figure 22B1: lane 3) had a correct length and no product of false length was amplified, showing the correct joining of exon 12 to exon 13 in the 3' non-coding region of the S-MAG-VSVG mRNA. The L-MAG-GFP-specific product (Figure 22B2: lane 3) also showed the expected length and no product of false length was detected. This L-MAG-GFP-specific product represents mRNAs having exon 11 joined to exon 13. To investigate the existence of a full-length L-MAG-GFP mRNA from the *pmag*-MAG-e12VSVG-e13GFP construct, we amplified the coding sequence by RT-PCR. The unique *Sma*I restriction site in exon 12 was used to digest all the products containing exon 12. This digest revealed that all products contained exon 12 and none encoded L-MAG-GFP. The same experiment carried out with *pmag*-MAG revealed L- and S-MAG-specific full-length products (data not shown). In summary, the specific amplification of mRNAs having exon 11 joined to exon 13 did not confirm the expected disturbed skipping of exon 12 for transcripts from *pmag*-MAG-e12VSVG-e13GFP. However, the absence of full-length mRNAs without exon 12 still underlines the possibility that the skipping of exon 12 containing VSVG generates a fragmented mRNA encoding GFP instead of L-MAG-GFP.

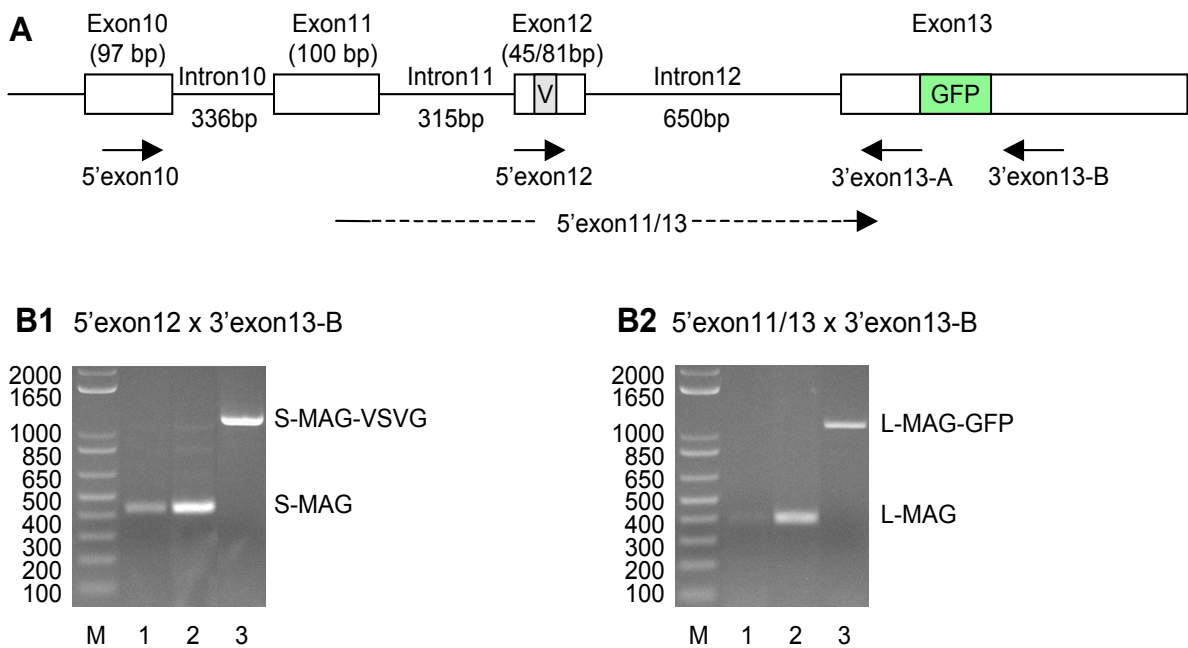


Figure 22 RT-PCR analysis of L- and S-MAG mRNA levels transcribed from the *pmag*-MAG-e12VSVG-e13GFP genomic construct in cAMP treated Oli-neu cells.

A: Schematic drawing spanning the mouse MAG genomic sequence from exon 10 to 13. The colored boxes in exon 12 and 13 represent the VSVG-tag (36 bp) and the GFP sequence (720 bp). Below the primers are shown in respect to their position. The primer 5'exon11/13 was designed to hybridise with the exon 11/13 junction. B1, B2: Oli-neu cells were grown in Sato medium containing 1 mM cAMP for 6 days (B1,B2: lane 1) and were transfected with wild-type *pmag*-MAG (B1,B2: lane 2) or with *pmag*-MAG-e12VSVG-e13GFP (B1,B2: lane 3). B1: The primer pair 5'exon12 x 3'exon13-B amplified specifically S-MAG mRNAs due to the position of the 5' primer in exon 12. The corresponding wild-type S-MAG products have a size of 409 bp, while the S-MAG-VSVG products have a size of 1165 bp, due to the additional 36 bp of the VSVG sequence in exon 12 and the 720 bp of the GFP sequence in exon 13. B2: The primer pair 5'exon11/13 x 3'exon13-B amplified specifically L-MAG products due to the hybridisation of the 5' primer with the exon 11/13 junction. The corresponding wild-type L-MAG products have a size of 377 bp, while the L-MAG-GFP products have a size of 1097 bp, due to the additional 720 bp of the GFP sequence. The molecular standard bands (M) are indicated in bp.

3.5. Constitutive Expression of L-MAG-GFP from the Genomic Expression Construct *pmag*-L-MAG-GFP

For a constitutive expression of L-MAG-GFP under the control of the endogenous mag promoter, we have replaced the region of *pmag*-MAG between its start codon (within exon 4) and the second stop codon (within exon 13), with the open reading-frame of L-MAG-GFP (Figure 18B-5). This *pmag*-L-MAG-GFP construct was reintroduced into Oli-neu cells to analyse the expression of the L-MAG-GFP protein. Upon cAMP stimulation, L-MAG-GFP was also expressed in rather differentiated cells containing various processes (Figure 23A,B). This shows that the L-MAG-GFP is constitutively expressed under the control of the mag promoter and is no longer restricted to the less differentiated bipolar cells due to the absence of the alternative splicing. The subcellular distribution of the L-MAG-GFP fusion protein, detected by the anti-L-MAG signal (Figure 23A) and the GFP-autofluorescence signal (Figure 23B), was restricted to the rER and Golgi (arrow) and the various cellular processes, whereas the nuclear region was negative (arrowhead). This pattern is comparable to that of L-MAG-GFP expressed from the \square actin-L-MAG-GFP (Figure 17C,D) or the *pmag*-MAG-e13GFP (Figure 20C,D) expression constructs.

However, the number of L-MAG-GFP-expressing cells was relatively small (beneath 1%), comparable to the situation observed for the expression of L-MAG-GFP from the genomic expression construct *pmag*-MAG-e13GFP.

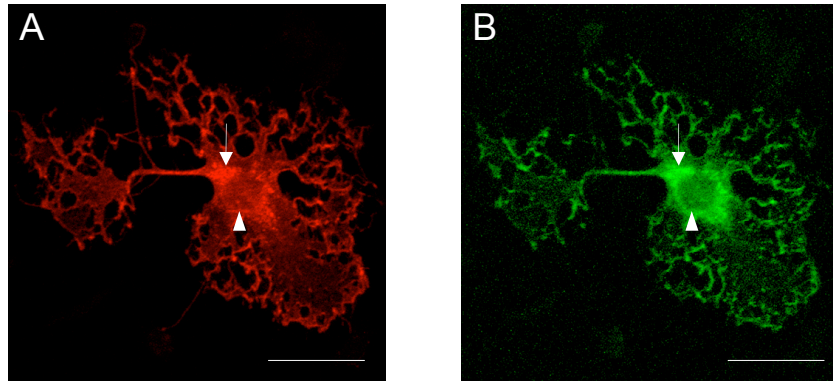


Figure 23 Constitutive expression of L-MAG-GFP driven by the *mag* promoter in Oli-neu cells
Laser scanning confocal microscopy was performed on Oli-neu cells upon transient transfection with the *pmag*-L-MAG-GFP genomic expression construct. Transfected cells were treated for 6 days with cAMP and were stained with anti-L-MAG antibody (A) or detected by its GFP autofluorescence (B). Note the relatively high degree of morphological differentiation of this L-MAG-GFP-positive cell. The position of the nucleus is marked by an arrowhead, and the position of the rER and Golgi is marked by an arrow. Bar: A, B: 43 μ m.

In summary the analysis of the genomic expression constructs encoding individually tagged MAG isoforms revealed that L-MAG is the predominant isoform in unstimulated, bipolar Oli-neu cells, whereas S-MAG expression is induced following cAMP stimulation in radial-shaped Oli-neu cells. Furthermore, the insertion of the GFP, or VSVG DNA sequences into the S-MAG-specific exon 12 leads to expression of the corresponding S-MAG fusion protein in a normally regulated manner and with a normal expression level. However, these insertions into exon 12 did affect the skipping of exon 12 for the expression of L-MAG. On the other hand, the insertion of the GFP DNA sequence into the L-MAG specific exon 13 led to expression of both isoforms in the expected regulated manner, but the number of L-MAG-GFP expressing cells was too small compared to those expressing L-MAG from the wild-type construct. A similarly small number of L-MAG-GFP-expressing cells could be observed when employing the *pmag*-L-MAG-GFP construct.

4. Generation of MAG-GFP Transgenic Mouse Lines

For a better investigation of the differential expression and localization of L- and S-MAG during myelin formation and maintenance and in mouse models for demyelinating neuropathies, we have generated three different transgenic mouse lines. We have used the following three constructs:

- *pmag*-MAG-e13GFP line (expression of L-MAG-GFP and untagged S-MAG under the control of the mag promoter and the regulatory process of alternative splicing)
- *pmag*-MAG-e12GFP line (expression of S-MAG-GFP under the control of the mag promoter and the regulatory process of alternative splicing)
- *pmag*-L-MAG-GFP line (constitutive expression of L-MAG-GFP under the control of the mag promoter in the absence of the regulatory process of alternative splicing)

The tail biopsy PCR analysis of the born animals that had developed out of the injected oocytes, revealed that one animal had incorporated the *pmag*-MAG-e13GFP DNA, one animal had incorporated the *pmag*-MAG-e12GFP DNA, and 7 animals had incorporated the *pmag*-L-MAG-GFP DNA into their genome. The sex and the date of birth of these founder animals are given in Table 2.

Construct:	Founder Number	Sex	Date of Birth
<i>pmag</i> -MAG-e13GFP	6	male	29/07/02
<i>pmag</i> -MAG-e12GFP	2	male	28/07/02
<i>pmag</i> -L-MAG-GFP	1	female	29/07/02
<i>pmag</i> -L-MAG-GFP	2	male	29/07/02
<i>pmag</i> -L-MAG-GFP	3	female	29/07/02
<i>pmag</i> -L-MAG-GFP	6	male	29/07/02
<i>pmag</i> -L-MAG-GFP	9	male	29/07/02
<i>pmag</i> -L-MAG-GFP	12	female	29/07/02
<i>pmag</i> -L-MAG-GFP	15	female	29/07/02

Table 2 List of founder animals that contain either the *pmag*-MAG-e13GFP, or the *pmag*-MAG-e12GFP, or the *pmag*-L-MAG-GFP transgenes.

4.1. The *pmag*-MAG-e13GFP Mouse Line

To analyse the L-MAG-GFP expression of the single founder animal, we performed immunohistochemistry on a tail biopsy that was taken at the age of one month. These tail peripheral nerves gave neither a GFP autofluorescence signal, nor an anti-GFP signal. The anti-MAG staining produced a periaxonal signal comparable to that observed in wild-

type animals. The L-MAG expression in the peripheral nervous system reaches its highest level around postnatal day 10, whereas at the age of one month, only background levels of L-MAG can be expected. The absence of the GFP and the anti-GFP signals might therefore result out of a predominant splicing of the primary MAG transcripts into the S-MAG splice variant.

The analysis of the L-MAG-GFP expression in the central nervous system has not been possible until now, because the founder animal has not yet passed the transgene on to the F1 animals (46 animals have been analyzed so far).

4.2. The *pmag*-MAG-e12GFP Mouse Line

4.2.1. The *pmag*-MAG-e12GFP Peripheral Myelin

To analyse the S-MAG-GFP expression of the single founder animal, we performed immunohistochemistry on a tail biopsy that was taken at the age of one month. In these peripheral nerves of the tail, a strong GFP autofluorescence, together with an overlapping anti-GFP signal was detected (Figure 24A,B).

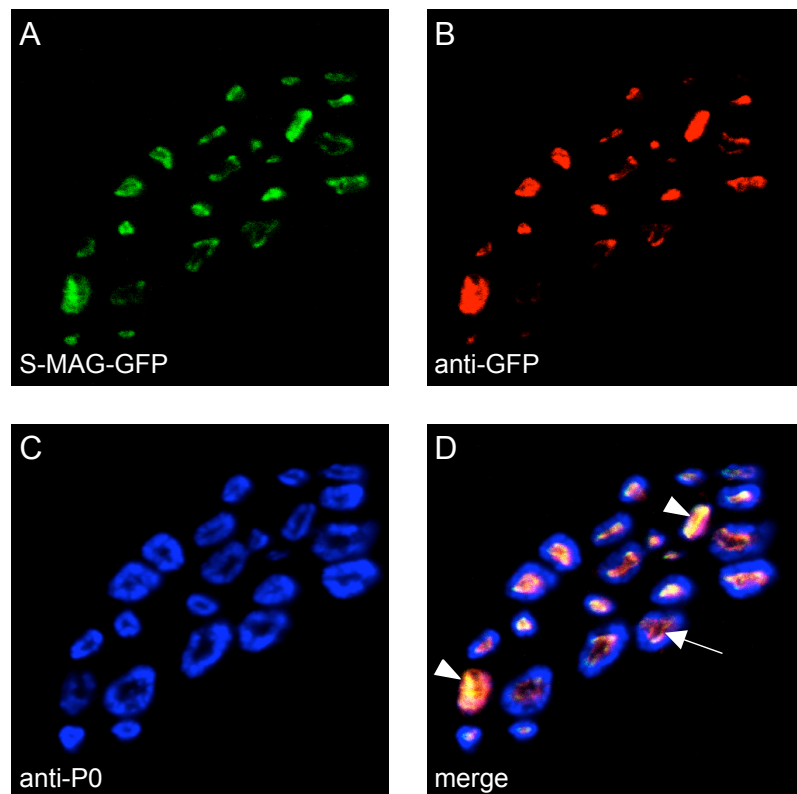


Figure 24 Analysis of the S-MAG-GFP expression in a tail biopsy from the *pmag*-MAG-e12GFP mouse. Laser scanning confocal microscopy was performed on a tail biopsy. The S-MAG-GFP expression was visualized by the GFP autofluorescent signal (green) and an anti-GFP signal (red). The anti-P0 signal (blue) depicts the compact myelin. Note the periaxonal localization of S-MAG-GFP (arrow, green and red signal), whereas P0 (blue) is localized in the compact myelin sheath. S-MAG-GFP expression in the region of 'compact myelin' together with low levels of P0 probably reflects Schmidt-Lanterman incisures (arrowheads).

Interestingly, S-MAG-GFP was localized within the periaxonal region, where MAG is known to be expressed. This expression pattern was clearly different from the pattern of the compact myelin protein zero (P0; Figure 24C). The expression pattern of the S-MAG-GFP shows that the C-terminal fusion of GFP to S-MAG does not affect its targeted trafficking and incorporation into the periaxonal membrane of peripheral myelin.

To analyse the S-MAG-GFP expression in the mouse sciatic nerve, we prepared teased fibres from a 2-month-old *pmag-MAG-e12GFP* transgenic mouse. The S-MAG-GFP was directly visualized by its GFP autofluorescent signal. Preliminary data showed a S-MAG-GFP localization in the periaxonal region (Figure 25, arrow), but only in a subset of all fibres. Interestingly, the expected localization in the paranodal region was almost undetectable.

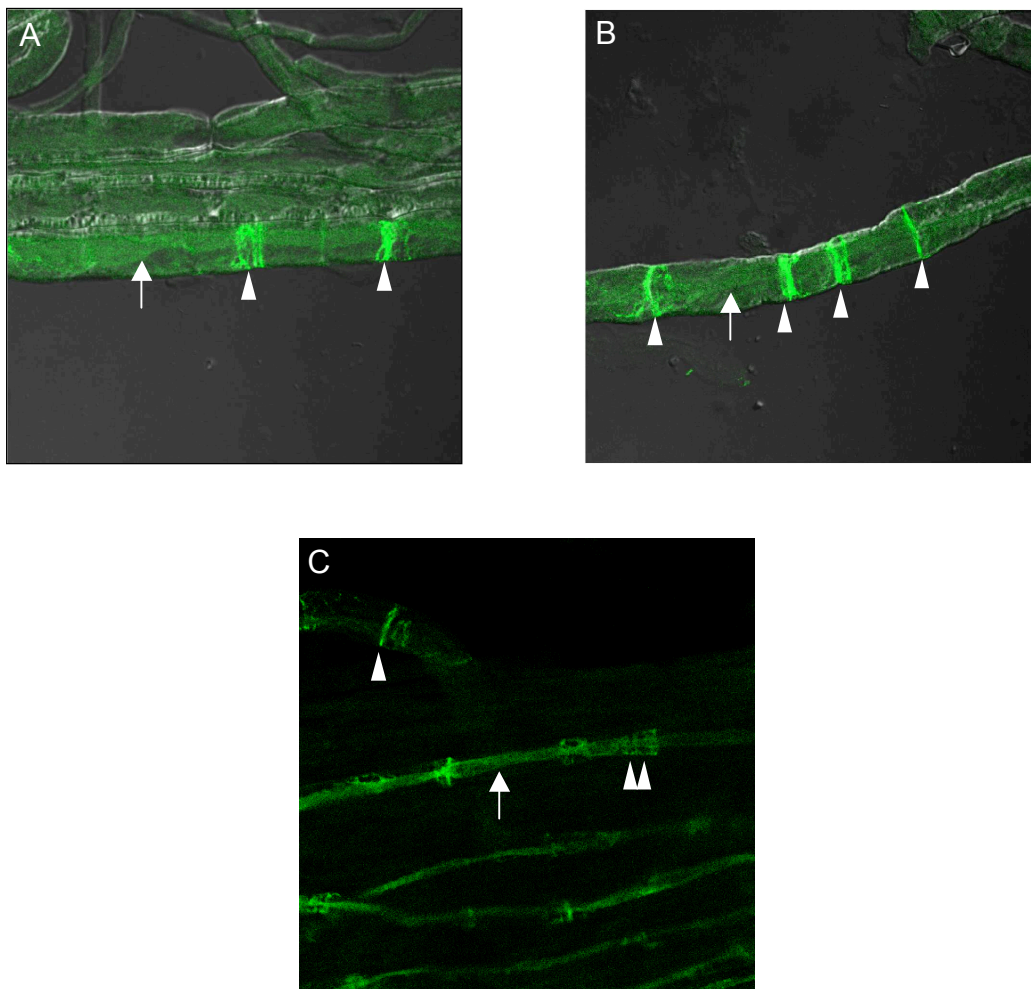


Figure 25 Analysis of S-MAG-GFP in a teased fibre preparation from *pmag-MAG-e12GFP* sciatic nerve. Laser scanning confocal microscopy was performed. The periaxonal signal is not detectable in all fibres, but is clearly visible in a subset of all fibres (arrow). The GFP signal of S-MAG-GFP often highlights ring-, or spiral-like structures (arrowhead). A typical V-shaped Schmidt-Lanterman incisure is indicated in C by a double arrowhead.

Furthermore, S-MAG-GFP was detected in many spiral, or ring-like structures (Figure 25, arrowheads) that are at least in some cases localized on the myelin sheath surface (Figure 25B, arrowhead on the left side). These ring-like structures were also detected in wild-type preparations by immunohistochemistry (data not shown). It was not evident whether these structures reflect Schmidt-Lanterman incisures, or some other as yet non-characterized MAG expression domain. However, S-MAG-GFP was also detected in typically V-shaped Schmidt-Lanterman incisures (Figure 25C, double arrowhead).

4.2.2. The *pmag*-MAG-e12GFP Central Myelin

To characterize the overall MAG and L-MAG levels in the brain of *pmag*-MAG-e12GFP transgenic mice, we isolated the myelin fraction from two one-month-old transgenic F1 animals and compared its levels with those of two age-matched wild-type animals (Figure 25). The hybridisation with the anti-MAG antibody showed the higher molecular weight of the S-MAG-GFP fusion protein relative to wild-type L- and S-MAG. The level of untagged MAG was slightly reduced in the transgenic animals, but the transgenic animals express the additional S-MAG-GFP fusion protein and might, therefore, express overall MAG levels comparable to those of wild-type animals. Interestingly, the L-MAG specific analysis showed no visible difference between transgenic and wild-type animals.

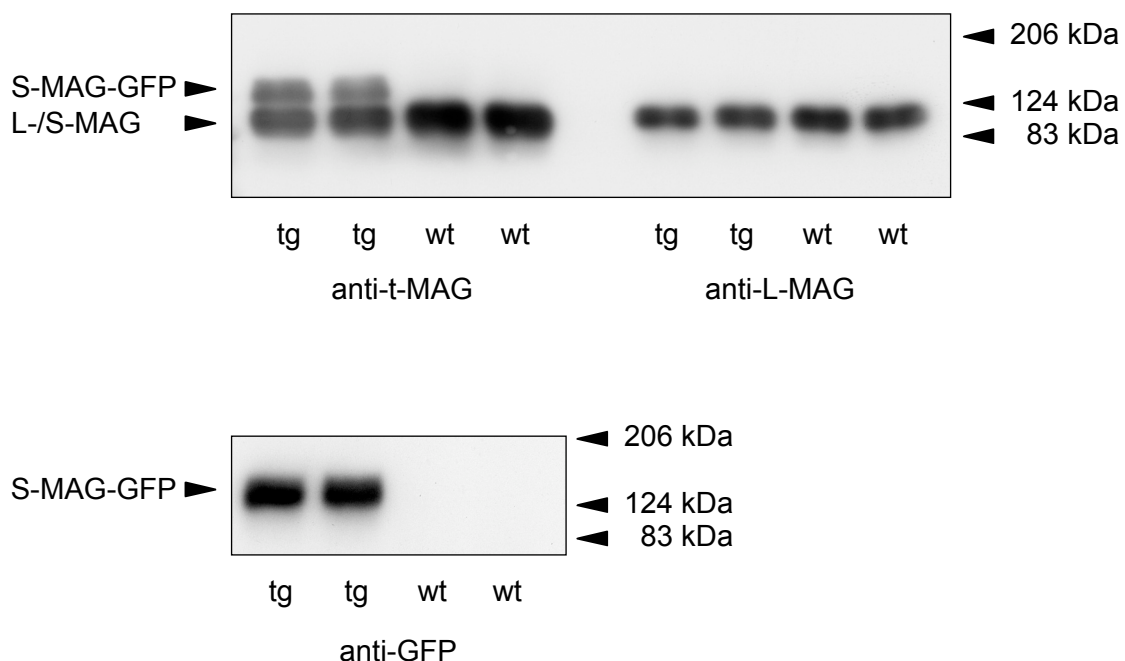


Figure 26 Western blot analysis of MAG isoforms in brain myelin from *pmag*-MAG-e12GFP mice. Brain myelin was isolated from one-month-old animals. Equal amounts of brain myelin from two transgenic and two wild-type animals were analysed using the t-MAG (total MAG) antibody that recognizes a common epitope of L- and S-MAG, the L-MAG specific antibody and the GFP-specific antibody. The S-MAG-GFP fusion protein expression is shown by the two bands detected by the t-MAG antibody and by the band detected by the anti-GFP antibody. The fusion protein has a higher molecular weight due to the additional 27 kDa from GFP. The wild-type MAG levels in the transgenic mice are slightly decreased, while their L-MAG levels are comparable to those observed in the wild-type mice; t-MAG: total MAG.

To analyse the S-MAG-GFP expression pattern in the brain, we performed confocal colocalization studies on a one-month-old transgenic F1 animal (Figure 27). The S-MAG-GFP autofluorescence signal clearly highlighted the myelinated fibre tracts of the cerebellum, the corpus callosum, the striatum, the hippocampus and the optic nerve.

The comparison of the anti-L-MAG (red) and anti-MAG (blue) staining with the S-MAG-GFP autofluorescence signal (green) revealed that the two MAG isoforms are differentially expressed within different brain structures.

Two neighbouring fibre tracts within the striatum (Striatum medullaris thalami) show a preferential expression of either L-MAG, or S-MAG (Figure 27A). The overall MAG levels were comparable in both fibre tracts. The long projecting fibres of the corpus callosum predominantly expressed S-MAG-GFP, whereas the underlying fibres were surrounded by a myelin sheath containing a higher amount of L-MAG (Figure 27B).

Taken together, the *pmag*-MAG-e12GFP transgenic animals seem to express comparable total MAG and L-MAG levels and revealed a differential expression of L- and S-MAG in distinct fibre tracts in the striatum and a prominent S-MAG expression in the corpus callosum.

4.3. The *pmag*-L-MAG-GFP Mouse Line

To analyse the L-MAG-GFP expression of the founder animals, we performed immunohistochemistry on tail biopsies taken from the founder animals (1, 2, 3 and 6) at the age of one month. Due to the used L-MAG-GFP open reading-frame, alternative splicing is excluded and we expect constitutive expression of L-MAG-GFP, in contrast to the *pmag*-MAG-e13GFP line that includes alternative splicing. However, also in these tail peripheral nerves, neither a GFP autofluorescence signal, nor an anti-GFP signal was detectable. The anti-MAG staining produced a periaxonal signal comparable to that observed in wild-type animals.

The analysis of the GFP autofluorescent signal in brain sections of transgenic F1 animals from two founders (2 and 3) also revealed no L-MAG-GFP expression.

Six of the seven founders passed the transgene to the F1 animals. The founder that did not pass the transgene to F1 generation was founder 6.

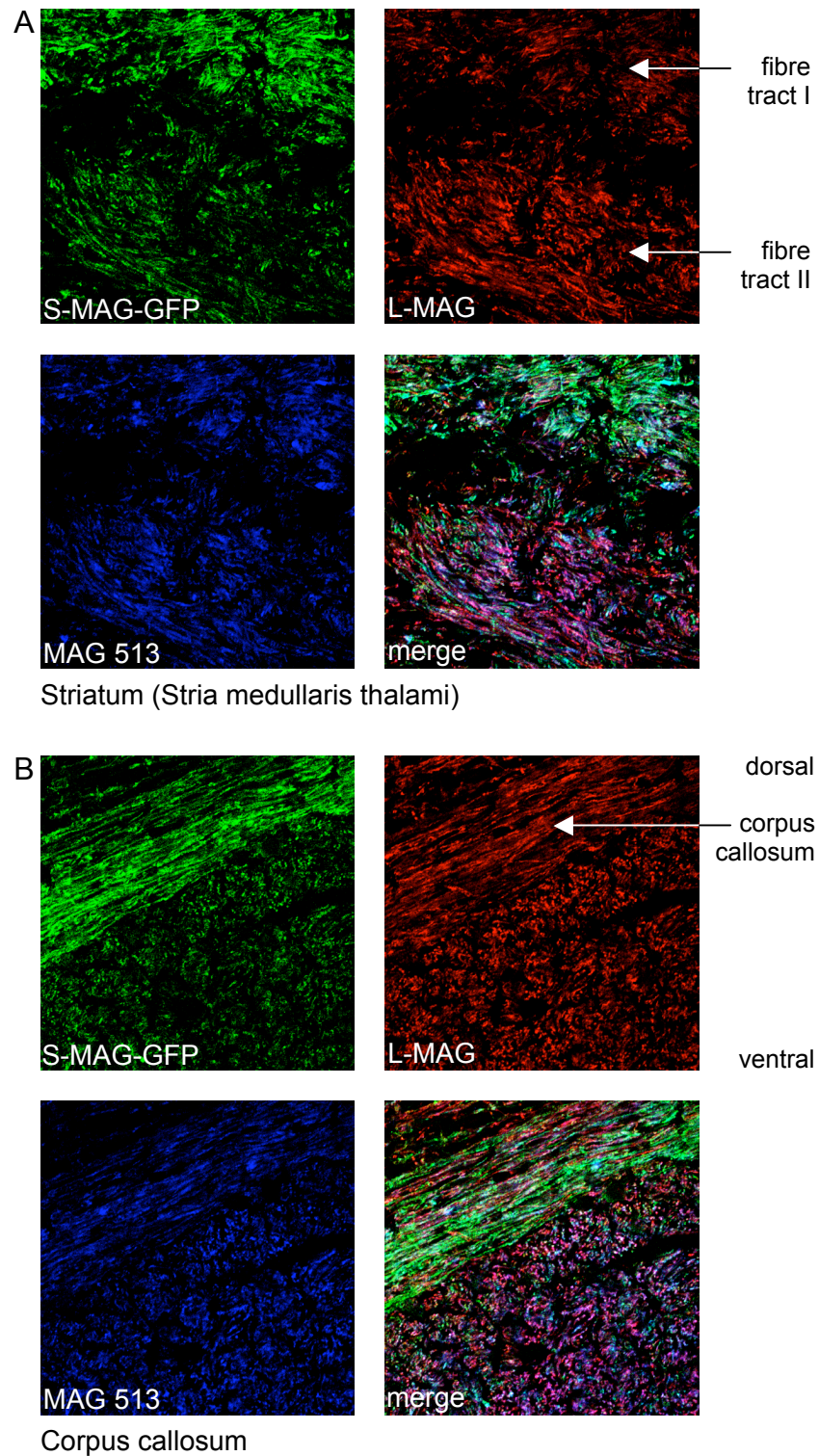


Figure 27 Localization of S-MAG-GFP and L-MAG in brain sections from a *pmag-MAG-e12GFP* mouse. Laser scanning confocal microscopy was performed on sagittal sections from one-month-old animals. S-MAG-GFP was analysed by the GFP autofluorescence (green) and immunohistochemistry for L-MAG (red) and total MAG (blue) was carried out. Depicted brain regions: Striatum (stria medullaris thalami; A) and Corpus callosum (B). **A:** The fibre tract I in the Striatum expresses more S-MAG-GFP (green) and the fibre tract II expresses more L-MAG (red), while the total MAG expression (blue) in these two tracts is comparable. **B:** High levels of S-MAG-GFP are detected in the Corpus callosum, while L-MAG seems to be expressed in a comparable manner in the Corpus callosum and the underlying brain region.

5. MAG Becomes Associated with Rafts in Adult CNS Myelin Membranes

The biological function of lipid-raft microdomains (DIGs) is ascribed to a variety of biological processes, including sorting, trafficking and signalling. Investigations of their relevance for myelin formation and maintenance have started only recently. We have analysed the composition of DIGs isolated from young (postnatal day 9), adult (3 months) and old (2 years) rodent brain myelin and adult human brain myelin.

5.1. MAG is not Raft-associated during Mouse CNS Myelin Formation

The analysis of DIGs isolated from postnatal day 9 mouse brain myelin revealed that the typical raft protein MAL was highly enriched in rafts (Figure 28A). The paranodal GPI-linked protein, F3/contactin, was found to be partially DIGs-associated. In contrast, we found that the two non-compact myelin proteins, L-MAG and MOG, were not recruited to DIGs during myelin formation. The analysis of DIGs isolated from the plasma membrane fraction of postnatal day 9 mouse brain revealed that neither F3/contactin, nor L-MAG were DIGs-associated (Figure 28B).

5.2. MAG Is Partially Raft-associated in Adult Mouse CNS Myelin

In adult rat (Figure 29A) and mouse (Figure 32) brain myelin, the MAL protein is exclusively localized in DIGs. In contrast to the situation during active myelination, in the adult CNS myelin, both MAG isoforms are partially incorporated into TritonX-100-insoluble (Figure 29A) and CHAPS-insoluble (Figure 32) DIGs. In two-years-old mouse brain myelin, total MAG is still incorporated to some extent into TritonX-100-insoluble DIGs (Figure 29B), but L-MAG is almost undetectable in the DIGs fraction. This is probably a matter of detection limits, because L-MAG seems to be poorly expressed in two-years-old mouse brain. The additional analysis of PLP and its splice variant DM20 in the two-years-old mouse brain myelin revealed that PLP is predominantly DIGs associated, whereas DM20 is almost exclusively incorporated into DIGs (Figure 29B, arrow).

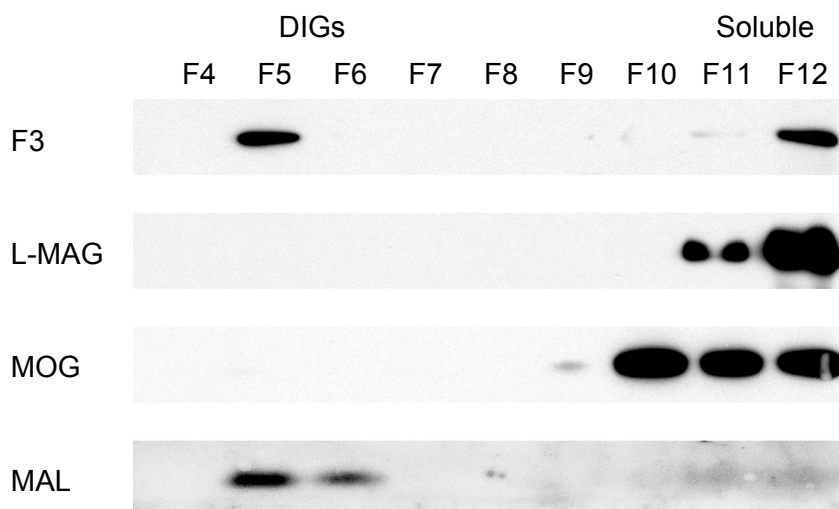
A: Mouse P9 Brain Compact Myelin TX-100 DIGs**B: Mouse P9 Brain Plasma Membrane TX-100 DIGs**

Figure 28 L-MAG is not associated with TritonX-100 resistant DIGs (lipid-rafts) from P9 mouse brain myelin

Myelin, or plasma membrane preparations were incubated for 30 minutes with 1% TritonX-100 at 4°C. The samples were adjusted to 40% sucrose, and 2 ml containing 400 µg protein were transferred to SW 41 centrifuge tubes; overlaid with 30% and 5% sucrose (5 ml each), and centrifuged for 21 hours at 36'000 rpm. Twelve 1 ml fractions (F1-F12) were collected from the top. Equal volumes of the fractions 4 to 12 were analysed by Western blotting. Detergent-insoluble complexes DIGs float to a low density on the sucrose gradient, due to the low density of the lipids associated with the proteins (F5 and F6). Detergent-soluble proteins stay in the bottom fractions F11 and F12. **A:** F3/contactin and MAL, but not L-MAG and MOG are incorporated into DIGs in compact brain myelin isolated from postnatal day 9 mice. **B:** F3/contactin and L-MAG are not found in DIGs of brain plasma membranes isolated from postnatal day 9 mice.

5.3. MAG is Almost Exclusively Raft-associated in the Adult Human Brain

In the old adult human brain myelin, we found a completely different situation for L-MAG (Figure 29C). L-MAG was found to be almost exclusively localized in DIGs. The same analysis using an antibody that recognizes both MAG isoforms, revealed the same distribution (not shown). The additional analysis of MBP showed that the MBP isoforms were partially DIGs-associated.

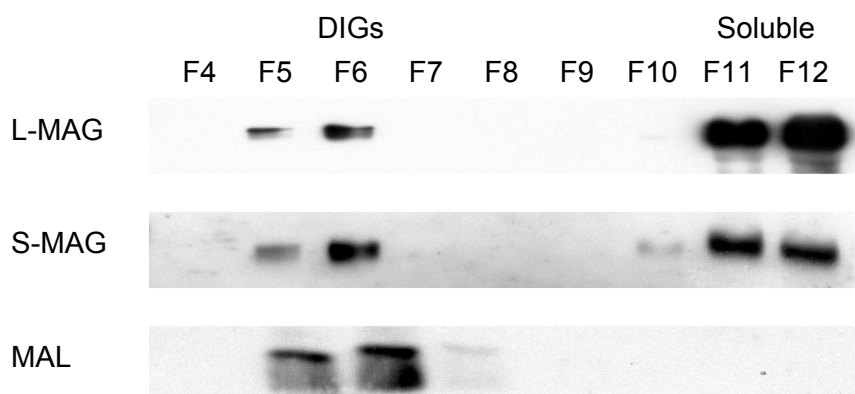
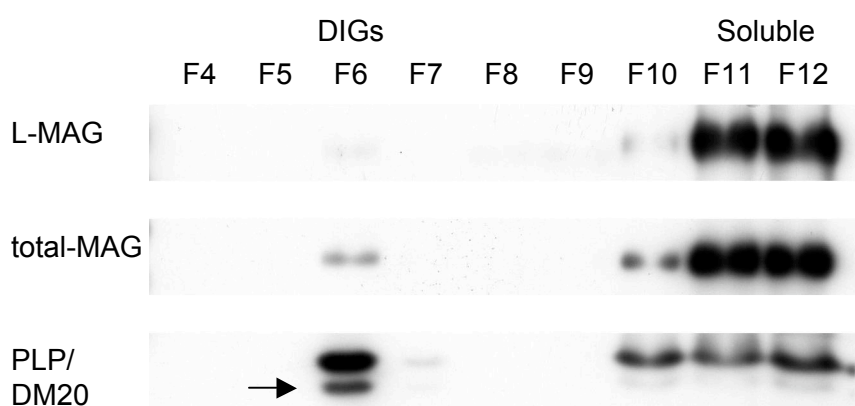
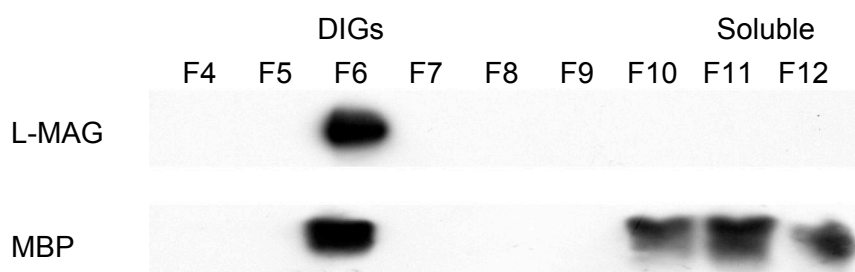
A: Rat 3 Months Brain Compact Myelin TritonX-100 DIGs**B: Mouse 2 Years Brain Compact Myelin TritonX-100 DIGs****C: Human Adult Brain Compact Myelin TritonX-100 DIGs**

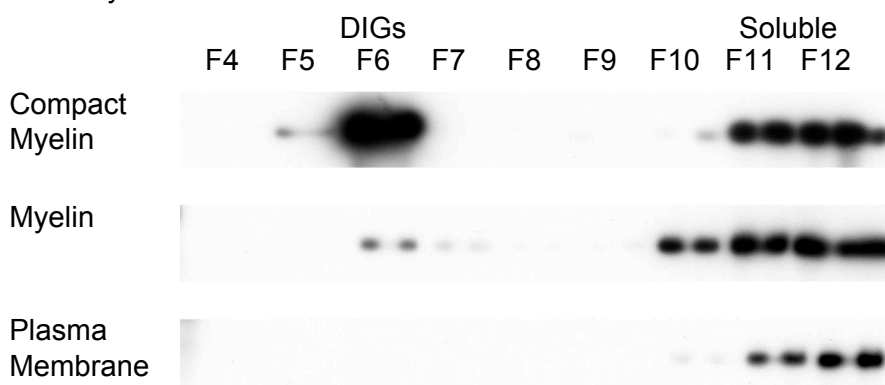
Figure 29 MAG is associated with TritonX-100-resistant DIGs (lipid-rafts) from adult rodent and human brain myelin

Detergent extraction and sucrose gradient ultracentrifugation were performed as described for Figure 15. **A:** MAL is fully and L- and S-MAG are partially incorporated into DIGs in brain compact myelin isolated from 3-months-old rat brain. **B:** MAG is only to a small extent, while PLP/DM20 is to at least 50%, incorporated into DIGs in brain myelin isolated from 2-years-old mouse brain. Note that the DM20 isoform (arrow) is found almost exclusively in DIGs. **C:** L-MAG is exclusively, and MBP is partially, incorporated into DIGs in brain compact myelin isolated from adult human brain.

5.4. MAG-Containing Rafts in the Human CNS are More Resistant to Detergent Extraction Using CHAPS than when Using TritonX-100

TritonX-100 and CHAPS are non-ionic and zwitterionic detergents, respectively, used for the isolation of detergent-insoluble rafts. We have compared the solubility of MAG-containing DIGs from the compact myelin, the myelin and the plasma membrane fractions isolated from autoptic adult human brain (Figure 30; autopsy A99-331). MAG-containing DIGs proved to be less soluble in CHAPS (Figure 30A) than in TritonX-100 (Figure 30B). Furthermore, all CHAPS and TritonX-100 detergent-insoluble MAG-containing DIGs were found to be accumulated in the compact myelin fraction and were absent from the myelin and plasma membrane fractions.

A: Analysis of L-MAG in Human Adult Brain CHAPS resistant DIGs



B: Analysis of L-MAG in Human Adult Brain TX100 resistant DIGs

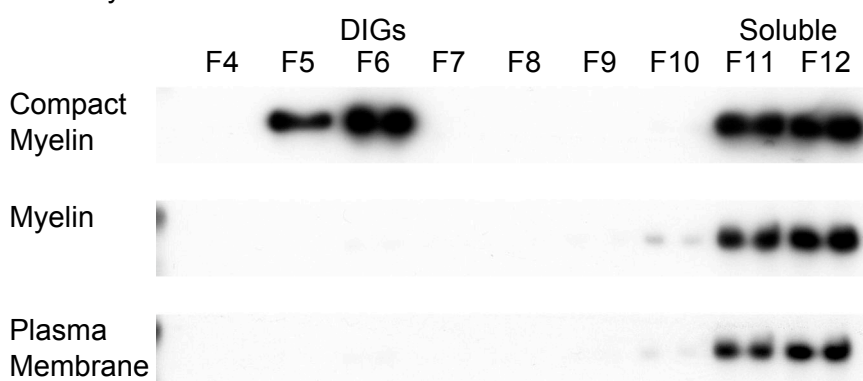


Figure 30 Comparison of CHAPS and TritonX-100 resistant DIGs (lipid-rafts) isolated from adult human brain myelin.

Detergent extraction and sucrose gradient ultracentrifugation were performed as described for Figure 15. CHAPS- (A) and TritonX-100- (B) resistant DIGs were isolated from the human brain compact myelin, myelin and plasma membrane fractions. All blots were processed in parallel and exposed to the same film to achieve comparable readouts. All L-MAG-containing detergent-resistant DIGs were found in the compact myelin fraction. More than half of L-MAG in the compact myelin was found to be localized in DIGs. L-MAG-containing DIGs are slightly more resistant to extraction with CHAPS than with TritonX-100.

6. The Incorporation of MAG and MBP into Brain Myelin Membranes is Dependent on MAL

Since the proteolipid MAL has been shown to be involved in the apical sorting within polarized cells (Cheong et al. 1999; Puertollano et al. 1999), and is highly enriched in myelin DIGs (lipid-rafts; Figure 28 and 29), we were interested in the functional implication of MAL on the myelin protein transport and their raft association. For this, we investigated the MAL knock-out mouse to study whether sorting and trafficking of particular myelin proteins are dependent on MAL.

6.1. The Myelin Protein Levels of MAG and MBP are decreased in 4-month-old MAL Deficient Mouse Brains

To analyse the myelin protein composition of adult (4-months-old) MAL-deficient mouse brains (Figure 31), we isolated myelin from 3 age-matched MAL knock-out and 3 wild-type animals. Therein, we analysed the relative myelin protein levels by Western blot analysis of MAL itself, two compact myelin proteins (PLP/DM20 and MBP), two non-compact myelin proteins (MAG and MOG), and two proteins that are involved in the attachment of the paranodal loops to the axonal membrane (F3/contactin and Caspr).

Interestingly, the levels of L-MAG and MBP were remarkably reduced in the MAL knock-out relative to the wild-type samples. Furthermore, the levels of F3/contactin and Caspr appear to be decreased in the knock-out brain myelin samples as well, whereas no significant difference could be observed for the protein levels of PLP/DM20 and MOG. The analysis of all 6 samples revealed very small inter individual differences within both genotypes, reflecting an accurate protein concentration measurement.

6.2. Reduced MAG Levels in the Detergent-Resistant and -Soluble Fractions isolated from MAL-Deficient Mouse Brain Myelin

For the investigation of the effect of the MAL depletion on the raft association of these MAG and MBP, we isolated the CHAPS-resistant DIGs from each of the 3 wild-type and the 3 knock-out brain myelin samples by detergent extraction and separation on a sucrose gradient (Figure 32). The fractions of each sucrose gradient were analysed separately by Western blot to determine whether the DIGs were floating in the same fractions in all gradients. All 6 gradients presented indistinguishable distributions: the large majority of the rafts were accumulated in fraction 6, while a minor part was found in the overlying fraction 5. Therefore, fraction 6 of each gradient was used to compare the raft association of the selected proteins between the wild-type and knock-out brain myelin samples. The same was true for the sucrose gradient fractions 11 and 12 that contain the detergent-soluble proteins. Therefore, the corresponding three fractions of each genotype were pooled for further analysis. This analysis showed in wild-type mice that the MAL-containing DIGs or the MAL molecules themselves, are not solubilized by the detergent CHAPS as they are with TritonX-100 (Figure 28 and 29).

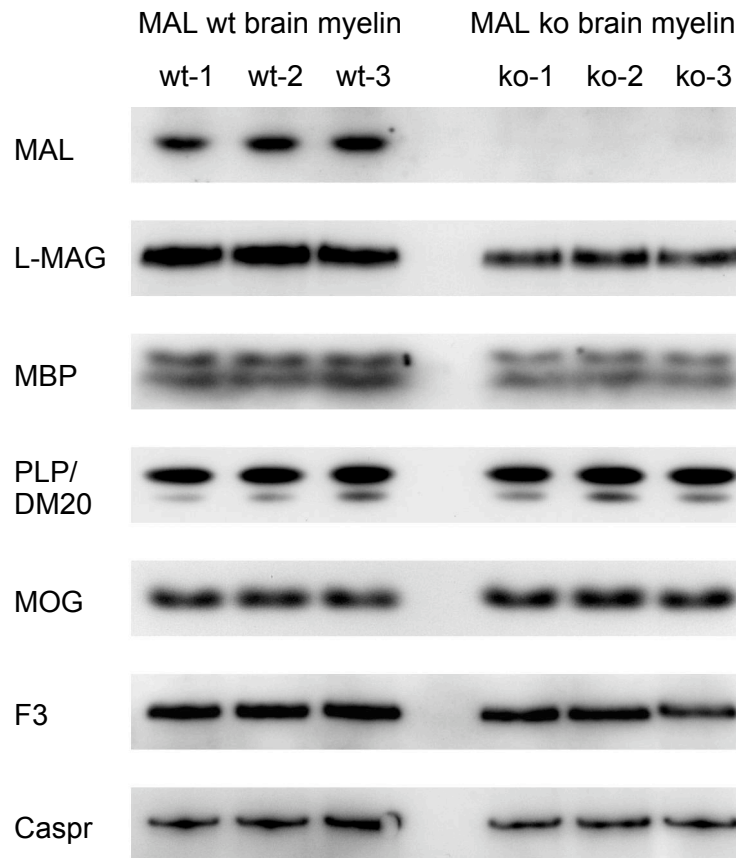


Figure 31 Western blot analysis of myelin protein levels from adult mouse MAL wild-type and knock-out brains

Brain myelin has been purified from three age-matched 4-month-old MAL-deficient and wild-type mice. Equal protein amounts from each myelin preparation was analysed by Western blotting. Besides the absence of the MAL protein, significantly reduced L-MAG and MBP protein levels were observed in the brain myelin of the three MAL knock-out animals. The levels of F3/contactin and Caspr seem to be slightly decreased in the MAL-deficient animals, whereas for PLP/DM20 and MOG no alteration was detectable. Note that the interindividual difference within each genotype are quite small, indicating an accurate protein measurement and equal loading.

The most prominent effect in the MAL-deficient mice was the profoundly decreased level of L-MAG protein in DIGs (F06, Figure 32). However, L-MAG was also decreased in the detergent-soluble fractions (F11 and F12; Figure 32). Besides the reduction of L-MAG, a significantly reduced level of MBP was visible in DIGs (F6; Figure 32). The analysis of PLP/DM20 revealed no obvious difference between the MAL knock-out and wild-type samples and both isoforms exhibited a high DIGs association, but the DM20 isoform showed a higher DIGs association than the PLP isoform (Figure 32).

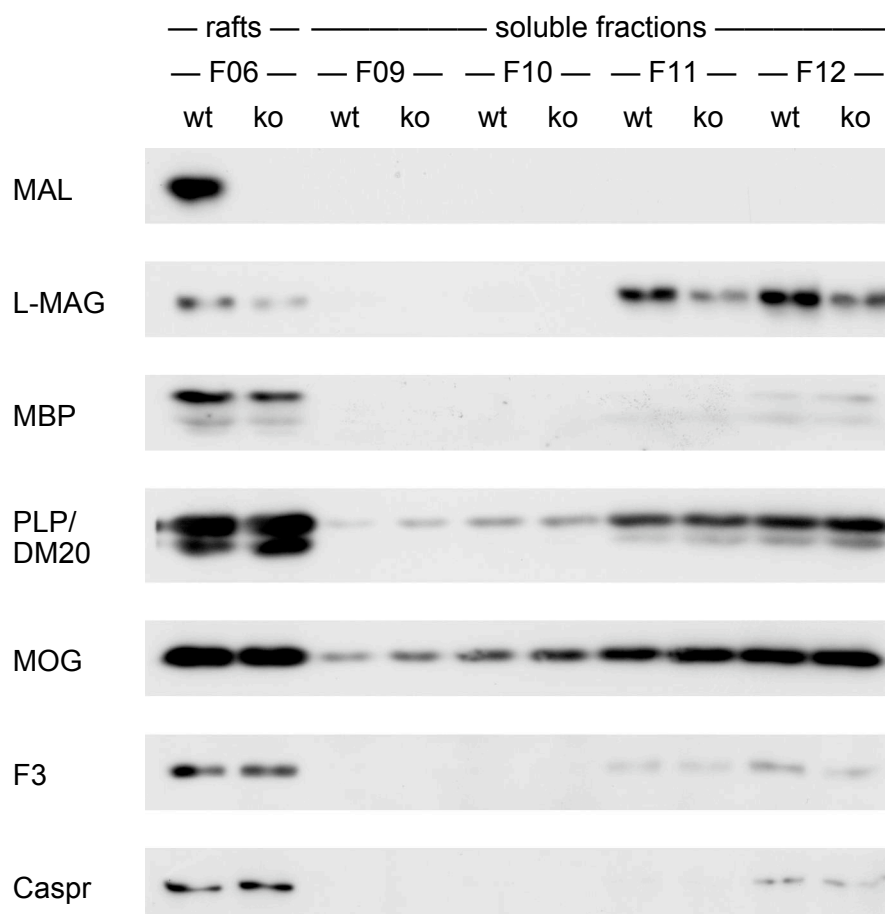


Figure 32 Analysis of the DIGs (lipid-raft) association of myelin proteins in MAL wt and ko adult (4 months) mouse brains using the detergent CHAPS

Detergent extraction and sucrose gradient ultracentrifugation were performed as described for Figure 15. The three myelin samples from both genotypes had been processed separately during detergent extraction and sucrose gradient centrifugation, but the corresponding fractions of each genotype were pooled thereafter. Equal volumes of the CHAPS-resistant fraction 6 (F06) and the soluble fractions 9 to 12 (F09-F12) were analysed by Western blotting. L-MAG and MBP showed a significant decrease in the DIGs fraction in the MAL knock-out samples compared to the wild-type levels. No significant alterations in the DIGs association were observed for PLP/DM20, MOG, F3/contactin and Caspr. Note, that DM20 shows a higher degree of raft association, or resistance to CHAPS extraction, than its larger isoform PLP; F3: F3/contactin.

6.3. Quantification of the Myelin Protein Levels in The MAL-Deficient Mouse Brain Myelin And Myelin-DIGs

To quantify the differences observed in the Western blot analysis of the brain myelin and their DIGs fractions from MAL wild-type and knock out animals, we established a Western blot protocol that allows a semi-quantitative readout (see Material and Methods section 3.8.).

The semi-quantitative analysis of the total MAG and L-MAG levels revealed, for both the brain myelin and the brain myelin DIGs fraction, a reduction to about 61-62% in the knock-out compared to wild-type animals (Figure 33). The analysis of the S-MAG-specific levels was not possible due to the lack of an S-MAG specific antibody, but the almost identical

results for both isoforms (total MAG) and for L-MAG alone, point to a similar reduction of L- and S-MAG. Taken together, the two MAG isoforms exhibited a similar reduction to about 61-61% in the myelin and myelin DIGs fractions of MAL knock-out mice relative to wild-type mice.

In a similar manner, MBP also exhibited a reduction in the myelin and myelin DIGs fractions of the knock-out brain samples. The myelin MBP levels were reduced to 75%, whereas the MBP levels in the DIGs were reduced to 67% of normal levels in MAL knock-out mice. The difference in the reduction of MBP in the myelin and myelin DIGs fractions was not statistically significant.

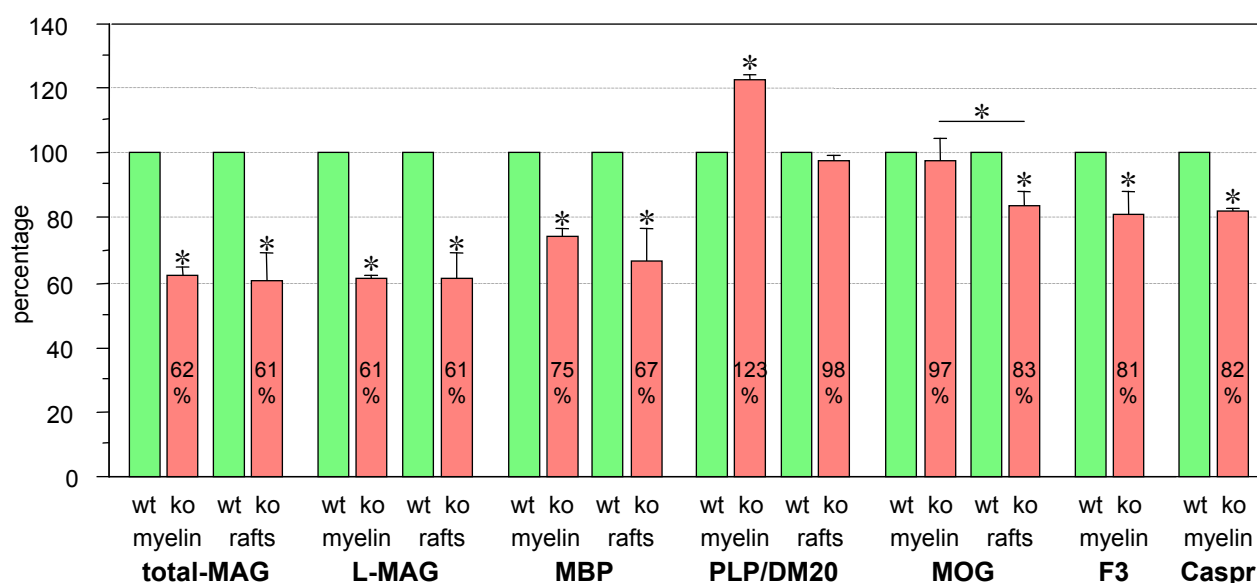


Figure 33 Quantitative analysis of the myelin protein levels and their DIGs (lipid-raft) association of MAL wt and ko adult (4 months) mouse brains

The relative protein levels in the brain myelin and in its CHAPS-insoluble fraction (F06) were analysed by Western blotting. For the detailed protocol see Material and Methods. The values of the wild-type levels were set to 100%. The number of experiments included in this quantification of the myelin and myelin DIGs protein levels were as follows: total MAG: 3 and 3; L-MAG: 3 and 4; MBP: 3 and 3; PLP/DM20: 3 and 6; MOG: 7 and 5; F3/contactin: 3; Caspr: 3. Statistically significant differences and standard errors are shown by asterisks and bars, respectively.

The analysis of the major myelin protein PLP, together with its splice variant DM20 revealed an increase of PLP/DM20 in the brain myelin of knock-out animals to 124% of the wild-type levels, whereas the PLP/DM20 levels in the myelin raft fraction were almost unaltered (98% of the wild-type levels). The elevated PLP/DM20 levels in the knock-out myelin are statistically different ($p < 0.0001$) from the almost unaltered levels in the knock-out myelin DIGs.

In contrast, the non-compact myelin protein MOG was the only protein that showed almost normal levels in myelin (97%), but a significant reduction (to 83%) in DIGs of MAL knock-out compared to wild-type brains. The difference between the MOG levels in myelin and in myelin DIGs (97 and 83% of wild-type levels) was statistically significant ($p < 0.0001$).

Caspr, F3/contactin and Neurofascin155 have been shown to form a complex that is responsible for the attachment of the paranodal loops to the axonal membrane (septate-

like junctions). Caspr and F3/contactin are localized on the axonal side, whereas Neurofascin155 is the glial binding partner. Since many paranodal loops are curving away from the paranode and the expression patterns of Caspr and Neurofascin155 are more diffuse in adult MAL deficient brains, we analysed their overall protein levels in MAL knock-out and wild-type brains. F3/contactin and Caspr revealed comparable reductions down to 81% and 82%, respectively, in knock-out compared to wild-type brains. The realization of the Western blot analysis of the glial binding partner Neurofascin155 was not possible due to the low affinity of the available anti-serum. The semi-quantitative analysis of the Caspr and F3/contactin DIGs levels was not carried out, but they are both found to be mainly raft-associated in both the wild-type and the MAL knock-out brain samples.

6.4. MAG and PLP Protein Levels in two-years-old MAL-Deficient Mouse Brains

To analyse the affects of two years of MAL depletion on the myelin protein composition in mouse brains, we purified myelin from two-years-old MAL wild-type and knock-out mouse brains (Figure 34). The analysis of the total MAG- and the L-MAG-specific protein levels in the two genotypes, revealed decreased MAG levels in the MAL deficient mouse brains (Figure 34A). In contrast, the analysis of the PLP/DM20 levels showed a rather strong increase in the myelin isolated from the MAL-deficient mouse brains. We have not yet quantified the alterations of the PLP/DM20 protein levels in the two-years-old MAL deficient mouse brains, as we did it for the four-months-old brains. But the increase of the PLP/DM20 protein levels in the two-years-old MAL deficient mice (Figure 34A) seems to be even bigger than the 24% increase in the four-months-old knock-out mice (Figure 31 and 33). The analysis of the DIGs association of MAG and PLP/DM20 in the two-years-old MAL-deficient and wild-type mouse brains (Figure 34B) revealed no significant differences for L-MAG and total MAG between the two genotypes, whereas the PLP/DM20 levels were increased in both the soluble and the insoluble fractions of the MAL knock-out compared to wild-type brains (Figure 34B).

In comparison to the situation after 4 months of MAL depletion, the depletion of MAL for 2 years results in a comparable, or milder reduction of the MAG levels, whereas the PLP/DM20 levels in total myelin and myelin DIGs seems to increase with age.

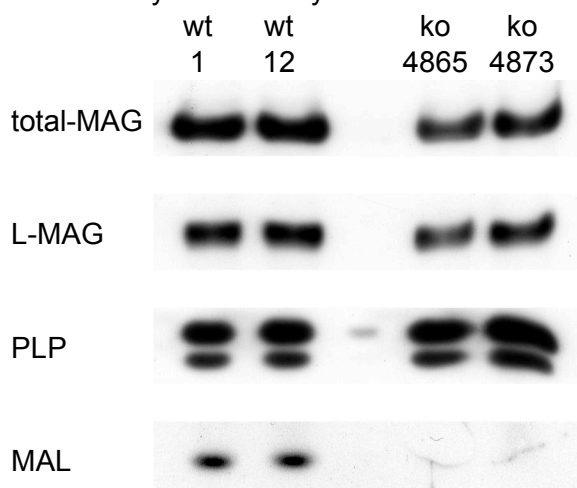
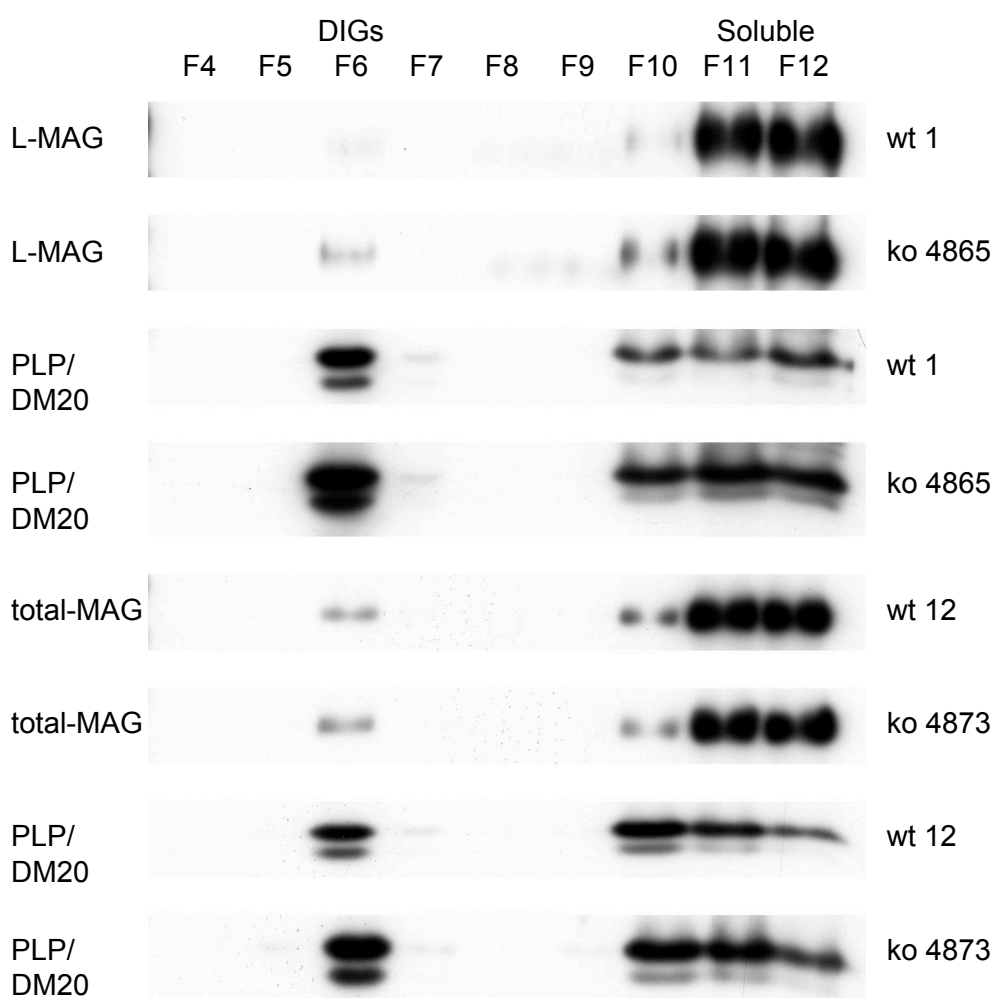
A: Brain Myelin from 2 years MAL wt/ko animals**B: Brain Myelin CHAPS DIGs from 2 years wt/ko animals**

Figure 34 MAG and PLP levels in myelin and myelin DIGs from 2-years-old MAL wt and ko brains
Brain myelin was isolated from two 2 years old mouse brains from both genotypes. **A:** The total MAG and the L-MAG levels are decreased, whereas the PLP/DM20 levels are increased in the MAL deficient brains. **B:** CHAPS extraction and sucrose gradient ultracentrifugation were performed as described for Figure 15. Equal volumes were loaded and blots incubated with the same antibody were processed in parallel and exposed to the same film to achieve comparable readouts. No significant alteration in the DIGs-association was observed for total- and L-MAG in the MAL deficient animals. But, a rather strong increase of PLP/DM20 levels could be observed in the CHAPS-insoluble DIGs fraction, as well as in the soluble fraction in the MAL-deficient brains.

7. MAG and PLP/DM20 Transcription are Altered in the MAL Knock-Out Brain in a Compensatory Manner

Since the lack of MAL led to reduced MAG levels in adult mouse brains (4 months), we analysed the total MAG and the L-MAG mRNA levels in 4- and 12-months-old MAL knock-out and wild-type mouse brains. This analysis should unravel the question of whether the reduced MAG levels are caused by an impaired trafficking and myelin membrane incorporation of the protein, or by an already decreased MAG transcriptional level. In addition to MAG, we also analysed the mRNA levels of PLP/DM20, MAL and GAPDH (internal standard).

7.1. Total-MAG and L-MAG mRNA Levels are Increased in the Adult MAL Knock-Out Brain

The analysis of the total MAG mRNA levels, using a primer pair that does not discriminate between the L- and S-MAG splice variants, and of the L-MAG-specific mRNA levels revealed that the total MAG mRNA levels were elevated in the 4-months-old MAL deficient mouse brains to about 140% of the wild-type levels (Figure 35). This is in clear contrast to the reduction of the MAG protein levels to about 60% of the wild-type levels. The analysis of 1-year-old MAL-deficient mouse brains revealed an up-regulation of the total MAG and L-MAG specific mRNA levels to about 122% and 167%, respectively, of the wild-type levels (Figure 35). Taken together, there seems to take place a general up-regulation of the MAG transcription to about 140% of the wild-type levels in the 4-months-old MAL deficient mouse brains. This up-regulation seems to be the result of a feedback mechanism that results in a compensatory up-regulation.

The overall MAG transcription levels in 4-month- and 1-years-old wild-type mouse brains were very similar (Figure 35; about 5.5% of the GAPDH levels). The comparison of the total MAG and the L-MAG-specific mRNA levels in the 4-months-old mouse brains revealed that about 23% of the primary MAG transcripts were spliced to the L-MAG-specific splice variant in a similar manner in both genotypes (Figure 36), whereas about 12% and 15% of the primary MAG transcripts are spliced to the L-MAG splice variant in the 1-years-old wild-type and MAL knock-out brains, respectively (Figure 36). Taken together, there seems to be no difference in the MAG transcriptional level between the ages of 4 and 12 months in wild-type brains, but the relative amount of the L-MAG-specific splice variant is decreased from 23% to 12% between the ages of 4 and 12 months in wild-type mouse brains. Interestingly, although the overall transcriptional level was increased in the MAL knock-out brains, the percentage of primary transcripts that are spliced to the L-MAG splice variant was almost identical in wild-type and knock-out brains.

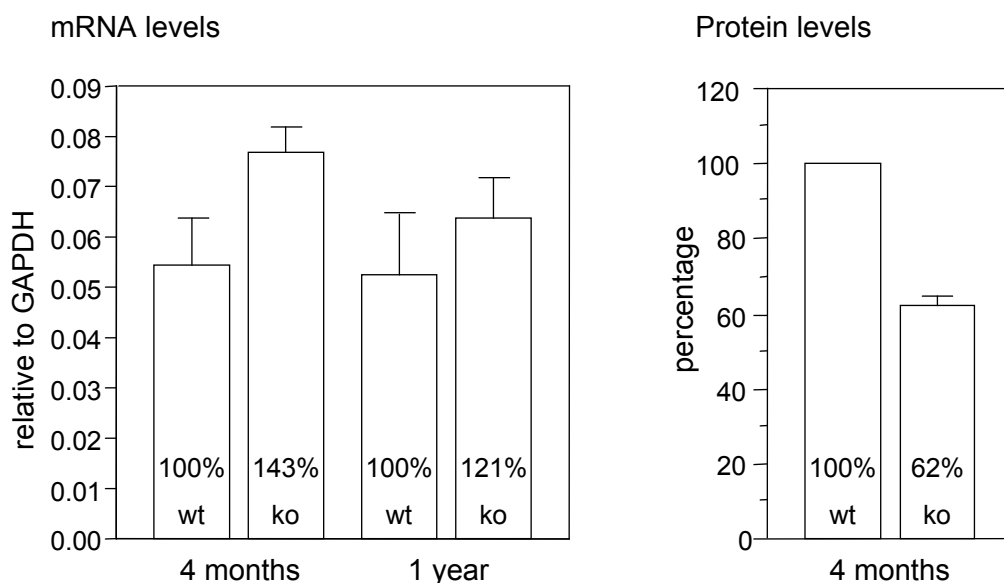
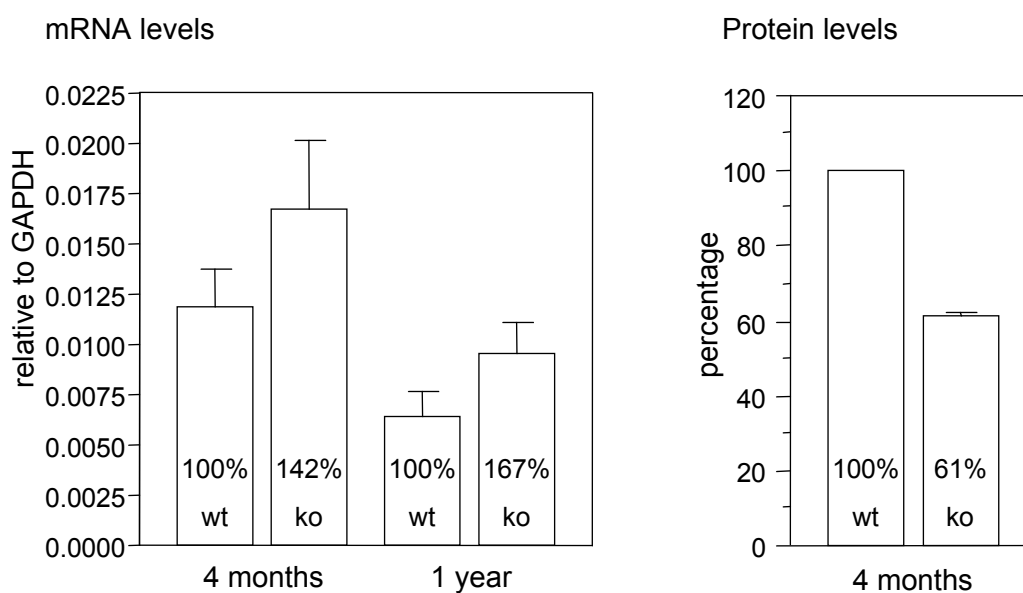
A: total-MAG mRNA and protein levels in MAL ko brains**B: L-MAG mRNA and protein levels in MAL ko brains**

Figure 35 Analysis of total MAG and L-MAG mRNA levels in MAL knock-out and wild-type mouse brain. Quantitative RT-PCR analysis (LightCycler) was carried out to determine the total MAG and L-MAG-specific mRNA levels in 4-months- and 1-years-old MAL knock-out and wild-type mouse brains. Total RNA was isolated from 3 mouse brains per age and genotype, while each sample was analysed once (n=3). The transcriptional levels were normalized to GAPDH. The error bars indicate the standard deviations. The differences in the transcriptional levels between the two genotypes were not significant. The analysis shows an increase of the MAG mRNA levels in the knock-out samples from both time points. On the right side, the results from the protein analysis (Figure 33) are shown for comparison.

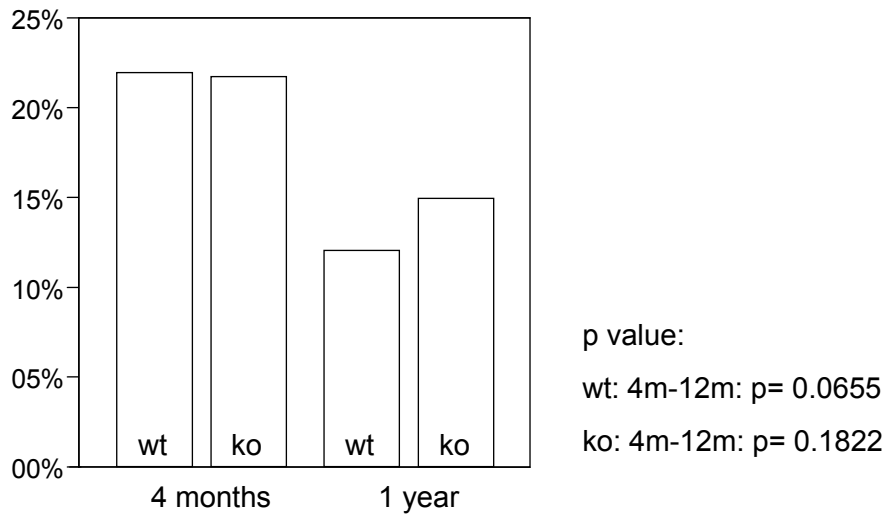
L-MAG to total-MAG mRNA level ratio in mouse brain

Figure 36 MAG alternative splicing: decreasing L-MAG mRNA levels in mouse brain with increasing age
The relative amount of L-MAG-specific mRNAs in 4-month-old wild-type mouse brains was about 22% of the total MAG (L- and S-MAG) mRNAs. In one-year-old mice, the relative amount of L-MAG specific transcripts was decreased to 12%. This decrease was almost significant ($n=3$; $p=0.0655$). In the MAL knock-out mice, the L-MAG fraction dropped from 22% to 15%.

7.2. Decreased PLP/DM20 mRNA Levels in Adult MAL-Deficient Brains

We originally chose to analyse the PLP/DM20 mRNA levels in the MAL knock-out brains as an internal control of a myelin protein that, before the quantitative Western blot analysis had been carried out, seemed not to be affected by the depletion of MAL. However, the quantitative PCR analysis did not reveal an up-regulation, but a reduction of the PLP/DM20 mRNA levels to 73% and 86% of the wild-type levels in the 4- and 12-months-old MAL deficient mouse brains, respectively (Figure 37). The PLP/DM20 mRNA levels in the 4- and 12-months-old mouse wild-type brains were comparable (Figure 37). In contrast to the situation observed for MAG, which exhibited reduced protein and increased mRNA levels, PLP/DM20 seems to exhibit the same compensatory feedback mechanisms with reversed premises, namely increased protein levels and with reduced mRNA levels.

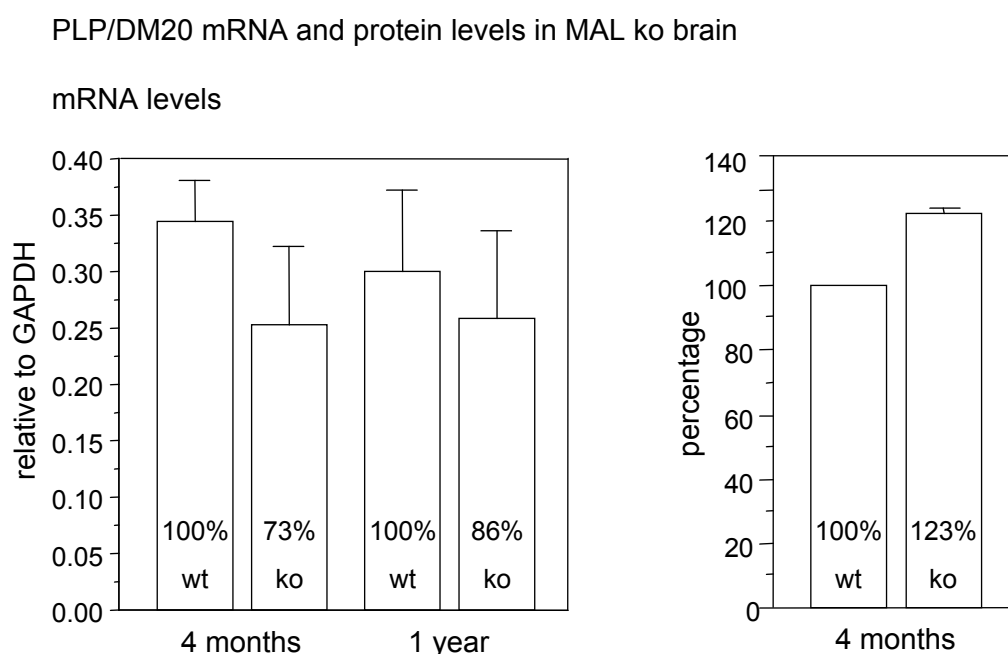


Figure 37 Analysis of PLP/DM20 mRNA levels in MAL knock-out and wild-type mouse brain. Quantitative RT-PCR analysis (LightCycler) was carried out to determine the PLP/DM20 mRNA levels in 4-months- and 1-year-old MAL knock-out and wild-type mouse brains. The primers were designed in a way that they do not discriminate between the PLP and the DM20 splice variant. Total RNA was isolated from 3 mouse brains per age and genotype, while each sample was analysed once ($n=3$). The transcriptional levels were normalized to GAPDH. The error bars indicate the standard deviations. The differences in the transcriptional level between the two genotypes were not significant. But, the analysis shows a decrease of the PLP/DM20 mRNA levels in the knock-out samples from both time-points. On the right side, the results from the protein analysis (Figure 33) are shown for comparison.

7.3. Lack of Exon 1-Containing MAL Transcripts in MAL Knock-Out Brains

The analysis of the MAL mRNA levels in the 4- and 12-months-old MAL knock-out and wild-type mouse brains revealed no significant difference between the two time points in the wild-type animals. Since the used primer pair was located in the MAL exon 1, which had been replaced in the MAL knock-out animals, the MAL transcripts were not detectable in the knock-out animals (Figure 38).

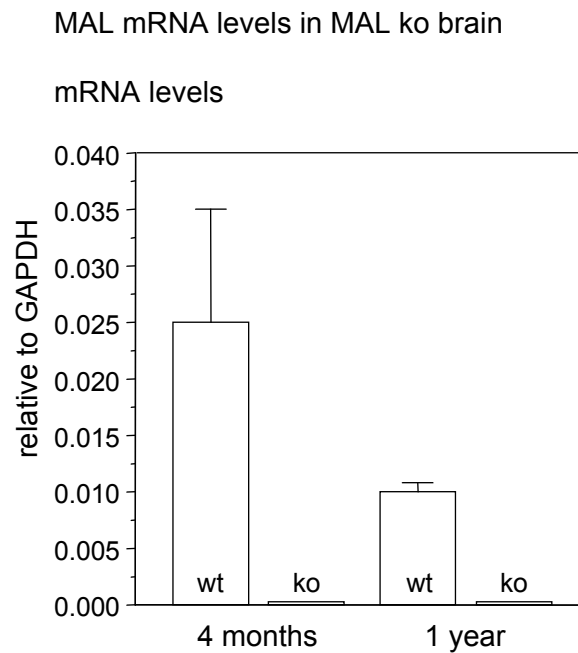


Figure 38 Analysis of the MAL mRNA levels in MAL knock-out and wild-type mouse brain. Quantitative RT-PCR analysis (LightCycler) was carried out to determine the MAL mRNA levels in 4-months- and 1-year-old MAL knock-out and wild-type mouse brains. The primers were designed to hybridize within the MAL exon 1. Since the exon 1 sequence is replaced in the knock-out mice, these primers are not expected to produce any signal in the knock-out mice. Total RNA was isolated from 3 mouse brains per age and genotype, while each sample was analysed once (n=3). The transcriptional levels were normalized to GAPDH. The error bars indicate the standard deviations. The differences in the transcriptional level between the 4-months- and the 1-year-old wild-type mice were not significant. The analysed knock-out samples did not express detectable levels of MAL exon 1-containing mRNAs, as expected.

Discussion

The myelin sheath is a unique and fundamental adaptation of both the central and peripheral nervous systems of vertebrates and is needed for rapid and efficient nerve impulse conduction. The formation of myelin around axons proceeds in various steps, requiring complex and reciprocal interactions between axons and myelin-forming oligodendrocytes and Schwann cells in the CNS and PNS, respectively. First, myelin-forming glial cells have to recognize those axons that are competent to become myelinated. The processes of myelin-forming glial cells have then to adhere to these axons and to envelope them. One molecule that has been implicated in the formation and maintenance of the axon-glia interaction is the MAG. The observations in MAG mutant mice support the role of MAG as a cell adhesion and receptor molecule that transduces signals into the interior of myelin-forming glial cells and contributes to the cross-talk between myelinating glia cells and axons. Interestingly, MAG does not appear to be necessary for the initial interactions between the myelinating glial cell and the axon, but for the maintenance of the axon-glia interaction in the adult.

The differential expression of the L-MAG and S-MAG isoforms (Inuzuka et al. 1991; Miescher et al. 1997) is likely to bear important consequences for signal transduction cascades, since the two isoforms have distinct intracellular domains (Lai et al. 1987). The non-receptor tyrosine kinase Fyn, has been identified as a signalling molecule downstream of L-MAG (Umemori et al. 1994). Beside Fyn, the calcium-binding protein S100beta has been shown to bind to the L-MAG specific domain (Kursula et al. 1999). The S-MAG specific domain has been reported to bind to tubulin and microtubules (Kursula et al. 2001). Therefore, L-MAG seems to have properties of a transmembrane receptor that transduces extracellular signals to the inside of oligodendrocytes and Schwann cells, whereas the S-MAG isoform appears to link the extracellular ligand to the cytoskeleton of the myelinating glial cell.

Differential Expression of L- and S-MAG in Oli-neu Cells upon CyclicAMP Treatment

To get further inside in the regulation of the differential expression of L-MAG and S-MAG, we have characterized their differential expression upon stimulation with cAMP in the mouse Oli-neu oligodendroglial cell line (Jung et al. 1995).

In vitro and *in vivo* studies showed that Oli-neu cells mimic in many aspects the behaviour of primary oligodendrocytes (Jung et al. 1995; Koch et al. 1997; Kramer et al., 1997; Kramer et al. 1999; Klein et al. 2002). The cells express the typical myelin lipids, GalC and sulfatide (Jung et al. 1995), and have been shown to express the GPI-anchored proteins, F3/contactin and NCAM120 (Koch et al. 1997), and the microtubule-associated proteins, Tau-1 and Tau-5 (Klein et al. 2002), in a manner similar to primary oligodendrocytes. Furthermore, Oli-neu cell transplantation into demyelinated CNS lesions showed that they express the components necessary for axonal interaction (Jung et al. 1995). Proliferating Oli-neu cells have a bipolar shape. Under the influence of cAMP, Oli-neu cells exit the cell cycle and develop a radial morphology with many processes. In parallel to their morphological maturation, they up-regulate the expression of MAG (Jung et al. 1995).

We have investigated the expression of the L- and S-MAG-encoding splice variants

following cAMP stimulation in the Oli-neu cells by RT-PCR. Furthermore, we have generated genomic expression constructs to express the individually tagged isoforms, regulated by the process of alternative splicing, under the control of their own promoter. These genomic constructs were reintroduced into Oli-neu cells to investigate the L- and S-MAG-specific protein expression upon cAMP stimulation in relation to the cellular morphology.

Our analysis revealed that elevated cAMP levels influenced the alternative splicing of the primary MAG transcripts. We observed a switch from primarily L-MAG to predominant S-MAG mRNA levels upon stimulation with cAMP. In addition, we could show, at both the cellular and the protein levels, that L-MAG was mainly expressed in bipolar cells, whereas the S-MAG up-regulation upon cAMP stimulation was restricted to the most morphologically differentiated cells having developed a radial shape. Our observations are in line with the differential expression of L- and S-MAG during development in the rodent CNS (Inuzuka et al. 1991; Ishiguro et al. 1991; Pedraza et al. 1991). L-MAG precedes S-MAG expression during myelination, whereas L- and S-MAG are co-expressed in the adult. The analysis of the L- and S-MAG levels in primary oligodendrocyte cultures and in the CG4 oligodendroglial cell line showed, on the contrary, a clear predominance of the L-MAG splice variant (Yim et al. 1995; Richter-Landsberg and Gorath 1999). In line with our data is the observation that primary oligodendrocytes co-cultured with neuronal cells showed a similar S-MAG up-regulation (Matsuda et al. 1997). In parallel to the S-MAG up-regulation, a morphological differentiation was induced upon neuronal co-culturing (Matsuda et al. 1997) comparable to that which we observed upon cAMP stimulation. It is very intriguing to speculate that the co-ordinate change in the MAG alternative splicing and the increase in morphological complexity are controlled by the same cAMP-responsive differentiation step mediated by neurons *via* a single, or multiple mechanisms, resulting in elevated cAMP levels. This hypothesis is supported by earlier observations, indicating that the absence of neuronal signals might cause a modulation of mRNA splicing (Barbarese and Pfeiffer 1981; Richter-Landsberg and Gorath 1999) and by the findings of Cohen and Almazan that cAMP levels of cultured oligodendrocytes can be elevated by a receptor-mediated interaction with neuroligands (Cohen and Almazan 1993). Interestingly, in oligodendrocytes isolated from postnatal day 2 rat cerebrum CREB was phosphorylated by neuroligands known to elevate Ca^{2+} -levels (e.g. histamine, carbachol, glutamate and ATP), whereas in primary oligodendrocytes from postnatal day 11, a time-point immediately preceding myelination, CREB phosphorylation was only stimulated by treatment with the β -adrenergic agonist isoproterenol, a neuroligand known to elevate cAMP levels (Sato-Bigbee et al. 1999). This is in line with the observations that S-MAG up-regulation occurs between postnatal day 10 and 15 in the rat cerebrum (Frail and Braun 1984; Matthieu et al. 1986; Inuzuka et al. 1991). Recently, the nuclear localized quaking isoform, QKI-5, was shown to repress the inclusion of exon 12 in the mature MAG mRNA and, therefore, promote the splicing leading to the L-MAG splice variant (Wu et al. 2002). QKI-5 is a product of the locus that is deleted in quaking mice (Ebersole et al. 1996). Quaking mice have a dysmyelinating phenotype and show a strong increase of S-MAG mRNA relative to the L-MAG level (Fujita et al. 1990). Therefore, QKI-5 was postulated to act as a negative regulator of MAG exon 12 integration (Wu et al. 2002). Hence, the elevated cAMP level may induce, besides an enhanced MAG transcription, a reduction of the transcription, or activity, of the nuclear factor QKI-5. Very recently, adenosine has been shown to act as a potent axon-glia transmitter that inhibits oligodendrocyte precursor proliferation, stimulates differentiation, and promotes the

formation of myelin (Stevens et al. 2002). This axon-glia signal provides a molecular mechanism for promoting oligodendrocyte development and myelination in response to impulse activity. Interestingly, the G-protein coupled adenosine receptors expressed by the oligodendrocyte precursors are known to activate adenylyl cyclase and, therefore, elevate the oligodendrocyte cAMP levels (Dunwiddie and Masino 2001). Therefore, cAMP appears to be the physiological mediator of the neuronal signal adenosine that promotes the exit of the oligodendrocyte from the cell cycle and its subsequent differentiation. The elevation of the MAG transcriptional level and the isoform type switch from L- to L- and S-MAG appear to be part of these early, cAMP-mediated, processes of the axon-glia interaction.

The Effect of Exonic Insertions on the Alternative Splicing of the MAG Pre-mRNAs

The genomic expression constructs encoding individually tagged L- and S-MAG isoforms were generated by the insertion of the tag-encoding DNA into the isoform specific exons. The compatibility of these exonic insertions with the process and regulation of alternative splicing of the primary MAG transcripts are discussed in the following section. The insertion of the GFP sequence into L-MAG specific exon 13, in the *pmag*-MAG-e13GFP genomic expression construct led to expression of L-MAG-GFP and untagged S-MAG. L-MAG-GFP was expressed mostly in bipolar cells, but the number of cells expressing L-MAG-GFP was decreased relative to the L-MAG-expressing cells from the wild-type construct. Interestingly, we also observed a decreased number of L-MAG-GFP-expressing Oli-neu cells from the *pmag*-L-MAG-GFP construct that was expected to constitutively express L-MAG-GFP under the control of the *mag* promoter. Hence, the L-MAG-GFP encoding mRNA might be less stable than the wild-type counterpart, or the L-MAG-GFP fusion protein gets targeted to the degradation pathway. However, the expression of the L-MAG-GFP fusion protein and wild-type L-MAG from the cDNA expression vectors (\square actin-promoter) both revealed comparably high expression levels and numbers of positive Oli-neu cells. However, the high level transcription due to the potent \square actin-promoter might have masked the hypothesized implications of the L-MAG-GFP mRNA and/or protein.

On the other hand, the elongation of exon 13 did not affect the splicing of exon 12. This contrasts with the insertion of the GFP, or VSVG sequences into the S-MAG specific exon 12. These two constructs led to the expression of tagged S-MAG (S-MAG-GFP, or S-MAG-VSVG), but not to the expression of L-MAG. The depletion of L-MAG was probably not due to a strong increase in inclusion of the elongated exon 12, because S-MAG-GFP and S-MAG-VSVG were expressed in multipolar rather than bipolar Oli-neu cells, a regulation comparable to that seen for S-MAG with the wild-type construct. In addition, our findings are supported by a recent report, showing that the regulatory element for exon 12 alternative splicing lies outside of exon 12, within the adjacent intron 12 (Wu et al. 2002). Since, we have not altered any intron sequence, the absence of the L-MAG splice variant cannot result from a strongly increased inclusion of exon 12 due to an alteration of the regulatory element within intron 12, or within any other intron. Interestingly, in the study by Wu and colleagues (2002), the sequence of exon 12 was replaced by that of exon 11, resulting in a strong increase in the inclusion of the modified exon 12. This increase of exon 12 inclusion was thought to be induced by the elongation of the exon from 45 to 100

bases since shorter fragments allowed repression of exon 12 inclusion by QKI-5. In our study, we did not observe enhanced inclusion of exon 12 due its elongation from 45 to 81 bases (S-MAG-VSVG), or even 762 bases (S-MAG-GFP). Therefore, the enhanced inclusion of the exon 12 replaced by the exon 11 sequence in the study of Wu et al. (2002) may be due to the presence of a strong exon splicing enhancer (ESE) within exon 11. Furthermore, the analysis of the *pmag*-MAG-e12VSVG-e13GFP construct demonstrated that the exon 12 is not included in bipolar cells, as shown by the sole expression of GFP (“soluble” GFP). These data indicate that it is the not regulation, but rather the skipping of exon 12 that is disturbed, generating a truncated “L-MAG-GFP” transcript that leads to the synthesis of GFP alone. This translation of GFP was probably initiated at the start codon of GFP itself. Otherwise, the upstream sequence of exon 13 would have been translated and the product would have been recognized by the L-MAG specific antibody, which was generated against this sequence.

Taken together, the results of the analysis of the differential expression of L- and S-MAG in Oli-neu cells demonstrated that this mouse oligodendroglial cell line is a valuable tool for analysing the regulation and mechanism of alternative splicing of L- and S-MAG mRNAs. The observed switch bears a resemblance to the situation observed during myelin formation in CNS development. Therefore, we hypothesize that the regulation of the MAG alternative splicing and the morphological differentiation in oligodendroglial cells may be controlled by a similar cAMP-responsive differentiation step. This step is probably mediated by adenosine, which is released by axons in activity dependent manner (Stevens et al., 2002). However, introducing VSVG, or GFP, into exon 12 interfered with the correct skipping of exon 12, but not its regulation.

Differential Expression of L- and S-MAG in the Adult Mouse Brain

We have generated three different transgenic mouse lines expressing individually tagged L-MAG-GFP, or S-MAG-GFP fusion proteins. The individually tagged MAG isoforms should allow us to investigate the differential expression during development, in the adult, during injury-induced regeneration and under hereditary de- and remyelinating conditions. The generation of a third mouse line to constitutively express L-MAG-GFP under the control of the MAG promoter should reveal, whether the overexpression of L-MAG leads to alterations in the axon-glia interaction. Such an L-MAG overexpression phenotype can be expected in both, the CNS and PNS of mice. Since L- and S-MAG are coexpressed in the mouse CNS, a L-MAG overexpression would mimic the situation of the human CNS, which is known to express exclusively L-MAG (Miescher et al. 1997). However, a more prominent L-MAG overexpression phenotype can be expected in the PNS, since only minor amounts of L-MAG are expressed during development and L-MAG is completely absent in the adult PNS. Along this line, cell culture experiments provided evidence for a critical role of MAG in the initiation of myelination. When levels of MAG expression were experimentally reduced in Schwann cells by infecting them with a retrovirus expressing MAG antisense RNA, they failed to segregate large calibre neurites of co-cultured dorsal root ganglion (DRG) neurons and myelination of DRG neurites was impaired (Owens and Bunge 1991). Therefore, one could imagine that L-MAG overexpression would lead to a shift of the ratio of myelinated and non-myelinated axons towards more myelinated axons. Such a shift would highlight the role of L-MAG as a receptor molecule that mediates the

axon-glia interaction and transduces a myelination-promoting signal into the Schwann cell. However, the analysis of the CNS and PNS myelin of several mouse lines expected to constitutively express L-MAG-GFP (*pmag*-L-MAG-GFP), revealed no expression of the transgene. Furthermore, we have analysed the mouse line expected to express L-MAG-GFP (*pmag*-MAG-e13GFP). Unfortunately, the single founder animal has not, so far, passed the transgene to the F1 generation. Therefore, our analysis was restricted to a tail biopsy from the one-month-old founder animal. The analysis revealed no detectable L-MAG-GFP expression in the myelinated fibres of the tail. This might be due to the already low expression of L-MAG in the one-month-old mouse PNS (Inuzuka et al. 1991; Lützel Schwab 1998). Taken together with the relatively low number of L-MAG-GFP-expressing Oli-neu cells from one of these two constructs, the fusion of GFP to the L-MAG C-terminus seems to interfere either with the RNA stability, protein synthesis, or with myelin incorporation.

Fortunately, the analysis of the mouse line planned to express individually tagged S-MAG-GFP (*pmag*-MAG-e12GFP) revealed a prominent expression the S-MAG-GFP fusion protein in the mouse CNS, as well as in the PNS myelin. The fusion of GFP to the S-MAG C-terminus does not seem to affect the normal targeting and myelin incorporation of S-MAG, since S-MAG-GFP was detected in the periaxonal membranes of PNS myelin sheaths. The expression of S-MAG-GFP from the transgene beside the endogenous MAG expression in the one-months-old mouse brain, leads neither to a significant MAG overexpression, nor to an alteration in the L-MAG expression level. This finding indicates that the MAG protein levels seem to be tightly controlled. The analysis of the *pmag*-MAG-e12GFP construct used in Oli-neu cells showed that S-MAG-GFP is expressed from the construct in a normally regulated manner, but that L-MAG expression was missing, since an anti-L-MAG signal was absent. The lack of the anti-L-MAG signal could have been the result of an impaired splicing of the artificially enlarged S-MAG specific exon 12 (insertion of the GFP DNA sequence), producing a MAG protein with a truncated C-terminus. But, the Western blot analysis of the transgenic mouse brain myelin revealed no truncated MAG protein. Thus, normal skipping of the enlarged exon 12 may take place *in vivo*, resulting in a normal L-MAG-encoding mRNA. This would be in clear contrast to the *in vitro* situation observed in Oli-neu. On the other hand, the truncated 'L-MAG' mRNA, or protein, is immediately degraded *in vivo*. For a final analysis of the existence of a correct L-MAG-encoding mRNA transcribed from the *pmag*-MAG-e12GFP construct, transgenic mice should be crossed with the MAG knock-out mouse. Taken together, the *pmag*-MAG-e12GFP mouse line expresses MAG levels comparable to those of wild-type mice, and the S-MAG-GFP fusion protein is targeted normally to the periaxonal membrane. Therefore, this mouse line can be used to analyse the differential expression of L- and S-MAG using the autofluorescence signal of S-MAG-GFP together with our L-MAG specific antibody.

In this line, our first results of the expression pattern of S-MAG-GFP and L-MAG in one-month-old mouse brains revealed a preferential expression of S-MAG in the corpus callosum and a reciprocal expression of L- and S-MAG in distinct fibre tracts within the striatum (Figure 27). This pattern contrasts with the findings of Butt and colleagues (1998b), who describe a constitutive L-MAG expression beside a specific S-MAG expression in large diameter fibres, so-called type III/IV units, but not in small diameter fibres, so-called type I/II type units, in the anterior medullar velum. However, care should be taken when interpreting these data, since their S-MAG antibody was raised against a peptide that is not absolutely S-MAG specific, but has an amino acid stretch that is

common to both MAG isoforms. Furthermore, they worked with unpurified rabbit sera that produced a strong unspecific signal in our hands (data not shown). Therefore, the high expression level of S-MAG-GFP in the corpus callosum could reflect a predominant expression of S-MAG in long projecting fibre tracts. S-MAG could help to stabilize the myelin sheath, since S-MAG has been reported to bind to tubulin and microtubules (Kursula et al. 2001). This hypothetical, predominant expression of the S-MAG isoform in long projecting CNS fibres can be tested by the analysis of the L- and S-MAG expression in the long projecting fibres of the spinal chord. This would support the role of S-MAG as a cell adhesion molecule that links the axonal surface to the myelinating glial cell cytoskeleton.

MAG has been shown to bind to extracellular matrix components such as collagen, tenascin-R, fibronectin and heparin (for review see Quarles et al., 2002). However, the physiological relevance of its binding to components of the extracellular matrix is not clear, because most MAG is localized in periaxonal and other spiralled glial membranes. Our investigation of teased fibres from the sciatic nerve of S-MAG-GFP expressing transgenic mice, revealed beside a rather weak periaxonal signal a strong expression of S-MAG-GFP in ring like structures in the outer myelin membranes (Figure 25). Since the myelinated fibres of the peripheral nervous system are surrounded by a basal lamina, this so far marginalized expression domain of S-MAG in the outer myelin membranes may be the physiological sites where S-MAG does interact with these ECM molecules within the Schwann cell basal lamina.

The analysis of the sciatic nerve teased fibres from the S-MAG-GFP transgenic mice revealed as well that not all myelinated axons in the mouse peripheral nervous system are surrounded by a myelin sheath with periaxonal MAG expression. The absence of the periaxonal MAG expression in mouse peripheral nerves had often been observed in our laboratory, but it was interpreted as a result of bad antibody penetration. But, the S-MAG-GFP transgenic mice confirm these earlier findings.

The absence of the periaxonal MAG expression in many myelinated fibres of the mouse PNS is clear contrast to the situation in the mouse CNS. In the mouse CNS, every myelinated fibre appears to be surrounded by a periaxonal MAG expression. This difference in the MAG expression between the mouse PNS and CNS might explain at least to a certain degree why in the MAG deficient mice the myelin maintenance in the CNS is much more affected than in the PNS (for review see, Schachner et al., 2000). Therefore, L- and S-MAG appear to be more important for the myelin maintenance and the axon-glia interaction in the mouse CNS compared to S-MAG in the PNS.

Raft Association of MAG During Myelination and Myelin Maintenance

A major question in the formation and maintenance of the myelin-axon interaction concerns the coordinated translocation of myelin proteins and lipids to the different myelin compartments. Recent results suggest that glycolipid-enriched microdomains, so-called 'lipid-rafts', are involved in particular sorting and trafficking mechanisms of membrane proteins and lipids in polarized cells. Furthermore, lipid-rafts can selectively incorporate, or exclude proteins, and thereby govern protein-protein and protein-lipid interactions (Brown and London 1998; Hooper 1999). Along this line, they are thought to serve as platforms for signal transduction mechanisms. This makes them interesting candidates as participants

in axon-myelin interactions, as well as in interactions between the apposed myelin membranes. Lipid-rafts are insoluble in detergents, such as non-ionic TritonX-100 and zwitterionic CHAPS, at 4°C, in which they form glycolipid-enriched complexes. Because of their high lipid content, these detergent-insoluble, glycolipid-enriched complexes (DIGs) float to a low density during gradient centrifugation, which enables any associated proteins to be identified and distinguishes DIGs from other detergent-insoluble complexes.

We could show that both MAG isoforms are recruited to TritonX-100- and CHAPS-insoluble DIGs in the adult rodent CNS. In contrast to the situation in the adult rodent brain, we found that, in very young rodent brain (postnatal day 9), MAG was exclusively localized in the soluble fraction and not in DIGs. This is of special interest, since MAG has so far described to be found mainly in the soluble fraction (Kramer et al. 1997; Kim and Pfeiffer 1999). The finding that L-MAG is incorporated into DIGs in the adult brain highlights the possibility that L-MAG transduces neuronal signals *via* the non-receptor tyrosine kinase Fyn. This hypothesis is supported by the fact that L-MAG has been shown to activate Fyn and Fyn-deficient mice displayed only 50-60% myelin compared to wild-type animals (Umemori et al. 1994). Interestingly, the degree of hypomyelination in the brain of MAG/Fyn double mutants was significantly increased when compared with MAG and Fyn single mutants (Biffiger et al. 2000). Fyn was shown to be associated with the two GPI-linked molecules, F3/contactin and NCAM-120, in rafts during CNS myelination (mouse postnatal day 9), while L-MAG is not incorporated into DIGs at this early phase of myelination (Kramer et al. 1999). However, since we could show that L-MAG is incorporated into DIGs in the adult rodent CNS, the L-MAG-Fyn interaction may be important for the axon-to-glia signalling to guarantee myelin maintenance during adulthood. Furthermore, MAG has been shown to interact with the sialic acid of the gangliosides GD1a and GT1b (Crocker et al. 1998; Collins et al. 1999). Therefore, MAG can mediate cell-cell *trans* interactions (axon-to-glia and/or glia-to-glia), as well as *cis* interactions with gangliosides located on the same myelin membrane (Crocker 2002). With respect to the MAG expression domains, L-MAG-Fyn signalling, supposed to be important for myelin maintenance, could be mediated by periaxonal (axon-to-glia) and paranodal (glia-to-glia) L-MAG (Bartsch et al. 1989).

L-MAG could play an even more prominent role in myelin maintenance in the adult human brain, because we could show that L-MAG represents only 22% and 12% of total MAG mRNA in 4- and 12-month-old mouse brains, respectively (Figure 36), while, in the adult human brain, L-MAG is the predominant MAG isoform (Miescher et al. 1997). Furthermore, we found a surprisingly high amount of L-MAG to be incorporated into TritonX-100- and CHAPS-insoluble DIGs isolated from adult human brain. The analysis of two human adult cortical white matter samples revealed that almost 100% of L-MAG in the first sample and about 60% of L-MAG in the second sample were incorporated into DIGs. This discrepancy could reflect brain region-, or structure-specific differences in the incorporation of L-MAG into DIGs. However, the predominance of L-MAG in the adult human brain myelin, together with its predominant localization in DIGs, suggests an important role for L-MAG in maintaining the integrity of the human brain myelin sheath.

Decreased MAG and MBP Protein Levels in the Brain Myelin from MAL Deficient Mice

During myelinogenesis, oligodendrocytes produce and target myelin membrane at a rate that ranks amongst the highest of all known cellular membrane-producing systems (Pfeiffer et al. 1993). Myelin is synthesized as a plasma membrane extension and maintains a characteristic biochemical composition during adult life. One molecule that is known to be involved in lipid-raft-associated protein sorting and trafficking, not only in myelinating glia cells, but also in polarized epithelial cells, is MAL. To investigate the role of MAL and rafts in CNS myelination and maintenance, we analysed the myelin protein composition of adult MAL-deficient mouse brain myelin and myelin DIGs. The depletion of MAL led to significant alterations in the protein levels of the non-compact myelin proteins, MAG and MOG, the compact myelin proteins, MBP and PLP, as well as of the paranodal proteins, F3/contactin and Caspr.

Among the analysed proteins, MAG was the protein whose incorporation into myelin membranes was most affected by the lack of MAL. The MAG protein levels in MAL knock-out brain myelin and myelin DIGs were reduced to about 60% of the wild-type levels. Interestingly, the MAL mutant CNS myelin contained ultrastructural abnormalities similar to those of the MAG mutant (Li et al. 1994; Montag et al. 1994; Marcus et al. 2002). These abnormalities include an increased number of multiply myelinated axons, overlapping myelinated segments, reversed paranodal glial loops (Figure 39) and periaxonal process splitting. They reflect disturbed axon-glia and/or glia-glia interactions.

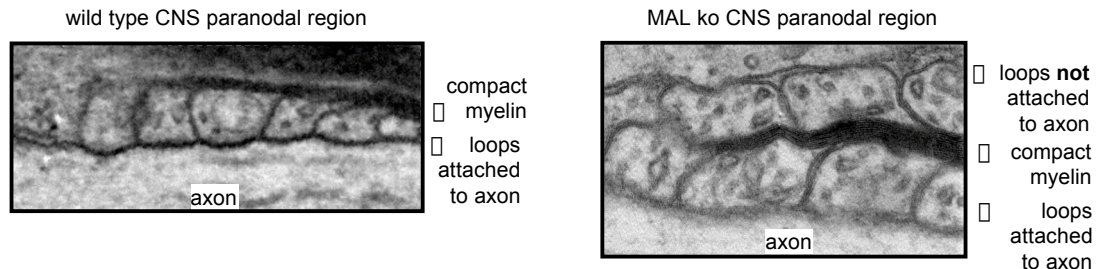


Figure 39 Paranodal loops in the nervus opticus of adult wild-type and MAL knock-out mice. In the wild-type situation, all loops are attached to the axonal membrane, whereas in the MAL knock-out mice, about half of the loops are not attached to the axonal membrane.

Due to the striking ultrastructural similarities between the MAL- and the MAG-deficient CNS myelin, the reduced MAG levels in the MAL mutant CNS appears to be responsible, at least to some extent, for the disturbed axon-glia interaction. Furthermore, mice lacking the two galactolipids GalC and sulfatide (CGT^{-/-}), two typical raft-associated lipids, revealed similar ultrastructural alterations. Whether, these alterations in the CGT knock-out mice are also caused by a partial lack of MAG is not known. The fact that the MAL-, MAG- and CGT-deficient mutants produce abnormal myelin containing similar ultrastructural abnormalities, suggests that these molecules may play an overlapping role in the axon-glia interaction, either by having a function in the sorting and trafficking of the involved receptor molecules, or by having receptor properties themselves. In line with these observations, the MAG/CGT double-mutant mice show a significantly more affected axon-myelin adhesion than the single mutants, supporting an overlapping function (Marcus et al. 2002). A very important feature of these mutants is that the paranodes, flanking the

nodes of Ranvier, form normally, independently of MAL, MAG, or galactolipids, but rapidly destabilize in their absence. Therefore, MAL, MAG, and the galactolipids do not appear to be necessary for the initial interactions between the oligodendrocyte and the axon, but these myelin components contribute significantly to the stabilization of the myelin–axon and myelin-myelin contacts in the CNS, even though they are structurally dissimilar. These data indicate that distinct molecular mechanisms are responsible for the formation and maintenance of axon-myelin and myelin-myelin interactions. MAG seem to play a major role in this maintenance process, either by stabilizing directly the glia-glia interaction in the paranodal region, as MAG is expressed in the paranodal loops at low levels in the CNS (Bartsch et al. 1989), or indirectly by mediating internodal axon-glia interactions, as MAG is expressed in the adaxonal (periaxonal) myelin membrane (Schachner and Bartsch 2000).

Our analysis of the MAG mRNA levels in the MAL-deficient mouse brains revealed that the transcription is elevated, even though not statistically significant. This shows that the lack of MAL does indeed affect the myelin incorporation of the MAG proteins. Furthermore, the reduced MAG levels appear to induce an up-regulation of MAG transcription in a compensatory manner.

Our investigation of the MAG protein levels in CHAPS-insoluble DIGs isolated from MAL knock-out and wild-type brain myelin, showed the same reduction that we had observed for MAG in the brain myelin. Thus, the detergent insolubility of total MAG and L-MAG was not affected by the lack of MAL. Therefore, within the brain myelin membrane, MAG appears to be still surrounded by, or interacting with, a comparable subset of myelin proteins and, even more important, with a comparable subset of myelin lipids. Along this line, our analysis of the lipid composition of the MAL-deficient brain myelin and brain myelin DIGs revealed no apparent differences. Therefore, the lack of MAL seems to affect primarily the sorting, trafficking and/or myelin membrane incorporation of MAG, and not its raft association in the mouse brain. Therefore, MAG may be partially incorporated into DIGs in the trans-Golgi network independently of MAL and MAL is involved in a similar manner in the transport of the DIG- and non-DIG-associated MAG to the myelin sheath. Alternatively, MAG may be transported to the myelin in a MAL-dependent manner as a non-DIG protein and is only then incorporated into DIGs independently of MAL. Yet another alternative is that in the absence of MAL, newly synthesized MAG molecules could be mistargeted and degraded, or endocytosed MAG could be targeted to the late endosomes/lysosomes instead of back to the myelin membranes. The analysis of the MAG protein levels in whole brain homogenates could help to determine whether the MAG that was not inserted into the myelin membranes in the absence of MAL, is still to some extent present, for instance, in the degradation pathway, or in the oligodendrocyte plasma membrane. The analysis of cerebellar slice cultures could also help to determine if and where the MAG protein that has not been incorporated into the myelin sheath in the absence of MAL, is localized within the myelinating oligodendrocytes.

The reduction of MAG in 2-years-old MAL-deficient mouse brains seems to be comparable or even milder, to that seen in 4-month-old brains. Therefore, the situation observed at the age of 4 months seems not to reflect a process of increasing reduction that had started, for example, during myelin compaction, but rather a steady-state situation. However, it is not known if the MAG trafficking has been already affected by the lack of MAL during the process of active myelination, before myelin compaction. The analysis of the MAG levels

from MAL-deficient mouse brains that are in the process of active myelination will reveal if the transport mechanisms of MAG in the forming, non-compacted myelin and in the adult, compact myelin sheath are both dependent on MAL, or if the transport mechanisms operative during myelin formation are independent of MAL. In the latter case, MAL would function especially in the transport mechanisms during the maintenance of the adult myelin sheath.

MBPs act as intracellular adhesion molecules, holding together the intracellular leaflets of myelin membranes to form the compact myelin (Omlin et al. 1982). Therefore, the aberrant cytoplasmic inclusions within the compact myelin in the MAL-deficient CNS (Figure 40) might be caused by the observed reduction of the MBP levels.

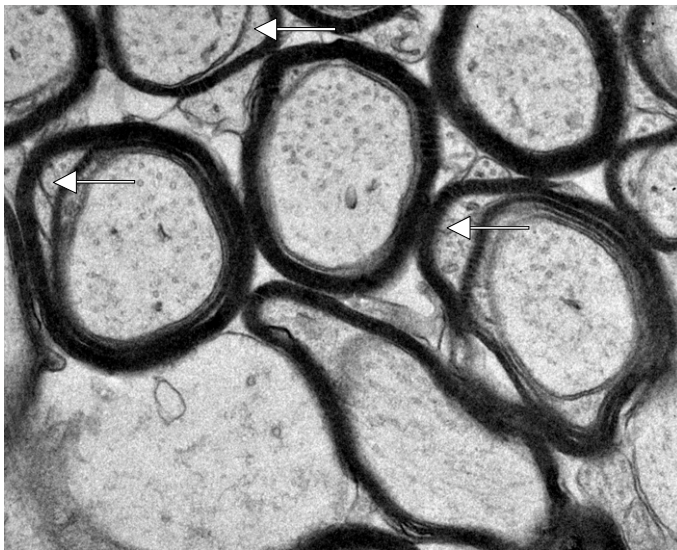


Figure 40 Splitting of CNS compact myelin in the absence of MAL
The lack of MAL leads to cytoplasmic inclusions (arrows) within the adult optic nerve that leads to a splitting of the compact myelin sheath.

Interestingly, the non-receptor tyrosine kinase Fyn has been shown to be necessary for MBP transcription (Umemori et al. 1999), while L-MAG is known to activate Fyn (Umemori et al. 1994). Since L-MAG is reduced to about 60% in MAL-deficient CNS myelin and DIGs, the lack of the L-MAG-Fyn cascade might be responsible for the reduced MBP levels. During CNS myelination, Fyn is thought to act in rafts through its association with F3/contactin and NCAM120, while L-MAG is not recruited to DIGs during this early developmental stage (Kramer et al. 1999). However, since L-MAG and Fyn are recruited to DIGs in the adult CNS myelin, L-MAG may activate Fyn in DIGs and, therefore, promote MBP transcription during the process of myelin maintenance. Therefore, the reduction of L-MAG in CNS myelin DIGs may be responsible for the reduced MBP transcription.

Since MBPs are basic, highly charged proteins, MBP mRNAs are selectively transported to the myelin sheath, where they are translated on free polysomes, in order to prevent unspecific membrane association (Colman et al. 1982; Trapp et al. 1987; Verity and Campagnoni 1988). Since myelin incorporation of MBP is independent of the normal protein sorting and trafficking machinery, the reduction of MBP in the MAL-deficient CNS cannot be explained by an impaired trafficking due to the absence of MAL and therefore supports the hypothesis that the lack of MAL results in a reduced MBP transcription perhaps through an impaired trafficking and signalling of L-MAG.

Among the proteins analysed in the brain myelin from adult MAL-deficient mice,

PLP/DM20 showed a unique pattern. In contrast with the decreased MAG, MBP and MOG levels, the amount of PLP/DM20 protein was increased in the adult MAL-deficient brain myelin membranes. Furthermore, in 2-years-old MAL-deficient mouse brains, the PLP/DM20 levels were strongly increased in the myelin, as well as in the myelin DIGs fraction. Interestingly, PLP/DM20 have other characteristics that are distinct from those of the other myelin proteins. The trafficking of PLP/DM20 appeared to be independent of other myelin markers, such as MAG, MOG and MBP (Hudson et al. 1989; Kramer et al. 2001). None of the latter colocalised with PLP/DM20 in intracellular compartments, arguing strongly against the existence of a common lipid-raft-dependent transport vesicle containing all myelin components. Moreover, PLP was found to be soluble in cold TritonX-100, contradicting one of the criteria for the association of a protein with lipid-rafts, while the myelin proteins MAG, MBP and MOG are at least partially resistant to TritonX-100 extraction (Kramer et al. 1997; Kim and Pfeiffer 1999; Taylor et al. 2002). The transport mechanism of the major myelin proteins PLP/DM20 seems, therefore, to be distinct from that of MAG, MOG and MBP. Kramer and collaborators (Kramer et al. 2001) proposed the transcytosis model as an alternative trafficking route for PLP/DM20 (Figure 41). According to this model, newly synthesised PLP/DM20 is transported to the oligodendrocyte plasma membrane *via* a general secretory pathway, independently of lipid-rafts. The incorporation of PLP/DM20 into the myelin sheath is achieved in a second step, by endocytic uptake into early/recycling endosomes, from where PLP/DM20 are sorted/recycled to the myelin sheath, or to the late endosomes/lysosomes.

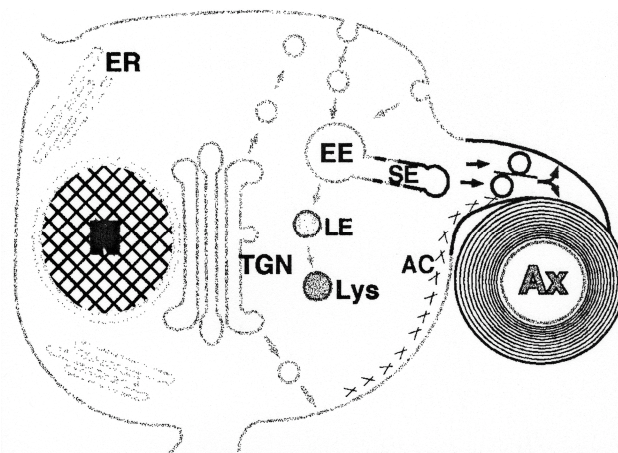


Figure 41 Transcytosis: model for the involvement of MAL in the transport/recycling of PLP

Newly synthesized PLP molecules follow a general secretory path from the *trans*-Golgi network (TGN) to the plasma membrane (bulk flow), from where they get transported to the early endosomes (EE) by endocytic uptake. From the early endosomes, newly synthesized, or recycled PLP gets either incorporated into the myelin sheath through sorting endosomes (SE), or it gets directed to the late endosomes/lysosomes (LE/Lys) for degradation. MAL appears to be involved in the regulation of the recycling/degradation of PLP in the early endosomes, since the lack of MAL leads to an accumulation of PLP in the myelin sheath. AC: actin cortex; Ax: axon; ER: endoplasmic reticulum; N: nucleus; copied from Kramer et. al., 2001:

But how can the lack of MAL lead to an accumulation of PLP/DM20 in brain myelin? Several *in vitro* overexpression experiments of PLP/DM20 led to an accumulation of PLP/DM20 in the late endosomes/lysosomes (Gow et al. 1994; Sinoway et al. 1994; Kalwy et al. 1997; Kramer et al. 2001; Simons et al. 2002). Therefore, the protein level of the major CNS myelin component PLP/DM20 seem to be tightly controlled and surplus

molecules are not recycled from the early/recycling endosomes back to the myelin sheath, but are targeted to the endosomal/lysosomal pathway for degradation. MAL could be involved in the endocytosis and recycling of PLP/DM20, since MAL has been shown to be localized in the early and recycling endosomes (Millan et al. 1997a; Puertollano et al. 1999). The lack of MAL could lead to an imbalance between recycling and degradation of PLP/DM20 in the early/recycling endosomes. This imbalance could lead to an increased recycling of PLP/DM20 back to the myelin sheath and, therefore, to an accumulation of PLP/DM20 in the brain with increasing age. An increased PLP/DM20 protein level due to an increased PLP/DM20 transcriptional activity can be excluded, since the transcriptional level in the MAL knock-out brains appeared to be decreased rather than elevated (Figure 37). Such a compensatory down-regulation further supports the hypothesis of an increased recycling of PLP/DM20 in the absence MAL. A possible involvement of MAL in the endosomal system is supported by recent findings in the Arylsulfatase-A knock-out mice (ASA knock-out; Franken et al. 2003). Due to the lack of the Arylsulfatase-A enzyme responsible for the normal degradation of the raft lipid sulfatide, MAL, together with sulfatide, is accumulated in the late endosomes/lysosomes of ASA knock-out kidney cells and maybe also in the ASA ko oligodendrocytes.

Taken together, the proteolipid MAL appears to be involved in the regulation of the recycling/degradation of the major CNS myelin protein PLP.

In the context of a possible involvement of MAL in the regulation of the recycling/degradation of myelin proteins in oligodendrocytes, the significantly decreased levels of MAG and MBP in the adult MAL-deficient mouse brains could result from an enhanced degradation of these myelin proteins *via* the endosomal/lysosomal system. Therefore, the MAG and MBP levels should also be analysed in whole brain preparations to detect possible MAG and MBP molecules that may have been misrouted to the late endosomes/lysosomes in the absence of MAL.

Outlook

MAL Knock-Out Brain Myelin: Analysis of the Myelin Protein Composition at the End of the Myelination Period and after 2 Years of Myelin Maintenance

The lack of MAL led to an altered myelin protein composition in adult (4-months-old) mouse brains. The altered myelin protein composition is probably caused by an impaired protein sorting/trafficking and/or recycling due to the lack of MAL. To determine if the MAL depletion affects the protein trafficking mainly during active myelination, or during the maintenance of the compact myelin sheath, the brain myelin composition could be quantitatively analysed in young (3 weeks old) and old (2 years old) MAL knock-out and wild-type mouse brains. The comparison of these new data sets with our data from adult MAL mutants could allow to determine which proteins have never been incorporated into myelin at normal levels during the initial phase of active myelination. Furthermore, it could allow determining which proteins have undergone normal incorporation into myelin during myelination, but that are affected by an impaired maintenance process and are, therefore, expected to show an even greater alteration in old mice compared to the adult mice.

An increased targeting of MAG and MBP to the endosomal/lysosomal system might cause their impaired levels in brain myelin from MAL-deficient mutants. Therefore, the analysis of their protein levels in whole brain homogenates, instead of the myelin preparations used so far, should also allow to detect these misrouted myelin proteins.

The analysis of cerebellar slice cultures from MAL knock-out and wild-type mice could be used to investigate the subcellular distribution of those myelin proteins that are affected by the lack of MAL. An accumulation of MAG, or MBP, in the endosomal/lysosomal system would explain their decreased levels in the brain myelin and would support a possible role for MAL in the regulation of the recycling of myelin proteins in early/recycling endosomes.

The verification of the MAG and PLP mRNA levels could allow to determine if the impaired protein levels in the MAL knock-out mice really do cause a compensatory mechanism at the transcriptional level. Furthermore, the analysis of the MBP mRNA levels could allow determining if the decreased MBP levels are caused by a decreased transcription, or an impaired turnover. A reduced MBP transcription would be in line with the hypothesis that a decreased L-MAG level causes a decreased Fyn activity and, thus, a decreased MBP transcription.

To investigate if the prominent reduction of MAG in the brain of MAL-deficient mice affects all brain regions in a similar manner, or if certain structures are especially affected, the S-MAG-GFP could be crossed with the MAL knock-out line. In these double transgenic mice, the S-MAG-GFP levels could be measured directly by the fluorescent signal intensity of the S-MAG-GFP fusion protein.

MAG-GFP expressing mouse lines

The combination of the S-MAG-GFP-expressing transgenic mouse, together with our L-MAG specific antibody, will allow the further characterisation of the differential expression of the two MAG isoforms during *in vivo* development and in the different regions of the adult brain. Furthermore, the cross-breeding of the S-MAG-GFP mice with animal models for the primary demyelinating peripheral neuropathies CMT1A and HNPP will allow the analysis of L- and S-MAG expression under the pathological conditions of de- and remyelination. Previous experiments have shown an up-regulation of the L-MAG isoform at the protein level in sural nerve biopsies from CMT1A and HNPP patients, while the analysis of the mRNA in the corresponding mouse models revealed an S-MAG up-regulation. Therefore, it will be interesting to see if these mice show an up-regulation of S-MAG at the protein level as well, or if they show an up-regulation of L-MAG as observed in patients.

Schmidt-Lanterman incisures are postulated to play a role in the maintenance and turnover of the compact myelin sheath. The incorporation of S-MAG-GFP fusion proteins into these Schmidt-Lanterman incisures should allow the investigation of their dynamics in myelinating co-cultures by video confocal microscopy. A putative dynamic property of Schmidt-Lanterman incisures that would move along the axon within the otherwise compact myelin could strongly highlight their role in the turnover of myelin proteins and lipids.

The analysis of the single *pmag*-MAG-e13GFP and *pmag*-L-MAG-GFP founder animal tail biopsies so far revealed no L-MAG-GFP transgene expression. Since this lack of the L-MAG-GFP fusion protein can result from the absence or instability of the corresponding mRNA, or from the degradation of the fusion protein itself, the existence of the mRNA should be established by RT-PCR analysis. If the L-MAG-GFP mRNA is detectable, the transcriptional level and the sequence of the mRNA should be analysed. If these two parameters are correct, the expression of the fusion protein should be analysed *in vitro* by the use of optic nerve cultures, to exclude the possibility that the fusion protein is down-regulated *in vivo*.

References

- Abe T. and Norton W. T. (1979) The characterization of sphingolipids of oligodendroglia from calf brain. *J Neurochem* **32**, 823-832.
- Adlkofer K., Martini R., Aguzzi A., Zielasek J., Toyka K. V. and Suter U. (1995) Hypermyelination and demyelinating peripheral neuropathy in Pmp22-deficient mice. *Nat Genet* **11**, 274-280.
- Adlkofer K., Frei R., Neuberg D. H., Zielasek J., Toyka K. V. and Suter U. (1997) Heterozygous peripheral myelin protein 22-deficient mice are affected by a progressive demyelinating tomaculous neuropathy. *J Neurosci* **17**, 4662-4671.
- Ainger K., Avossa D., Diana A. S., Barry C., Barbarese E. and Carson J. H. (1997) Transport and localization elements in myelin basic protein mRNA. *J Cell Biol* **138**, 1077-1087.
- Alonso M. A. and Weissman S. M. (1987) cDNA cloning and sequence of Mal, a hydrophobic protein associated with human T-cell differentiation. *Proc Natl Acad Sci U S A* **84**, 1997-2001.
- Arroyo E. J. and Scherer S. S. (2000) On the molecular architecture of myelinated fibers. *Histochem Cell Biol* **113**, 1-18.
- Bachmann M., Conscience J. F., Probstmeier R., Carbonetto S. and Schachner M. (1995) Recognition molecules myelin-associated glycoprotein and tenascin-C inhibit integrin-mediated adhesion of neural cells to collagen. *J Neurosci Res* **40**, 458-470.
- Bajt M. L., Schmitz B., Schachner M. and Zipser B. (1990) Carbohydrate epitopes involved in neural cell recognition are conserved between vertebrates and leech. *J Neurosci Res* **27**, 276-285.
- Ballice-Gordon R. J., Bone L. J. and Scherer S. S. (1998) Functional gap junctions in the schwann cell myelin sheath. *J Cell Biol* **142**, 1095-1104.
- Bansal R., Winkler S. and Bheddah S. (1999) Negative regulation of oligodendrocyte differentiation by galactosphingolipids. *J Neurosci* **19**, 7913-7924.
- Barbarese E. and Pfeiffer S. E. (1981) Developmental regulation of myelin basic protein in dispersed cultures. *Proc Natl Acad Sci U S A* **78**, 1953-1957.
- Bartsch S., Montag D., Schachner M. and Bartsch U. (1997) Increased number of unmyelinated axons in optic nerves of adult mice deficient in the myelin-associated glycoprotein (MAG). *Brain Res* **762**, 231-234.
- Bartsch U., Kirchoff F. and Schachner M. (1989) Immunohistological localization of the adhesion molecules L1, N-CAM, and MAG in the developing and adult optic nerve of mice. *J Comp Neurol* **284**, 451-462.
- Bergoffen J., Scherer S. S., Wang S., Scott M. O., Bone L. J., Paul D. L., Chen K., Lensch M. W., Chance P. F. and Fischbeck K. H. (1993) Connexin mutations in X-linked Charcot-Marie-Tooth disease. *Science* **262**, 2039-2042.
- Bhat M. A., Rios J. C., Lu Y., Garcia-Fresco G. P., Ching W., St Martin M., Li J., Einheber S., Chesler M., Rosenbluth J., Salzer J. L. and Bellen H. J. (2001) Axon-glia interactions and the domain organization of myelinated axons requires neurexin IV/Caspr/Paranodin. *Neuron* **30**, 369-383.
- Biffiger K., Bartsch S., Montag D., Aguzzi A., Schachner M. and Bartsch U. (2000) Severe hypomyelination of the murine CNS in the absence of myelin-associated glycoprotein and fyn tyrosine kinase. *J Neurosci* **20**, 7430-7437.
- Bird T. D., Farrell D. F. and Sumi S. M. (1978) Brain lipid composition of the shiverer mouse: (genetic defect in myelin development). *J Neurochem* **31**, 387-391.
- Black J. A. and Waxman S. G. (1988) The perinodal astrocyte. *Glia* **1**, 169-183.
- Blank W. F., Jr., Bunge M. B. and Bunge R. P. (1974) The sensitivity of the myelin sheath, particularly the Schwann cell-axolemmal junction, to lowered calcium levels in cultured sensory ganglia. *Brain Res* **67**, 503-518.
- Boggs J. M. and Wang H. (2001) Effect of liposomes containing cerebroside and cerebroside sulfate on cytoskeleton of cultured oligodendrocytes. *J Neurosci Res* **66**, 242-253.
- Bogler O., Wren D., Barnett S. C., Land H. and Noble M. (1990) Cooperation between two growth factors promotes extended self-renewal and inhibits differentiation of oligodendrocyte-type-2 astrocyte (O-2A) progenitor cells. *Proc Natl Acad Sci U S A* **87**, 6368-6372.
- Boison D. and Stoffel W. (1994) Disruption of the compacted myelin sheath of axons of the central nervous system in proteolipid protein-deficient mice. *Proc Natl Acad Sci U S A* **91**, 11709-11713.
- Bosio A., Bussow H., Adam J. and Stoffel W. (1998) Galactosphingolipids and axono-glia interaction in myelin of the central nervous system. *Cell Tissue Res* **292**, 199-210.
- Boyle M. E., Berglund E. O., Murai K. K., Weber L., Peles E. and Ranscht B. (2001) Contactin orchestrates assembly of the septate-like junctions at the paranode in myelinated peripheral nerve. *Neuron* **30**, 385-397.
- Bronstein J. M., Chen K., Tiwari-Woodruff S. and Kornblum H. I. (2000) Developmental expression of OSP/claudin-11. *J Neurosci Res* **60**, 284-290.
- Brown D. A. and Rose J. K. (1992) Sorting of GPI-anchored proteins to glycolipid-enriched membrane subdomains during transport to the apical cell surface. *Cell* **68**, 533-544.

- Brown D. A. and London E. (1998) Functions of lipid-rafts in biological membranes. *Annu Rev Cell Dev Biol* **14**, 111-136.
- Bunge R. P. (1993) Expanding roles for the Schwann cell: ensheathment, myelination, trophism and regeneration. *Curr Opin Neurobiol* **3**, 805-809.
- Burger D., Pidoux L. and Steck A. J. (1993) Identification of the glycosylated sequons of human myelin-associated glycoprotein. *Biochem Biophys Res Commun* **197**, 457-464.
- Burkart T., Caimi L. and Wiesmann U. N. (1983) Synthesis and subcellular transport of sulfogalactosyl glycerolipids in the myelinating mouse brain. *Biochim Biophys Acta* **753**, 294-299.
- Butt A. M., Ibrahim M. and Berry M. (1997) The relationship between developing oligodendrocyte units and maturing axons during myelinogenesis in the anterior medullary velum of neonatal rats. *J Neurocytol* **26**, 327-338.
- Butt A. M., Ibrahim M. and Berry M. (1998a) Axon-myelin sheath relations of oligodendrocyte unit phenotypes in the adult rat anterior medullary velum. *J Neurocytol* **27**, 259-269.
- Butt A. M., Ibrahim M., Ruge F. M. and Berry M. (1995) Biochemical subtypes of oligodendrocyte in the anterior medullary velum of the rat as revealed by the monoclonal antibody Rip. *Glia* **14**, 185-197.
- Butt A. M., Ibrahim M., Gregson N. and Berry M. (1998b) Differential expression of the L- and S-isoforms of myelin associated glycoprotein (MAG) in oligodendrocyte unit phenotypes in the adult rat anterior medullary velum. *J Neurocytol* **27**, 271-280.
- Caduff J., Sansano S., Bonnet A., Suter U. and Schaeren-Wiemers N. (2001) Characterization of GFP-MAL expression and incorporation in rafts. *Microsc Res Tech* **52**, 645-655.
- Cameron-Curry P., Dulac C. and Le Dourain N. M. (1991) A Monoclonal Antibody Defining a Carbohydrate Epitope Restricted to Glial Cells. *Eur J Neurosci* **3**, 126-139.
- Campagnoni A. T., Pribyl T. M., Campagnoni C. W., Kampf K., Amur-Umarjee S., Landry C. F., Handley V. W., Newman S. L., Garbay B. and Kitamura K. (1993) Structure and developmental regulation of Golli-mbp, a 105-kilobase gene that encompasses the myelin basic protein gene and is expressed in cells in the oligodendrocyte lineage in the brain. *J Biol Chem* **268**, 4930-4938.
- Carson J. H., Nielson M. L. and Barbarese E. (1983) Developmental regulation of myelin basic protein expression in mouse brain. *Dev Biol* **96**, 485-492.
- Chandross K. J., Kessler J. A., Cohen R. I., Simburger E., Spray D. C., Bieri P. and Dermietzel R. (1996) Altered connexin expression after peripheral nerve injury. *Mol Cell Neurosci* **7**, 501-518.
- Charles P., Tait S., Faivre-Sarrailh C., Barbin G., Gunn-Moore F., Denisenko-Nehrbass N., Guennoc A. M., Girault J. A., Brophy P. J. and Lubetzki C. (2002) Neurofascin is a glial receptor for the paranodin/Caspr-contactin axonal complex at the axoglia junction. *Curr Biol* **12**, 217-220.
- Cheong K. H., Zacchetti D., Schneeberger E. E. and Simons K. (1999) VIP17/MAL, a lipid-raft-associated protein, is involved in apical transport in MDCK cells. *Proc Natl Acad Sci U S A* **96**, 6241-6248.
- Chou K. H., Nolan C. E. and Jungalwala F. B. (1982) Composition and metabolism of gangliosides in rat peripheral nervous system during development. *J Neurochem* **39**, 1547-1558.
- Coetzee T., Dupree J. L. and Popko B. (1998) Demyelination and altered expression of myelin-associated glycoprotein isoforms in the central nervous system of galactolipid-deficient mice. *J Neurosci Res* **54**, 613-622.
- Coetzee T., Fujita N., Dupree J., Shi R., Blight A., Suzuki K. and Popko B. (1996) Myelination in the absence of galactocerebroside and sulfatide: normal structure with abnormal function and regional instability. *Cell* **86**, 209-219.
- Cohen R. I. and Almazan G. (1993) Norepinephrine-stimulated PI hydrolysis in oligodendrocytes is mediated by alpha 1A-adrenoceptors. *Neuroreport* **4**, 1115-1118.
- Collins B. E., Ito H., Sawada N., Ishida H., Kiso M. and Schnaar R. L. (1999) Enhanced binding of the neural siglecs, myelin-associated glycoprotein and Schwann cell myelin protein, to Chol-1 (alpha-series) gangliosides and novel sulfated Chol-1 analogs. *J Biol Chem* **274**, 37637-37643.
- Colman D. R., Kreibich G., Frey A. B. and Sabatini D. D. (1982) Synthesis and incorporation of myelin polypeptides into CNS myelin. *J Cell Biol* **95**, 598-608.
- Crocker P. R. (2002) Siglecs: sialic-acid-binding immunoglobulin-like lectins in cell-cell interactions and signalling. *Curr Opin Struct Biol* **12**, 609-615.
- Crocker P. R., Clark E. A., Filbin M., Gordon S., Jones Y., Kehrl J. H., Kelm S., Le Douarin N., Powell L., Roder J., Schnaar R. L., Sgroi D. C., Stamenkovic K., Schauer R., Schachner M., van den Berg T. K., van der Merwe P. A., Watt S. M. and Varki A. (1998) Siglecs: a family of sialic-acid binding lectins. *Glycobiology* **8**, v.
- DeBellard M. E., Tang S., Mukhopadhyay G., Shen Y. J. and Filbin M. T. (1996) Myelin-associated glycoprotein inhibits axonal regeneration from a variety of neurons via interaction with a sialoglycoprotein. *Mol Cell Neurosci* **7**, 89-101.
- Dermietzel R., Farooq M., Kessler J. A., Althaus H., Hertzberg E. L. and Spray D. C. (1997) Oligodendrocytes express gap junction proteins connexin32 and connexin45. *Glia* **20**, 101-114.
- Detering N. K. and Wells M. A. (1976) Detection of myelin in the optic nerve of young rats by sedimentation equilibrium in a CsCl gradient. *J Neurochem* **26**, 247-252.

- Devor M., Govrin-Lippmann R. and Angelides K. (1993) Na⁺ channel immunolocalization in peripheral mammalian axons and changes following nerve injury and neuroma formation. *J Neurosci* **13**, 1976-1992.
- Dickinson P. J., Fanarraga M. L., Griffiths I. R., Barrie J. M., Kyriakides E. and Montague P. (1996) Oligodendrocyte progenitors in the embryonic spinal cord express DM-20. *Neuropathol Appl Neurobiol* **22**, 188-198.
- Domeniconi M., Cao Z., Spencer T., Sivasankaran R., Wang K., Nikulina E., Kimura N., Cai H., Deng K., Gao Y., He Z. and Filbin M. (2002) Myelin-associated glycoprotein interacts with the Nogo66 receptor to inhibit neurite outgrowth. *Neuron* **35**, 283-290.
- Dong Z., Sinanan A., Parkinson D., Parmantier E., Mirsky R. and Jessen K. R. (1999) Schwann cell development in embryonic mouse nerves. *J Neurosci Res* **56**, 334-348.
- Doyle J. P. and Colman D. R. (1993) Glial-neuron interactions and the regulation of myelin formation. *Curr Opin Cell Biol* **5**, 779-785.
- Duckett S., Said G., Streletz L. G., White R. G. and Galle P. (1979) Tellurium-induced neuropathy: correlative physiological, morphological and electron microprobe studies. *Neuropathol Appl Neurobiol* **5**, 265-278.
- Dunwiddie T. V. and Masino S. A. (2001) The role and regulation of adenosine in the central nervous system. *Annu Rev Neurosci* **24**, 31-55.
- Dupree J. L., Suzuki K. and Popko B. (1998a) Galactolipids in the formation and function of the myelin sheath. *Microsc Res Tech* **41**, 431-440.
- Dupree J. L., Girault J. A. and Popko B. (1999) Axo-glial interactions regulate the localization of axonal paranodal proteins. *J Cell Biol* **147**, 1145-1152.
- Dupree J. L., Coetzee T., Suzuki K. and Popko B. (1998b) Myelin abnormalities in mice deficient in galactocerebroside and sulfatide. *J Neurocytol* **27**, 649-659.
- Dupree P., Parton R. G., Raposo G., Kurzchalia T. V. and Simons K. (1993) Caveolae and sorting in the trans-Golgi network of epithelial cells. *Embo J* **12**, 1597-1605.
- Dyer C. A. (1993) Novel oligodendrocyte transmembrane signaling systems. Investigations utilizing antibodies as ligands. *Mol Neurobiol* **7**, 1-22.
- Dyer C. A. and Benjamins J. A. (1989) Organization of oligodendroglial membrane sheets. I: Association of myelin basic protein and 2',3'-cyclic nucleotide 3'-phosphohydrolase with cytoskeleton. *J Neurosci Res* **24**, 201-211.
- Dyer C. A. and Benjamins J. A. (1990) Glycolipids and transmembrane signaling: antibodies to galactocerebroside cause an influx of calcium in oligodendrocytes. *J Cell Biol* **111**, 625-633.
- Dyer C. A., Philibotte T. M., Wolf M. K. and Billings-Gagliardi S. (1994) Myelin basic protein mediates extracellular signals that regulate microtubule stability in oligodendrocyte membrane sheets. *J Neurosci Res* **39**, 97-107.
- Ebersole T. A., Chen Q., Justice M. J. and Artzt K. (1996) The quaking gene product necessary in embryogenesis and myelination combines features of RNA binding and signal transduction proteins. *Nat Genet* **12**, 260-265.
- Einheber S., Milner T. A., Giancotti F. and Salzer J. L. (1993) Axonal regulation of Schwann cell integrin expression suggests a role for alpha 6 beta 4 in myelination. *J Cell Biol* **123**, 1223-1236.
- Einheber S., Zanazzi G., Ching W., Scherer S., Milner T. A., Peles E. and Salzer J. L. (1997) The axonal membrane protein Caspr, a homologue of neurexin IV, is a component of the septate-like paranodal junctions that assemble during myelination. *J Cell Biol* **139**, 1495-1506.
- Erne B., Sansano S., Frank M. and Schaeren-Wiemers N. (2002) Rafts in adult peripheral nerve myelin contain major structural myelin proteins and myelin and lymphocyte protein (MAL) and CD59 as specific markers. *J Neurochem* **82**, 550-562.
- Faivre-Sarrailh C., Gauthier F., Denisenko-Nehrbass N., Le Bivic A., Rougon G. and Girault J. A. (2000) The glycosylphosphatidyl inositol-anchored adhesion molecule F3/contactin is required for surface transport of paranodin/contactin-associated protein (caspr). *J Cell Biol* **149**, 491-502.
- Fannon A. M., Sherman D. L., Ilyina-Gragerova G., Brophy P. J., Friedrich V. L., Jr. and Colman D. R. (1995) Novel E-cadherin-mediated adhesion in peripheral nerve: Schwann cell architecture is stabilized by autotypic adherens junctions. *J Cell Biol* **129**, 189-202.
- Feltri M. L., Scherer S. S., Nemni R., Kamholz J., Vogelbacker H., Scott M. O., Canal N., Quaranta V. and Wrabetz L. (1994) Beta 4 integrin expression in myelinating Schwann cells is polarized, developmentally regulated and axonally dependent. *Development* **120**, 1287-1301.
- Fields R. D. and Stevens B. (2000) ATP: an extracellular signaling molecule between neurons and glia. *Trends Neurosci* **23**, 625-633.
- Fong J. W., Ledeen R. W., Kundu S. K. and Brostoff S. W. (1976) Gangliosides of peripheral nerve myelin. *J Neurochem* **26**, 157-162.
- Fra A. M., Williamson E., Simons K. and Parton R. G. (1994) Detergent-insoluble glycolipid microdomains in lymphocytes in the absence of caveolae. *J Biol Chem* **269**, 30745-30748.
- Frail D. E. and Braun P. E. (1984) Two developmentally regulated messenger RNAs differing in their coding region may exist for the myelin-associated glycoprotein. *J Biol Chem* **259**, 14857-14862.

- Frank M. (2000) MAL, a proteolipid in glycosphingolipid enriched domains: functional implications in myelin and beyond. *Prog Neurobiol* **60**, 531-544.
- Frank M., van der Haar M. E., Schaeren-Wiemers N. and Schwab M. E. (1998) rMAL is a glycosphingolipid-associated protein of myelin and apical membranes of epithelial cells in kidney and stomach. *J Neurosci* **18**, 4901-4913.
- Frank M., Schaeren-Wiemers N., Schneider R. and Schwab M. E. (1999) Developmental expression pattern of the myelin proteolipid MAL indicates different functions of MAL for immature Schwann cells and in a late step of CNS myelinogenesis. *J Neurochem* **73**, 587-597.
- Frank M., Atanasoski S., Sancho S., Magyar J. P., Ruelicke T., Schwab M. E. and Suter U. (2000) Progressive segregation of unmyelinated axons in peripheral nerves, myelin alterations in the CNS, and cyst formation in the kidneys of myelin and lymphocyte protein-overexpressing mice. *J Neurochem* **75**, 1927-1939.
- Franken S., Schaeren-Wiemers N., D. K., Sandhoff R., Schwarz A., Yaghoofam A., Saravanan K. and Gieselmann V. (2003) Effects of lipid storage on raft associated myelin proteins in a glycolipid storage disorder. *submitted*.
- Franzen R., Tanner S. L., Dashiell S. M., Rottkamp C. A., Hammer J. A. and Quarles R. H. (2001) Microtubule-associated protein 1B: a neuronal binding partner for myelin-associated glycoprotein. *J Cell Biol* **155**, 893-898.
- Friede R. L. and Samorajski T. (1968) Myelin formation in the sciatic nerve of the rat. A quantitative electron microscopic, histochemical and radioautographic study. *J Neuropathol Exp Neurol* **27**, 546-570.
- Fruttiger M., Montag D., Schachner M. and Martini R. (1995) Crucial role for the myelin-associated glycoprotein in the maintenance of axon-myelin integrity. *Eur J Neurosci* **7**, 511-515.
- Fujita N., Sato S., Ishiguro H., Inuzuka T., Baba H., Kurihara T., Takahashi Y. and Miyatake T. (1990) The large isoform of myelin-associated glycoprotein is scarcely expressed in the quaking mouse brain. *J Neurochem* **55**, 1056-1059.
- Fujita N., Kemper A., Dupree J., Nakayasu H., Bartsch U., Schachner M., Maeda N., Suzuki K. and Popko B. (1998) The cytoplasmic domain of the large myelin-associated glycoprotein isoform is needed for proper CNS but not peripheral nervous system myelination. *J Neurosci* **18**, 1970-1978.
- Garbay B., Heape A. M., Sargueil F. and Cassagne C. (2000) Myelin synthesis in the peripheral nervous system. *Prog Neurobiol* **61**, 267-304.
- Gard A. L., Maughon R. H. and Schachner M. (1996) In vitro oligodendroglial properties of cell adhesion molecules in the immunoglobulin superfamily: myelin-associated glycoprotein and N-CAM. *J Neurosci Res* **46**, 415-426.
- Ghitescu L., Fixman A., Simionescu M. and Simionescu N. (1986) Specific binding sites for albumin restricted to plasmalemmal vesicles of continuous capillary endothelium: receptor-mediated transcytosis. *J Cell Biol* **102**, 1304-1311.
- Givogri M. I., Bongarzone E. R. and Campagnoni A. T. (2000) New insights on the biology of myelin basic protein gene: the neural-immune connection. *J Neurosci Res* **59**, 153-159.
- Gluzman Y. (1981) SV40-transformed simian cells support the replication of early SV40 mutants. *Cell* **23**, 175-182.
- Gow A., Friedrich V. L., Jr. and Lazzarini R. A. (1994) Intracellular transport and sorting of the oligodendrocyte transmembrane proteolipid protein. *J Neurosci Res* **37**, 563-573.
- Griffiths I. R. (1996) Myelin mutants: model systems for the study of normal and abnormal myelination. *Bioessays* **18**, 789-797.
- Hammang J. P., Duncan I. D. and Gilmore S. A. (1986) Degenerative changes in rat intraspinal Schwann cells following tellurium intoxication. *Neuropathol Appl Neurobiol* **12**, 359-370.
- Hooper N. M. (1999) Detergent-insoluble glycosphingolipid/cholesterol-rich membrane domains, lipid-rafts and caveolae (review). *Mol Membr Biol* **16**, 145-156.
- Howe J. R. and Ritchie J. M. (1990) Sodium currents in Schwann cells from myelinated and non-myelinated nerves of neonatal and adult rabbits. *J Physiol* **425**, 169-210.
- Hudson L. (1990) Molecular biology of myelin proteins in the central and peripheral nervous system. *The Neurosci* **2**, 483-496.
- Hudson L. D., Friedrich V. L., Jr., Behar T., Dubois-Dalcq M. and Lazzarini R. A. (1989) The initial events in myelin synthesis: orientation of proteolipid protein in the plasma membrane of cultured oligodendrocytes. *J Cell Biol* **109**, 717-727.
- Ichimura T. and Ellisman M. H. (1991) Three-dimensional fine structure of cytoskeletal-membrane interactions at nodes of Ranvier. *J Neurocytol* **20**, 667-681.
- Inouye H., Ganser A. L. and Kirschner D. A. (1985) Shiverer and normal peripheral myelin compared: basic protein localization, membrane interactions, and lipid composition. *J Neurochem* **45**, 1911-1922.
- Inuzuka T., Fujita N., Sato S., Baba H., Nakano R., Ishiguro H. and Miyatake T. (1991) Expression of the large myelin-associated glycoprotein isoform during the development in the mouse peripheral nervous system. *Brain Res* **562**, 173-175.
- Ishiguro H., Sato S., Fujita N., Inuzuka T., Nakano R. and Miyatake T. (1991) Immunohistochemical

- localization of myelin-associated glycoprotein isoforms during the development in the mouse brain. *Brain Res* **563**, 288-292.
- Jaramillo M. L., Afar D. E., Almazan G. and Bell J. C. (1994) Identification of tyrosine 620 as the major phosphorylation site of myelin-associated glycoprotein and its implication in interacting with signaling molecules. *J Biol Chem* **269**, 27240-27245.
- Juguelin H., Heape A., Boiron F. and Cassagne C. (1986) A quantitative developmental study of neutral lipids during myelinogenesis in the peripheral nervous system of normal and trembler mice. *Brain Res* **390**, 249-252.
- Jung M., Kramer E., Grzenkowski M., Tang K., Blakemore W., Aguzzi A., Khazaie K., Chlichlia K., von Blankenfeld G., Kettenmann H. and et al. (1995) Lines of murine oligodendroglial precursor cells immortalized by an activated neu tyrosine kinase show distinct degrees of interaction with axons *in vitro* and *in vivo*. *Eur J Neurosci* **7**, 1245-1265.
- Kalwy S. A., Smith R. and Kidd G. J. (1997) Myelin proteolipid protein expressed in COS-1 cells is targeted to actin-associated surfaces. *J Neurosci Res* **48**, 201-211.
- Kelm S., Pelz A., Schauer R., Filbin M. T., Tang S., de Bellard M. E., Schnaar R. L., Mahoney J. A., Hartnell A., Bradfield P. and et al. (1994) Sialoadhesin, myelin-associated glycoprotein and CD22 define a new family of sialic acid-dependent adhesion molecules of the immunoglobulin superfamily. *Curr Biol* **4**, 965-972.
- Kessaris N., Pringle N. and Richardson W. D. (2001) Ventral neurogenesis and the neuron-glia switch. *Neuron* **31**, 677-680.
- Kim T. and Pfeiffer S. E. (1999) Myelin glycosphingolipid/cholesterol-enriched microdomains selectively sequester the non-compact myelin proteins CNP and MOG. *J Neurocytol* **28**, 281-293.
- Kim T., Fiedler K., Madison D. L., Krueger W. H. and Pfeiffer S. E. (1995) Cloning and characterization of MVP17: a developmentally regulated myelin protein in oligodendrocytes. *J Neurosci Res* **42**, 413-422.
- Kimura M., Sato M., Akatsuka A., Nozawa-Kimura S., Takahashi R., Yokoyama M., Nomura T. and Katsuki M. (1989) Restoration of myelin formation by a single type of myelin basic protein in transgenic shiverer mice. *Proc Natl Acad Sci U S A* **86**, 5661-5665.
- Klein C., Kramer E. M., Cardine A. M., Schraven B., Brandt R. and Trotter J. (2002) Process outgrowth of oligodendrocytes is promoted by interaction of fyn kinase with the cytoskeletal protein tau. *J Neurosci* **22**, 698-707.
- Klugmann M., Schwab M. H., Puhlhofer A., Schneider A., Zimmermann F., Griffiths I. R. and Nave K. A. (1997) Assembly of CNS myelin in the absence of proteolipid protein. *Neuron* **18**, 59-70.
- Koch T., Brugger T., Bach A., Gennarini G. and Trotter J. (1997) Expression of the immunoglobulin superfamily cell adhesion molecule F3 by oligodendrocyte-lineage cells. *Glia* **19**, 199-212.
- Kramer E. M., Schardt A. and Nave K. A. (2001) Membrane traffic in myelinating oligodendrocytes. *Microsc Res Tech* **52**, 656-671.
- Kramer E. M., Koch T., Niehaus A. and Trotter J. (1997) Oligodendrocytes direct glycosyl phosphatidylinositol-anchored proteins to the myelin sheath in glycosphingolipid-rich complexes. *J Biol Chem* **272**, 8937-8945.
- Kramer E. M., Klein C., Koch T., Boytinck M. and Trotter J. (1999) Compartmentation of Fyn kinase with glycosylphosphatidylinositol-anchored molecules in oligodendrocytes facilitates kinase activation during myelination. *J Biol Chem* **274**, 29042-29049.
- Kroepfl J. F. and Gardinier M. V. (2001) Mutually exclusive apicobasolateral sorting of two oligodendroglial membrane proteins, proteolipid protein and myelin/oligodendrocyte glycoprotein, in Madin-Darby canine kidney cells. *J Neurosci Res* **66**, 1140-1148.
- Kroepfl J. F., Viise L. R., Charron A. J., Linington C. and Gardinier M. V. (1996) Investigation of myelin/oligodendrocyte glycoprotein membrane topology. *J Neurochem* **67**, 2219-2222.
- Kunzelmann P., Blumcke I., Traub O., Dermietzel R. and Willecke K. (1997) Coexpression of connexin45 and -32 in oligodendrocytes of rat brain. *J Neurocytol* **26**, 17-22.
- Kursula P., Lehto V. P. and Heape A. M. (2001) The small myelin-associated glycoprotein binds to tubulin and microtubules. *Brain Res Mol Brain Res* **87**, 22-30.
- Kursula P., Tikkanen G., Lehto V. P., Nishikimi M. and Heape A. M. (1999) Calcium-dependent interaction between the large myelin-associated glycoprotein and S100beta. *J Neurochem* **73**, 1724-1732.
- Kusumi A. and Sako Y. (1996) Cell surface organization by the membrane skeleton. *Curr Opin Cell Biol* **8**, 566-574.
- Laemmli U. K. (1970) Cleavage of structural proteins during the assembly of the head of bacteriophage T4. *Nature* **227**, 680-685.
- Lai C., Brow M. A., Nave K. A., Noronha A. B., Quarles R. H., Bloom F. E., Milner R. J. and Sutcliffe J. G. (1987) Two forms of 1B236/myelin-associated glycoprotein, a cell adhesion molecule for postnatal neural development, are produced by alternative splicing. *Proc Natl Acad Sci U S A* **84**, 4337-4341.
- Lampert P., Garro F. and Pentschew A. (1970) Tellurium neuropathy. *Acta Neuropathol (Berl)* **15**, 308-317.
- Lampert P. W. and Garrett R. S. (1971) Mechanism of demyelination in tellurium neuropathy. Electron microscopic observations. *Lab Invest* **25**, 380-388.

- Landry C. F., Ellison J., Skinner E. and Campagnoni A. T. (1997) Golli-MBP proteins mark the earliest stages of fiber extension and terminal arboration in the mouse peripheral nervous system. *J Neurosci Res* **50**, 265-271.
- Lemke G. (1988) Unwrapping the genes of myelin. *Neuron* **1**, 535-543.
- Letourneau P. C., Roche F. K., Shattuck T. A., Lemmon V. and Takeichi M. (1991) Interactions of Schwann cells with neurites and with other Schwann cells involve the calcium-dependent adhesion molecule, N-cadherin. *J Neurobiol* **22**, 707-720.
- Li C., Tropak M. B., Gerlai R., Clapoff S., Abramow-Newerly W., Trapp B., Peterson A. and Roder J. (1994) Myelination in the absence of myelin-associated glycoprotein. *Nature* **369**, 747-750.
- Linington C., Izumo S., Suzuki M., Uyemura K., Meyermann R. and Wekerle H. (1984) A permanent rat T cell line that mediates experimental allergic neuritis in the Lewis rat *in vivo*. *J Immunol* **133**, 1946-1950.
- Lützelshwab R. (1998) Differential expression of myelin associated glycoprotein isoforms in human nervous system and in mouse models for demyelinating neuropathies., in *Philosophisch-Naturwissenschaftlichen Fakultät*, p 138. Universität Basel, Basel.
- Magyar J. P., Ebensperger C., Schaeren-Wiemers N. and Suter U. (1997) Myelin and lymphocyte protein (MAL/MVP17/VIP17) and plasmalogen are members of an extended gene family. *Gene* **189**, 269-275.
- Marcus J., Dupree J. L. and Popko B. (2002) Myelin-associated glycoprotein and myelin galactolipids stabilize developing axo-glial interactions. *J Cell Biol* **156**, 567-577.
- Martin-Belmonte F., Puertollano R., Millan J. and Alonso M. A. (2000) The MAL proteolipid is necessary for the overall apical delivery of membrane proteins in the polarized epithelial Madin-Darby canine kidney and fischer rat thyroid cell lines. *Mol Biol Cell* **11**, 2033-2045.
- Martin-Belmonte F., Kremer L., Albar J. P., Marazuela M. and Alonso M. A. (1998) Expression of the MAL gene in the thyroid: the MAL proteolipid, a component of glycolipid-enriched membranes, is apically distributed in thyroid follicles. *Endocrinology* **139**, 2077-2084.
- Martini R. and Schachner M. (1997) Molecular bases of myelin formation as revealed by investigations on mice deficient in glial cell surface molecules. *Glia* **19**, 298-310.
- Martini R., Mohajeri M. H., Kasper S., Giese K. P. and Schachner M. (1995) Mice doubly deficient in the genes for P0 and myelin basic protein show that both proteins contribute to the formation of the major dense line in peripheral nerve myelin. *J Neurosci* **15**, 4488-4495.
- Matsuda Y., Koito H. and Yamamoto H. (1997) Induction of myelin-associated glycoprotein expression through neuron-oligodendrocyte contact. *Brain Res Dev Brain Res* **100**, 110-116.
- Matthieu J. M., Roch J. M., Omlin F. X., Rambaldi I., Almazan G. and Braun P. E. (1986) Myelin instability and oligodendrocyte metabolism in myelin-deficient mutant mice. *J Cell Biol* **103**, 2673-2682.
- Mentaberry A., Adesnik M., Atchison M., Norgard E. M., Alvarez F., Sabatini D. D. and Colman D. R. (1986) Small basic proteins of myelin from central and peripheral nervous systems are encoded by the same gene. *Proc Natl Acad Sci U S A* **83**, 1111-1114.
- Messier A. M. and Bizzozero O. A. (2000) Conserved fatty acid composition of proteolipid protein during brain development and in myelin subfractions. *Neurochem Res* **25**, 449-455.
- Mi H., Harris-Warrick R. M., Deerinck T. J., Inman I., Ellisman M. H. and Schwarz T. L. (1999) Identification and localization of Ca(2+)-activated K⁺ channels in rat sciatic nerve. *Glia* **26**, 166-175.
- Miescher G. C., Lützelshwab R., Erne B., Ferracin F., Huber S. and Steck A. J. (1997) Reciprocal expression of myelin-associated glycoprotein splice variants in the adult human peripheral and central nervous systems. *Brain Res Mol Brain Res* **52**, 299-306.
- Millan J., Puertollano R., Fan L. and Alonso M. A. (1997b) Caveolin and MAL, two protein components of internal detergent-insoluble membranes, are in distinct lipid microenvironments in MDCK cells. *Biochem Biophys Res Commun* **233**, 707-712.
- Millan J., Puertollano R., Fan L., Rancano C. and Alonso M. A. (1997a) The MAL proteolipid is a component of the detergent-insoluble membrane subdomains of human T-lymphocytes. *Biochem J* **321**, 247-252.
- Molineaux S. M., Engh H., de Ferra F., Hudson L. and Lazzarini R. A. (1986) Recombination within the myelin basic protein gene created the dysmyelinating shiverer mouse mutation. *Proc Natl Acad Sci U S A* **83**, 7542-7546.
- Montag D., Giese K. P., Bartsch U., Martini R., Lang Y., Bluthmann H., Karthigasan J., Kirschner D. A., Wintergerst E. S., Nave K. A. and et al. (1994) Mice deficient for the myelin-associated glycoprotein show subtle abnormalities in myelin. *Neuron* **13**, 229-246.
- Morita K., Sasaki H., Fujimoto K., Furuse M. and Tsukita S. (1999) Claudin-11/OSP-based tight junctions of myelin sheaths in brain and Sertoli cells in testis. *J Cell Biol* **145**, 579-588.
- Mukhopadhyay G., Doherty P., Walsh F. S., Crocker P. R. and Filbin M. T. (1994) A novel role for myelin-associated glycoprotein as an inhibitor of axonal regeneration. *Neuron* **13**, 757-767.
- Newman S., Kitamura K. and Campagnoni A. T. (1987) Identification of a cDNA coding for a fifth form of myelin basic protein in mouse. *Proc Natl Acad Sci U S A* **84**, 886-890.
- Norton W. T. and Cammer W. (1984) Isolation and characterization of myelin, in *Myelin*, second Edition (Morell P., ed.), pp 147-195. Plenum Publishing Corp., New York/London.
- Nussbaum J. L., Neskovic N. and Mandel P. (1969) A study of lipid components in brain of the 'Jimpy'

- mouse, a mutant with myelin deficiency. *J Neurochem* **16**, 927-934.
- Omlin F. X., Webster H. D., Palkovits C. G. and Cohen S. R. (1982) Immunocytochemical localization of basic protein in major dense line regions of central and peripheral myelin. *J Cell Biol* **95**, 242-248.
- Owens G. C. and Bunge R. P. (1991) Schwann cells infected with a recombinant retrovirus expressing myelin-associated glycoprotein antisense RNA do not form myelin. *Neuron* **7**, 565-575.
- Parton R. G. (1996) Caveolae and caveolins. *Curr Opin Cell Biol* **8**, 542-548.
- Parton R. G. and Simons K. (1995) Digging into caveolae. *Science* **269**, 1398-1399.
- Pedraza L., Huang J. K. and Colman D. R. (2001) Organizing principles of the axoglial apparatus. *Neuron* **30**, 335-344.
- Pedraza L., Frey A. B., Hempstead B. L., Colman D. R. and Salzer J. L. (1991) Differential expression of MAG isoforms during development. *J Neurosci Res* **29**, 141-148.
- Pesheva P., Gloor S., Schachner M. and Probstmeier R. (1997) Tenascin-R is an intrinsic autocrine factor for oligodendrocyte differentiation and promotes cell adhesion by a sulfatide-mediated mechanism. *J Neurosci* **17**, 4642-4651.
- Peters A., Palay S. L. and Webster H. D. (1991), in *The fine structure of the nervous system*, pp 494-499. Oxford University Press, New York.
- Pfeiffer S. E., Warrington A. E. and Bansal R. (1993) The oligodendrocyte and its many cellular processes. *Trends Cell Biol* **3**, 191-197.
- Pirollet F., Derancourt J., Haiech J., Job D. and Margolis R. L. (1992) Ca(2+)-calmodulin regulated effectors of microtubule stability in bovine brain. *Biochemistry* **31**, 8849-8855.
- Pribyl T. M., Campagnoni C. W., Kampf K., Kashima T., Handley V. W., McMahon J. and Campagnoni A. T. (1993) The human myelin basic protein gene is included within a 179-kilobase transcription unit: expression in the immune and central nervous systems. *Proc Natl Acad Sci U S A* **90**, 10695-10699.
- Pringle N. P. and Richardson W. D. (1993) A singularity of PDGF alpha-receptor expression in the dorsoventral axis of the neural tube may define the origin of the oligodendrocyte lineage. *Development* **117**, 525-533.
- Pringle N. P., Mudhar H. S., Collarini E. J. and Richardson W. D. (1992) PDGF receptors in the rat CNS: during late neurogenesis, PDGF alpha-receptor expression appears to be restricted to glial cells of the oligodendrocyte lineage. *Development* **115**, 535-551.
- Privat A., Jacque C., Bourre J. M., Dupouey P. and Baumann N. (1979) Absence of the major dense line in myelin of the mutant mouse "shiverer". *Neurosci Lett* **12**, 107-112.
- Probstmeier R., Fahrig T., Spiess E. and Schachner M. (1992) Interactions of the neural cell adhesion molecule and the myelin-associated glycoprotein with collagen type I: involvement in fibrillogenesis. *J Cell Biol* **116**, 1063-1070.
- Puertollano R. and Alonso M. A. (1998) A short peptide motif at the carboxyl terminus is required for incorporation of the integral membrane MAL protein to glycolipid-enriched membranes. *J Biol Chem* **273**, 12740-12745.
- Puertollano R., Li S., Lisanti M. P. and Alonso M. A. (1997) Recombinant expression of the MAL proteolipid, a component of glycolipid-enriched membrane microdomains, induces the formation of vesicular structures in insect cells. *J Biol Chem* **272**, 18311-18315.
- Puertollano R., Martinez-Menarguez J. A., Batista A., Ballesta J. and Alonso M. A. (2001) An intact dilysine-like motif in the carboxyl terminus of MAL is required for normal apical transport of the influenza virus hemagglutinin cargo protein in epithelial Madin-Darby canine kidney cells. *Mol Biol Cell* **12**, 1869-1883.
- Puertollano R., Martin-Belmonte F., Millan J., de Marco M. C., Albar J. P., Kremer L. and Alonso M. A. (1999) The MAL proteolipid is necessary for normal apical transport and accurate sorting of the influenza virus hemagglutinin in Madin-Darby canine kidney cells. *J Cell Biol* **145**, 141-151.
- Quarles R. H. (1983) Myelin-associated glycoprotein in development and disease. *Dev Neurosci* **6**, 285-303.
- Raff M. C., Abney E. R. and Miller R. H. (1984) Two glial cell lineages diverge prenatally in rat optic nerve. *Dev Biol* **106**, 53-60.
- Raff M. C., Mirsky R., Fields K. L., Lisak R. P., Dorfman S. H., Silberberg D. H., Gregson N. A., Leibowitz S. and Kennedy M. C. (1978) Galactocerebroside is a specific cell-surface antigenic marker for oligodendrocytes in culture. *Nature* **274**, 813-816.
- Raine C. S. (1982) Differences between the nodes of Ranvier of large and small diameter fibres in the P.N.S. *J Neurocytol* **11**, 935-947.
- Rambukkana A., Yamada H., Zanazzi G., Mathus T., Salzer J. L., Yurchenco P. D., Campbell K. P. and Fischetti V. A. (1998) Role of alpha-dystroglycan as a Schwann cell receptor for Mycobacterium leprae. *Science* **282**, 2076-2079.
- Rasband M. N. and Shrager P. (2000) Ion channel sequestration in central nervous system axons. *J Physiol* **525 Pt 1**, 63-73.
- Remahl S. and Hildebrand C. (1990) Relations between axons and oligodendroglial cells during initial myelination. II. The individual axon. *J Neurocytol* **19**, 883-898.
- Richter-Landsberg C. and Gorath M. (1999) Developmental regulation of alternatively spliced isoforms of mRNA encoding MAP2 and tau in rat brain oligodendrocytes during culture maturation. *J Neurosci Res*

- 56, 259-270.
- Roach A., Boylan K., Horvath S., Prusiner S. B. and Hood L. E. (1983) Characterization of cloned cDNA representing rat myelin basic protein: absence of expression in brain of shiverer mutant mice. *Cell* **34**, 799-806.
- Roach A., Takahashi N., Pravtcheva D., Ruddle F. and Hood L. (1985) Chromosomal mapping of mouse myelin basic protein gene and structure and transcription of the partially deleted gene in shiverer mutant mice. *Cell* **42**, 149-155.
- Rosenbluth J. (1980) Peripheral myelin in the mouse mutant Shiverer. *J Comp Neurol* **193**, 729-739.
- Rosenbluth J., Liang W. L., Liu Z., Guo D. and Schiff R. (1995) Paranodal structural abnormalities in rat CNS myelin developing *in vivo* in the presence of implanted O1 hybridoma cells. *J Neurocytol* **24**, 818-824.
- Roth H. J., Hunkeler M. J. and Campagnoni A. T. (1985) Expression of myelin basic protein genes in several dysmyelinating mouse mutants during early postnatal brain development. *J Neurochem* **45**, 572-580.
- Rothberg K. G., Ying Y. S., Kamen B. A. and Anderson R. G. (1990) Cholesterol controls the clustering of the glycopospholipid-anchored membrane receptor for 5-methyltetrahydrofolate. *J Cell Biol* **111**, 2931-2938.
- Said G. and Duckett S. (1981) Tellurium-induced myelinopathy in adult rats. *Muscle Nerve* **4**, 319-325.
- Saito F., Masaki T., Kamakura K., Anderson L. V., Fujita S., Fukuta-Ohi H., Sunada Y., Shimizu T. and Matsumura K. (1999) Characterization of the transmembrane molecular architecture of the dystroglycan complex in schwann cells. *J Biol Chem* **274**, 8240-8246.
- Salzer J. L., Bunge R. P. and Glaser L. (1980) Studies of Schwann cell proliferation. III. Evidence for the surface localization of the neurite mitogen. *J Cell Biol* **84**, 767-778.
- Sargiacomo M., Sudol M., Tang Z. and Lisanti M. P. (1993) Signal transducing molecules and glycosylphosphatidylinositol-linked proteins form a caveolin-rich insoluble complex in MDCK cells. *J Cell Biol* **122**, 789-807.
- Sato-Bigbee C., Pal S. and Chu A. K. (1999) Different neuroligands and signal transduction pathways stimulate CREB phosphorylation at specific developmental stages along oligodendrocyte differentiation. *J Neurochem* **72**, 139-147.
- Sawada N., Ishida H., Collins B. E., Schnaar R. L. and Kiso M. (1999) Ganglioside GD1 alpha analogues as high-affinity ligands for myelin-associated glycoprotein (MAG). *Carbohydr Res* **316**, 1-5.
- Schachner M. and Bartsch U. (2000) Multiple functions of the myelin-associated glycoprotein MAG (siglec-4a) in formation and maintenance of myelin. *Glia* **29**, 154-165.
- Schaeren-Wiemers N., Valenzuela D. M., Frank M. and Schwab M. E. (1995b) Characterization of a rat gene, rMAL, encoding a protein with four hydrophobic domains in central and peripheral myelin. *J Neurosci* **15**, 5753-5764.
- Schaeren-Wiemers N., Schaefer C., Valenzuela D. M., Yancopoulos G. D. and Schwab M. E. (1995a) Identification of new oligodendrocyte- and myelin-specific genes by a differential screening approach. *J Neurochem* **65**, 10-22.
- Schaeren-Wiemers N., Lützel Schwab R., Erne B., Atanasoski S., Sancho S., Suter U. and Steck A. J. (1999) Differential expression of L- and S-MAG in human and mouse models of peripheral neuropathies. *J Neurol* **246**, 71.
- Scherer S. S. (1996) Molecular specializations at nodes and paranodes in peripheral nerve. *Microsc Res Tech* **34**, 452-461.
- Scherer S. S., Deschenes S. M., Xu Y. T., Grinspan J. B., Fischbeck K. H. and Paul D. L. (1995) Connexin32 is a myelin-related protein in the PNS and CNS. *J Neurosci* **15**, 8281-8294.
- Schlesinger M. J. (1981) Proteolipids. *Annu Rev Biochem* **50**, 193-206.
- Schroeder R., London E. and Brown D. (1994) Interactions between saturated acyl chains confer detergent resistance on lipids and glycosylphosphatidylinositol (GPI)-anchored proteins: GPI-anchored proteins in liposomes and cells show similar behavior. *Proc Natl Acad Sci U S A* **91**, 12130-12134.
- Seilheimer B., Persohn E. and Schachner M. (1989) Antibodies to the L1 adhesion molecule inhibit Schwann cell ensheathment of neurons *in vitro*. *J Cell Biol* **109**, 3095-3103.
- Sheikh K. A., Sun J., Liu Y., Kawai H., Crawford T. O., Proia R. L., Griffin J. W. and Schnaar R. L. (1999) Mice lacking complex gangliosides develop Wallerian degeneration and myelination defects. *Proc Natl Acad Sci U S A* **96**, 7532-7537.
- Shimizu-Okabe C., Matsuda Y., Koito H. and Yoshida S. (2001) L-isoform but not S-isoform of myelin associated glycoprotein promotes neurite outgrowth of mouse cerebellar neurons. *Neurosci Lett* **311**, 203-205.
- Simons K. and van Meer G. (1988) Lipid sorting in epithelial cells. *Biochemistry* **27**, 6197-6202.
- Simons K. and Ikonen E. (1997) Functional rafts in cell membranes. *Nature* **387**, 569-572.
- Simons M., Kramer E. M., Macchi P., Rathke-Hartlieb S., Trotter J., Nave K. A. and Schulz J. B. (2002) Overexpression of the myelin proteolipid protein leads to accumulation of cholesterol and proteolipid protein in endosomes/lysosomes: implications for Pelizaeus-Merzbacher disease. *J Cell Biol* **157**, 327-336.
- Singer S. J. and Nicolson G. L. (1972) The fluid mosaic model of the structure of cell membranes. *Science*

- 175, 720-731.
- Sinoway M. P., Kitagawa K., Timsit S., Hashim G. A. and Colman D. R. (1994) Proteolipid protein interactions in transfectants: implications for myelin assembly. *J Neurosci Res* **37**, 551-562.
- Skibbens J. E., Roth M. G. and Matlin K. S. (1989) Differential extractability of influenza virus hemagglutinin during intracellular transport in polarized epithelial cells and nonpolar fibroblasts. *J Cell Biol* **108**, 821-832.
- Sommer I. and Schachner M. (1981) Monoclonal antibodies (O1 to O4) to oligodendrocyte cell surfaces: an immunocytochemical study in the central nervous system. *Dev Biol* **83**, 311-327.
- Spagnol G., Williams M., Srinivasan J., Golier J., Bauer D., Lebo R. V. and Latov N. (1989) Molecular cloning of human myelin-associated glycoprotein. *J Neurosci Res* **24**, 137-142.
- Stensaas L. J. and Stensaas S. S. (1968) Astrocytic neuroglial cells, oligodendrocytes and microgliaocytes in the spinal cord of the toad. II. Electron microscopy. *Z Zellforsch Mikrosk Anat* **86**, 184-213.
- Sternberger N. H., Quarles R. H., Itoyama Y. and Webster H. D. (1979) Myelin-associated glycoprotein demonstrated immunocytochemically in myelin and myelin-forming cells of developing rat. *Proc Natl Acad Sci U S A* **76**, 1510-1514.
- Stevens B., Porta S., Haak L. L., Gallo V. and Fields R. D. (2002) Adenosine: a neuron-glia transmitter promoting myelination in the CNS in response to action potentials. *Neuron* **36**, 855-868.
- Streng K., Schauer R. and Kelm S. (1999) Binding partners for the myelin-associated glycoprotein of N2A neuroblastoma cells. *FEBS Lett* **444**, 59-64.
- Streng K., Brossmer R., Ihrig P., Schauer R. and Kelm S. (2001) Fibronectin is a binding partner for the myelin-associated glycoprotein (siglec-4a). *FEBS Lett* **499**, 262-267.
- Tait S., Gunn-Moore F., Collinson J. M., Huang J., Lubetzki C., Pedraza L., Sherman D. L., Colman D. R. and Brophy P. J. (2000) An oligodendrocyte cell adhesion molecule at the site of assembly of the paranodal axo-glia junction. *J Cell Biol* **150**, 657-666.
- Takahashi N., Roach A., Teplow D. B., Prusiner S. B. and Hood L. (1985) Cloning and characterization of the myelin basic protein gene from mouse: one gene can encode both 14 kd and 18.5 kd MBPs by alternate use of exons. *Cell* **42**, 139-148.
- Takahashi T. (1981) Experimental study on segmental demyelination in tellurium neuropathy. *Hokkaido Igaku Zasshi* **56**, 105-131.
- Taylor C. M., Coetzee T. and Pfeiffer S. E. (2002) Detergent-insoluble glycosphingolipid/cholesterol microdomains of the myelin membrane. *J Neurochem* **81**, 993-1004.
- Timsit S., Martinez S., Allinquant B., Peyron F., Puelles L. and Zalc B. (1995) Oligodendrocytes originate in a restricted zone of the embryonic ventral neural tube defined by DM-20 mRNA expression. *J Neurosci* **15**, 1012-1024.
- Toews A. D., Lee S. Y., Popko B. and Morell P. (1990) Tellurium-induced neuropathy: a model for reversible reductions in myelin protein gene expression. *J Neurosci Res* **26**, 501-507.
- Toews A. D., Hostettler J., Barrett C. and Morell P. (1997) Alterations in gene expression associated with primary demyelination and remyelination in the peripheral nervous system. *Neurochem Res* **22**, 1271-1280.
- Toews A. D., Jurevics H., Hostettler J., Roe E. B. and Morell P. (1996) Tissue-specific coordinate regulation of enzymes of cholesterol biosynthesis: sciatic nerve versus liver. *J Lipid Res* **37**, 2502-2509.
- Tran D., Carpentier J. L., Sawano F., Gorden P. and Orci L. (1987) Ligands internalized through coated or noncoated invaginations follow a common intracellular pathway. *Proc Natl Acad Sci U S A* **84**, 7957-7961.
- Trapp B. D. (1990) Myelin-associated glycoprotein. Location and potential functions. *Ann N Y Acad Sci* **605**, 29-43.
- Trapp B. D., Andrews S. B., Wong A., O'Connell M. and Griffin J. W. (1989) Co-localization of the myelin-associated glycoprotein and the microfilament components, F-actin and spectrin, in Schwann cells of myelinated nerve fibres. *J Neurocytol* **18**, 47-60.
- Trapp B. D., Moench T., Pulley M., Barbosa E., Tennekoon G. and Griffin J. (1987) Spatial segregation of mRNA encoding myelin-specific proteins. *Proc Natl Acad Sci U S A* **84**, 7773-7777.
- Trotter J., Klein C. and Krämer E.-M. (2000) GPI-anchored proteins and glycosphingolipid-rich rafts: platforms for adhesion and signalling. *The Neuroscientist* **6**, 271-284.
- Umemori H., Sato S., Yagi T., Aizawa S. and Yamamoto T. (1994) Initial events of myelination involve Fyn tyrosine kinase signalling. *Nature* **367**, 572-576.
- Umemori H., Kadowaki Y., Hirose K., Yoshida Y., Hironaka K., Okano H. and Yamamoto T. (1999) Stimulation of myelin basic protein gene transcription by Fyn tyrosine kinase for myelination. *J Neurosci* **19**, 1393-1397.
- Vabnick I., Novakovic S. D., Levinson S. R., Schachner M. and Shrager P. (1996) The clustering of axonal sodium channels during development of the peripheral nervous system. *J Neurosci* **16**, 4914-4922.
- van Helvoort A., Smith A. J., Sprong H., Fritzsche I., Schinkel A. H., Borst P. and van Meer G. (1996) MDR1 P-glycoprotein is a lipid translocase of broad specificity, while MDR3 P-glycoprotein specifically translocates phosphatidylcholine. *Cell* **87**, 507-517.
- van Meer G. (1989) Lipid traffic in animal cells. *Annu Rev Cell Biol* **5**, 247-275.

- Verity A. N. and Campagnoni A. T. (1988) Regional expression of myelin protein genes in the developing mouse brain: in situ hybridization studies. *J Neurosci Res* **21**, 238-248.
- Vyas A. A., Patel H. V., Fromholt S. E., Heffer-Lauc M., Vyas K. A., Dang J., Schachner M. and Schnaar R. L. (2002) Gangliosides are functional nerve cell ligands for myelin-associated glycoprotein (MAG), an inhibitor of nerve regeneration. *Proc Natl Acad Sci U S A* **99**, 8412-8417.
- Weimbs T. and Stoffel W. (1992) Proteolipid protein (PLP) of CNS myelin: positions of free, disulfide-bonded, and fatty acid thioester-linked cysteine residues and implications for the membrane topology of PLP. *Biochemistry* **31**, 12289-12296.
- Weiss M. D., Hammer J. and Quarles R. H. (2000) Oligodendrocytes in aging mice lacking myelin-associated glycoprotein are dystrophic but not apoptotic. *J Neurosci Res* **62**, 772-780.
- Wiley-Livingston C. A. and Ellisman M. H. (1982) Return of axonal and glial membrane specializations during remyelination after tellurium-induced demyelination. *J Neurocytol* **11**, 65-80.
- Wu J. I., Reed R. B., Grabowski P. J. and Artzt K. (2002) Function of quaking in myelination: Regulation of alternative splicing. *Proc Natl Acad Sci U S A* **99**, 4233-4238.
- Yamashita T., Higuchi H. and Tohyama M. (2002) The p75 receptor transduces the signal from myelin-associated glycoprotein to Rho. *J Cell Biol* **157**, 565-570.
- Yang H., Xiao Z. C., Becker B., Hillenbrand R., Rougon G. and Schachner M. (1999) Role for myelin-associated glycoprotein as a functional tenascin-R receptor. *J Neurosci Res* **55**, 687-701.
- Yang L. J., Zeller C. B., Shaper N. L., Kiso M., Hasegawa A., Shapiro R. E. and Schnaar R. L. (1996) Gangliosides are neuronal ligands for myelin-associated glycoprotein. *Proc Natl Acad Sci U S A* **93**, 814-818.
- Yasargil G. M., Greeff N. G., Luescher H. R., Akert K. and Sandri C. (1982) The structural correlate of saltatory conduction along the Mauthner axon in the tench (*Tinca tinca* L.): identification of nodal equivalents at the axon collaterals. *J Comp Neurol* **212**, 417-424.
- Yates A. J. and Wherrett J. R. (1974) Changes in the sciatic nerve of the rabbit and its tissue constituents during development. *J Neurochem* **23**, 993-1003.
- Yim S. H., Farrer R. G. and Quarles R. H. (1995) Expression of glycolipids and myelin-associated glycoprotein during the differentiation of oligodendrocytes: comparison of the CG-4 glial cell line to primary cultures. *Dev Neurosci* **17**, 171-180.
- Yin X., Crawford T. O., Griffin J. W., Tu P., Lee V. M., Li C., Roder J. and Trapp B. D. (1998) Myelin-associated glycoprotein is a myelin signal that modulates the caliber of myelinated axons. *J Neurosci* **18**, 1953-1962.
- Zacchetti D., Peranen J., Murata M., Fiedler K. and Simons K. (1995) VIP17/MAL, a proteolipid in apical transport vesicles. *FEBS Lett* **377**, 465-469.
- Zeller N. K., Hunkeler M. J., Campagnoni A. T., Sprague J. and Lazzarini R. A. (1984) Characterization of mouse myelin basic protein messenger RNAs with a myelin basic protein cDNA clone. *Proc Natl Acad Sci U S A* **81**, 18-22.
- Zhou Q. and Anderson D. J. (2002) The bHLH transcription factors OLIG2 and OLIG1 couple neuronal and glial subtype specification. *Cell* **109**, 61-73.
- Zhou Q., Choi G. and Anderson D. J. (2001) The bHLH transcription factor Olig2 promotes oligodendrocyte differentiation in collaboration with Nkx2.2. *Neuron* **31**, 791-807.

Curriculum Vitae

Personal Details:

Name: Michael Erb

Address: Mülhauserstrasse 73
CH-4056 Basel
061 322 46 88

Neurobiologie
Pharmazentrum/Biozentrum
Klingelbergstrasse 50
CH-4056 Basel
061 267 15 40

Date of birth: 1st December 1968

Place of Birth: Aarau

Marital status: Married

Languages: German mother tongue
English fluent
French

Academic Education:

1999 - 2003 Ph.D. Thesis in Neurobiology in the laboratory of Dr. N. Schaeren-Wiemers and Prof. A.J. Steck at the Department of Research, University Hospital Basel

1998 - 1999 Diploma Thesis in Developmental Biology in the laboratory of Prof. V. Schmid at the Zoological Institute, University of Basel.
Title: 'BMP5-8 in the Jellyfish *Podocoryne carnea*: A Role in Neurogenesis?'

1994 - 1998 Biology I, University of Basel (Diplom)

1991 - 1993 Anthropology, University of Zürich

1989 - 1991 Biology, University of Bern (Vordiplom)

1985 – 1988 College, Alte Kantonsschule Aarau

Publications:

M. Erb, A.J. Steck, K. A. Nave, N. Schaeren-Wiemers (2003). Differential expression of L- and S-MAG upon cAMP stimulated differentiation in oligodendroglial cells. *Journal of Neuroscience Research* 71(3), 326-37.

N. Schaeren-Wiemers, A. Bonnet, B. Erne, M. Erb, U. Bartsch, F. Kern, U. Suter (2003). The raft associated protein MAL is required for normal paranodal structure maintenance. *Manuscript for submission in June 2003.*

Congresses with Poster Presentation:

Neurex Annual Meeting in Basel, April 2003. Poster Presentation: The Lipid-Raft Protein MAL is required for Myelin Structure Maintenance.

International Congress of Peripheral Neuropathy in Vancouver, Canada, July 2002. Poster presentation: Expressing individually tagged L-MAG and S-MAG isoforms from a single genomic expression construct: L-MAG-GFP and S-MAG-VSV.

Gordon Research Conference on Myelin, Ventura Beach, California, February 2002. Poster presentation: Expressing individually tagged L-MAG and S-MAG isoforms from single genomic constructs: L-MAG-GFP and S-MAG-VSVG.

Eleventh Meeting European Neurological Society (ENS), Paris, France, April 2001. Poster presentation: Differential Expression of the Myelin-Associated Glycoprotein Isoforms in Development, De- and Remyelination; Tagging the Isoforms individually with GFP